To the Graduate Council:

I am submitting herewith a thesis written by Ravinder Nair entitled " Processing and Characterization of Blends of Polyarylate and a Thermotropic Copolymer ". I have examined the final copy of this thesis for form and content and recommend that it be accepted in partial fulfillment of the requirements for the degree of Master of Science, with a major in Polymer Engineering.

Joseph E. Spruiell, Major Professor

We have read thesis

and recommend its acceptance:

Accepted for the Council:

Associate Vice Chancellor

and Dean of Graduate School

PROCESSING AND CHARACTERIZATION OF BLENDS OF POLYARYLATE AND A THERMOTROPIC POLYMER

A Thesis

Presented for the

Master of Science

Degree

The University of Tennessee, Knoxville

Ravinder Nair

December, 1992

ACKNOWLEDGEMENT

I would like to express deep gratitude to my major professor, Dr. J. E. Spruiell for his continued support and invaluable guidance offered through the entire duration of this work. His interest in embarking on new and potential subjects were truly admirable and were a constant source of motivation. I would also like to extend my sincere gratitude to my joint advisor Dr. J. F. Fellers for his priceless contribution through a continued evaluation and healthy discussion making this effort a truly enjoyable experience. Appreciation is also expressed to Dr. R. S. Benson for his interest in the subject and for being in my commitee.

The author is indebted to the University of Tennessee for providing personal support in the form of teaching assistantship for the entire duration of this project. The help provided by the staff in the department machine shop and the electronic shop through a skilful maintenance of the equipments relating to this project are also greatly appreciated.

Special thanks are also extended to Mr B. L. McGill for his assistance with the scanning electronic microscopy. The author would also like to thank Mr. D. Fielden for his assistance with the fabrication work on the extruder.

Lastly, I would like to thank my fellow polymer students for their moral and physical support provided at all times.

ABSTRACT

Blends of polyarylate and a thermotropic copolymer of HBA/HNA (75/25) were studied for their general phase behavior and mechanical properties. The compatibility of the two polymers has been analyzed using DSC and polarizing optical microscope. Polyarylate has been found to give incompatible blends showing a two phase morphology up to 20% by weight of LCP. Low composition blends (1-4% LCP) show a decrease in T_g of the polarylate phase as shown by the DSC traces of the blends.

Mechanical properties of the fibers prepared by melt drawing of these biphasic blends have been analyzed using SEM images of the fracture surface. Estimates of the aspect ratio of the reinforcing LCP fibrils were obtained from the counts of the pulled out fibrils on the fracture surfaces and their average diameters. It is seen that the aspect ratio of the fibrils increases with the decrease in the corresponding number of pulled out fibrils as the concentration of LCP increases from 1% to 15% by weight. An optimum melt shear rate of 150-200 sec^{-1} and a temperature of 300°C has been shown to give favourable morphologies for enhanced mechanical properties of the composite fibers.

Melt viscosity of the blends measured for capillary flow decreased with increasing LCP composition at a steady shear of 100 sec^{-1} showing over a 12 fold drop at 5% level of LCP. All blends showed Newtonian behaviour of the matrix in the shear rate region of 10 to 200 sec^{-1}. Blends with 1% by weight of LCP however showed a shear thinning behavior up to about 100 sec^{-1}.

TABLE OF CONTENTS

Chapter	Subject	Page
1.	**INTRODUCTION**	1
	1.1 General Introduction	1
	1.2 Liquid Crystal Polymer Mesophases	3
	1.3 Literature Review	10
	1.3.1 Thermodynamics and Phase Behavior	15
	1.3.2 Rheology and Processing	20
	1.3.3 Mechanical Properties and Morphology	27
	1.4 Over View of the Present Work	38
2.	**EXPERIMENTAL**	40
	2.1 Materials	40
	2.2 Processing	40
	2.3 Characterization	42
	2.3.1 Differential Scanning Calorimetry	42
	2.3.2 Dynamic Mechanical Thermal Analysis.	42
	2.3.3 Polarized Optical Microscopy	43
	2.3.4 Scanning Electron Microscopy	43
	2.3.5 Mechanical Properties	44
	2.3.6 Rheometry Measurements	44
3.	**RESULTS**	45
	3.1 Differential Scanning Calorimetry	45
	3.2 Polarized Optical Microscopy	52
	3.3 Scanning Electron Microscopy Studies	57
	3.4 Dynamic Shear Viscosity of the Blends	66
	3.5 Mechanical Properties	72
4.	**DISCUSSION**	89
	4.1 Thermal Analysis of Neat Polymers and Blends	89
	4.2 Polarized Optical Microscopy of the Blends	92
	4.3 Scanning Electron Microscopy of Fracture Surface	94
	4.4 Melt Rheology of the Blends	100
	4.6 Mechanical Properties of the Blends	103
5.	**CONCLUSIONS AND FUTURE WORK**	108

6. **BIBLIOGRAPHY** 110

7. **APPENDIX** 119

8. **VITA** 122

LIST OF FIGURES

Fig.		Page
1.1	Different possible mesophases and their interconversion paths	4
1.2	General structures of main chain and side chain LCPs	5
1.3	Three basic liquid crystalline structures	7
1.4	Chemical structures of commercial thermotropic polymers	8
1.5	Phase diagram for a mixture of EBBA and polystyrene	13
1.6	Phase diagram for PC/PHB-PET blends from cloud point determination at 2°C/min.	19
1.7	Polydomain representation of mesomorphic state and effect of flow	29
1.8	Schematic of rotational annular die and squeezing flow apparatus	30
3.1	DSC traces for polyarylate with different thermal histories	46
3.2	Glass transition temperature of polyarylate stored under different moisture conditions	48
3.3	DSC traces for Vectra A910 under different thermal histories	50
3.4	T_g of the polyarylate rich phase of PAr/Vectra blends	51
3.5	Microscope view of 90/10 blends (extrudates) from transmitted light and under cross polars	54
3.6	Microscope view of the blends (extrudates) using transmitted light and under cross polars	55
3.7	Microscope view of the blends (extrudates) using transmitted light and under bright field.	56
3.8	a) SEM fracture surface view of extrudates from 90/10 blends b) Melt drawn fibers from 90/10 blends (D.R. 30.6)	58
3.9	SEM images of the fracture surface of fibers melt drawn from the blends	60
3.10	SEM images of the fracture surface of fibers melt drawn from the blends	61

3.11 SEM images of fracture surface of fibers melt drawn from 90/10 blend. 62

3.12 SEM images of fracture surface of the fibers spun from different melt temperatures. 64

3.13 SEM images of fracture surface of the fibers obtained under different melt shear rates 65

3.14 Melt viscosities of the blends for capillary flow measured at 300°C .. 67

3.15 Melt viscosities of the blends for capillary flow measured at 300°C. .. 68

3.16 Melt viscosities of PAr/V blends for capillary flow under a steady shear 69

3.17 Melt viscosity of PAr/V blend (90/10) at different melt temperatures 70

3.18 Melt viscosity of PAr/V blend (90/10) at different melt temperatures 71

3.19 Determination of flow activation energy of PAr/V blend (90/10) using Arhenius type relation 73

3.20 Modulus of elasticity of PAr/V blend fibers of varying composition .. 74

3.21 Stress-at-break of PAr/V blend fibers with varying LCP compositions 75

3.22 Strain-at- break of PAr/V blend fibers of different LCP compositions 76

3.23 Modulus of elasticity of fibers spun under different draw ratios. 79

3.24 Stress-at-break of fibers spun under different draw ratios. 80

3.25 Strain-at-break of fibers spun at different melt draw ratios 81

3.26 Modulus of elasticity of fibers spun at different melt temperatures ... 82

3.27 Stress-at-break of fibers spun at different melt temperatures 83

3.28 Strain-at-break of fibers spun at different melt temperatures 84

3.29 Modulus of elasticity of fibers spun at different melt shear rates 85

3.30 Stress-at-break of fibers spun at different melt shear rates 86

3.31 Strain-at-break of fibers spun at different melt shear rates 87

3.32 Modulus of elasticity of fibers spun from pure LCP at varying melt D.R. ..... .88

4.1 Fraction of added LCP volume obtained as pulled out fibrils on the fracture surface of the blend fibers ..... .98

CHAPTER 1

INTRODUCTION

1.1 General Introduction

Thermoplastic polymers used in engineering applications have traditionally been blended with a variety of natural and synthetic filler materials with an aim to improve one or more of the end properties. Typical examples include elastomers to improve the impact strength, mineral fillers or glass fibers for high heat distortion temperatures, fluoropolymers to increase the lubricity of molded materials. These heterogeneous fillers are incorporated into the thermoplastic matrix using an appropriate compounding process to achieve the desired properties. Processing of heterogeneous blends containing the dispersed chopped fibers, mainly glass, has been the source of composite materials having exceptionally high modulus, strength and the dimensional stability that is often required in engineering applications.

It is, however, widely recognized that the processing and fabrication of such filled resins is beset with many problems. Glass fibers, being solid, present their extremely hard surfaces to the fine machined parts that are in relative motion, producing excessive wear and eventual damage of the machine. Product quality suffers because of the drift in the process due to contamination from the wearing parts and a change in the critical dimensions of the mold and dies. Additionally, an increase in the viscosity of heterogeneous blends necessitates an increase in pressure

resulting in flash and short shots. Increased temperatures to reduce the viscosity may sometimes causes the degradation of the resin affecting the product quality. For this and many other reasons, the compounding process is an expensive step requiring expenditure of high energy and the time required to impart it. These problems often put restrictions on the maximum allowable loadings of the solid filler.

Various attempts have been made in the past to incorporate a meltable reinforcement. Such materials would not cause a viscosity rise during processing. However, it would tend to solidify during the forming step to yield a reinforcing structure within the polymer matrix[1,2,3,4,5]. One of the earliest techniques employed with this objective involved either *insitu* crystallization from low molecular weight materials or an *insitu* polymerization in the solid state using trioxane and di- and tri-acetylene monomers. Then came the concept of molecular composites obtained by mixing flexible chain polymers in solution with lyotropic polymers having a high degree of chain stiffness. Poly(p-phenyleneterephthalamide), poly(parabenzamide) are two of the commercially available lyotropic polymers commonly used in this type of blends. However, the thermotropic polymers developed later also had high chain stiffness but with sufficient flexibility to show melting. Therefore these polymers lend themselves to be processed from the melt state. These polymers, collectively called liquid crystalline polymers, exhibited extremely low viscosity with a high tendency to chain alignment in a shear flow field.

1.2 Liquid Crystal Polymer Mesophases

Characteristic properties of low molar mass materials exhibiting mesophases have been studied and cited in the literature for over a hundred years now[6]. A conventional view of the liquid crystalline order is that it possesses many of the characterisitic mechanical properties of fluids yet it has sufficient degree of molecular order to diffract X-rays according to Bragg's law. Hence this texture is appropriately denoted as mesophase[7]. Properties of the blends of polymers with these low molecular weight mesophase materials have been widely studied and well understood in terms of their physical interactions and phase behavior. However, since the discovery of stiff chain polymers exhibiting anisotropic behavior in solution[8,9] and some in the melt state[10], a large amount of work has been carried out to study the structure and conditions of their formation. Their physical properties such as low melt viscosities and high degree of birefringence together with high temperature stability has enhanced their scope for potential material applications. Liquid crystalline order can be described in relation to two other possible mesophases by appropriate thermal changes as shown in Fig. 1.1[11]. However, depending upon the chemical structure and symmetry, one of the three phases is much more stable than the other two phases. Polymer mesophases are recognized as liquid crystalline in nature. Thermotropic polymers that exhibit liquid crystallinity in the melt state can be classified as having side chain or main chain mesogen groups. The general structure of these two different mesogen group types may be given as shown in Fig. 1.2[12]. Three different mesomorphic forms of liquid crystal order have been

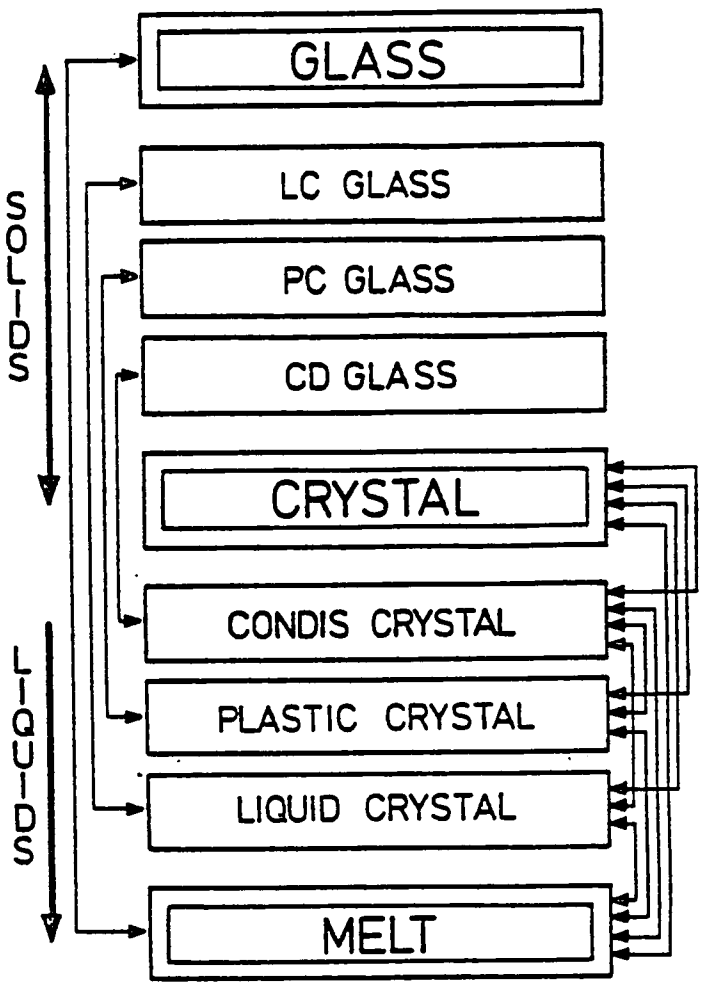

Fig. 1.1 : Different possible mesophases and their interconversion paths (Ref. 11).

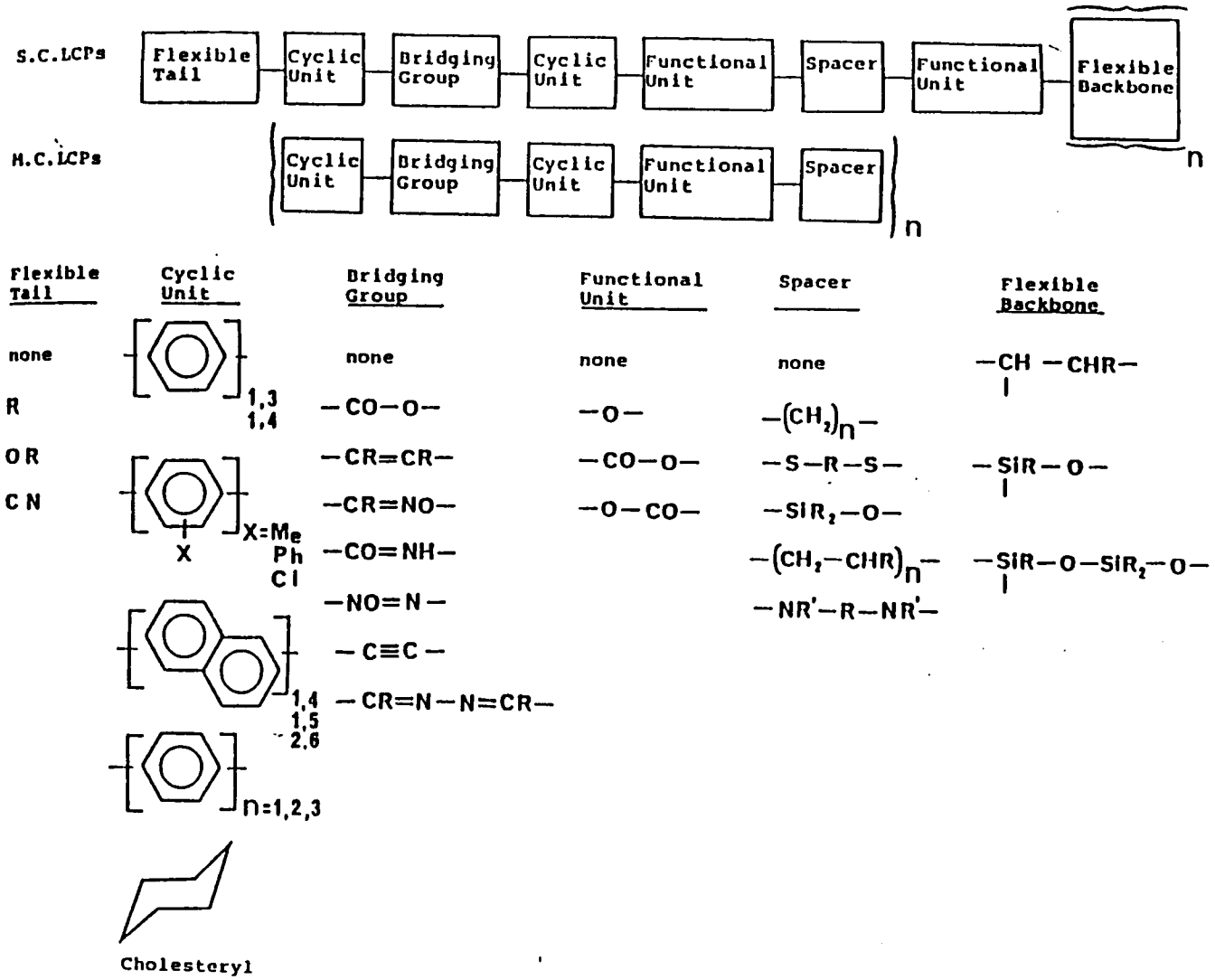

Fig. 1.2 : General structures of main chain (M.C.) and side (S.C.) chain LCPs (Ref. 12).

recognized in general. , i.e., cholesteric, smectic and nematic. A schematic of these different structures is reproduced in Fig. 1.3[13,14]. Physically the nematic phase may be described as an arrangement in which the center of gravity of the rigid chains is put at random with no long range positional order. However, the axes of rigid polymer chains are all oriented in a specific direction within a small volume element. The cholesteric phase is similar to the nematic phase except that the direction of the long axes of the molecules changes continuously producing a twist about an axis perpendicular to the long axes. In the smectic modification the center of gravity of the long molecules is arranged in equidistant planes with a certain orientation of the long axes with respect to the layer normal. There may be a two dimensional short or long range order within each of these planes. Within each of these different mesophases there can be textural changes due to different macroscopic orientation of the molecules. These changes can be brought about by mechanical, thermal, electric and magnetic forces. These textural changes are reversible and often directly relate to the molecular structure of the material[15]. It is the nematic phase of the main chain liquid crystalline polymers which has been recognized as having unique rheological properties combined with inherently high molecular orientation and high temperature stability. The chemical structure of some of the commercially available thermotropic LC polymers is shown in Fig. 1.4. The applications of these polymers make use of some of the characterisitic properties attributed to the liquid crystalline order.

Copolymers of PET and PHB have been investigated by far the most for their characteristic properties[16,17]. It is believed that the liquid crystalline order in these

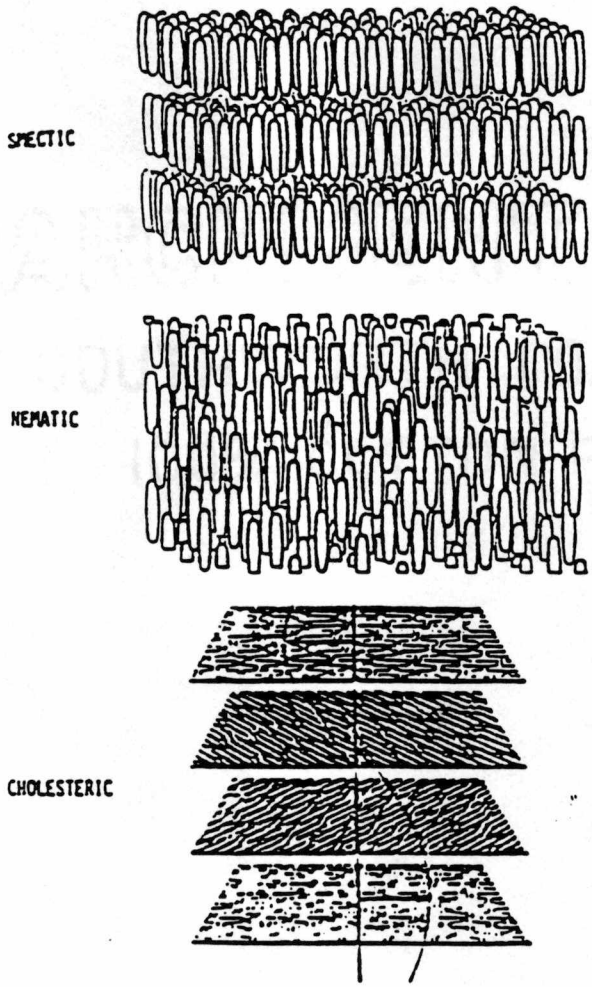

Fig. 1.3 : Three basic liquid crystalline structures (Ref. 13 & 14).

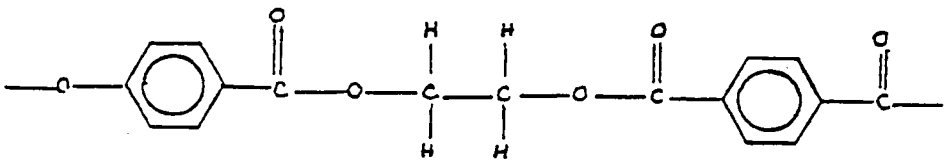

PHB-PET (Eastman Kodak)

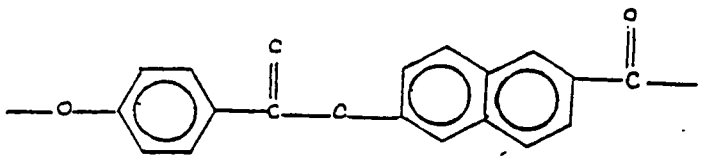

PHB-HNA (Celanese)

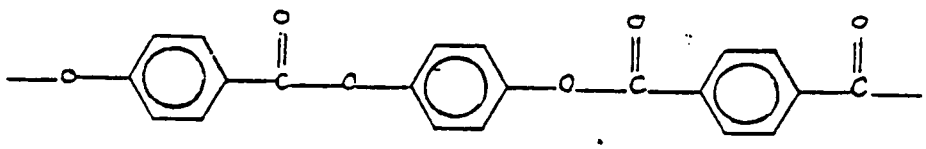

PHB-BPT

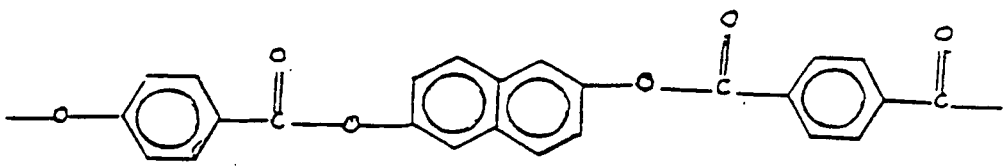

PHB-NDT

Fig. 1.4 : Chemical structures of some commercial thermotropic polymers.

copolymers arise from a unique combination of flexible conformation due to PET and a rigid rod like conformation of PHB. Development of liquid crystallinity is accompanied by an anomolously reduced viscosity of the melt combined with a high degree of anisotropy during their melt processing completely in contrast with the conventional flexible chain polymers. The chain structure of these materials described as completely random[18] initially, has now been shown to be some what non-random[19] and with a heterogeneous phase morphology[20]. The rheological properties of these thermotropic melts have been analyzed by Wissbrun[21] and he showed that they exhibit very long relaxation times and appeared to be highly elastic. Negligible die swell, first reported for lyotropic systems[22], were initially assigned to finite yield stresses especially at low temperatures. Negative normal stresses were reported for some lyotropic systems[23] and for some thermotropic copolymers at some temperatures. At high temperatures, however, these values reportedly become positive, and contribute to a die swell value of greater than 1. Absence of corresponding rise in the viscosity due to generation of isotropic regions at elevated temperatures have made the authors conclude that a combination of both the finite yield stresses and negative normal stresses are in fact contributing to the observed negligible die swell. Similar rheological and phase characteristics were reported for the anisotropic melts from other thermotropic polymers, such as copolyester based on PHB and HNA and another based on HBA/HNA/HQ/ET[24]. Phase and thermodynamic studies conducted on a mixture of liquid crystalline polymer with flexible chain polymer has indicated its potential in improving the processibility of

some of the high temperature flexible chain polymers by having a lower viscosity for the blend. Due to strong anisotropy of the LC polymer melts under low stresses, these polymer blends have been viewed as a potential method of getting some type of self reinforced material, formed during processing. One of the earliest studies on blending of liquid crystalline polymers with thermoplastic polymers appears to have been done by Cogswell and coworkers[25]. They examined a range of thermoplastic polymers blended with a series of structurally different thermotropic and lyotropic liquid crystalline polymers for their effectiveness in reducing the viscosity of the neat resin without significantly affecting the mechanical properties of the products. A large reduction in viscosity has been claimed for various different resins at the shear rates encountered during conventional melt processing. This study also revealed that the interaction between the isotropic and anisotropic polymer seems to influence the rheological response of the blends.

1.3 Literature Review

Mixing liquid crystalline materials of low molecular weight with flexible chain polymers has been investigated as far back as 1977 by Gebhard et al.[26]. Ever since then, most of the studies involving blends of low molecular weight LC's and a polymer have concentrated on their thermodynamics and phase behavior aspects in line with their potential as plasticizer for thermoplastic materials. Huh et al.[27] used thermotropic LC's, EBBA and terephthal-bis-4-n-butyaniline (TBBA), as platicizers for polystyrene. Plasticization was evidenced through a decrease in the

glass transition temperature and melt viscosity with increasing LC content up to the solubility limits of LC in the polymer. Low molecular weight liquid crystal molecules have been used to reduce the melt viscosities of polyolefins and polystyrenes by as much as 25 to 30 percent below the melt viscosities of the neat polymers[28]. Polymer dispersed liquid crystal material (PDLC) have found widespread applications in systems based on electro optical displays[29,30,31]. These materials essentially consist of microdroplets of liquid crystals distributed in a polymer matrix using various techniques[32]. The electro-optical properties of these two phase materials results from the alignment of the optical axis of the microdroplet LC phase under an applied electric field. Initial mismatch of the refractive index between the two materials is due to random orientation of the liquid crystal director axes within the droplet. However, on application of electric field the LC director axis lie preferential parallel to the polymer wall with a bipolar-like configuration. This aligned LC droplet then has a refractive index equal to the ordinary refractive index of the liquid crystal, which is essentially equal to that of the polymer binder. The electro-optical properties of these materials have been shown to be strongly dependent on the LC phase morphology. Morphology and the resulting properties can be controlled by varying the polymerization temperature and rate of cooling. These blend systems are formed as two phase materials from a one phase melt region by nucleation and growth of the dissolved LCP quite unlike the situations seen with polymer-polymer blends.

Membrane applications have also been derived from some monomeric

LC/polymer blends. The morphology of these blends consists of a three dimensional network of polymer fibrils in an LC continuous phase. The unique transport properties of these blends is because of the diffusion through the LC phase trapped between the polymer fibrils. The permeability of gases through these membranes is enhanced due to solubility in addition to increased diffusion above the crystal-nematic transition temperature. Kajiyama et al.[33,34] have described the structure-permeation property relationship for the membranes made from blends of EBBA with PVC and PC.

Flory and coworkers[35] have carried out a theoretical analysis of the thermodynamics of rod like molecules and polymers of varying flexibilities. They derived the expressions for phase equilibria in a mixture of low molar mass mesogens and polymers of varying flexibilities. Ballauf[36] modified the simple lattice theory for the mixture of nematic LC's and flexible polymers to include the effect of isotropic interactions between the components. This theory successfully explains the main features of the phase diagram for the mixture of a monomeric LC, EBBA and polystyrene. The cooling diagrams at varying compositions of polystyrene may be reproduced as shown in Fig. 1.5. Cooling of a low concentration polymer mixture leads to a two phase system consisting of a nematic and isotropic phase. This on further cooling through the triple point is shown to generate an equilibrium mixture of an another nematic phase and a polymer rich isotropic phase. Similarly, cooling of mixtures with higher polymer concentration led to phase separation into two isotropic phases which changes finally to a coexisting polymer rich isotropic phase

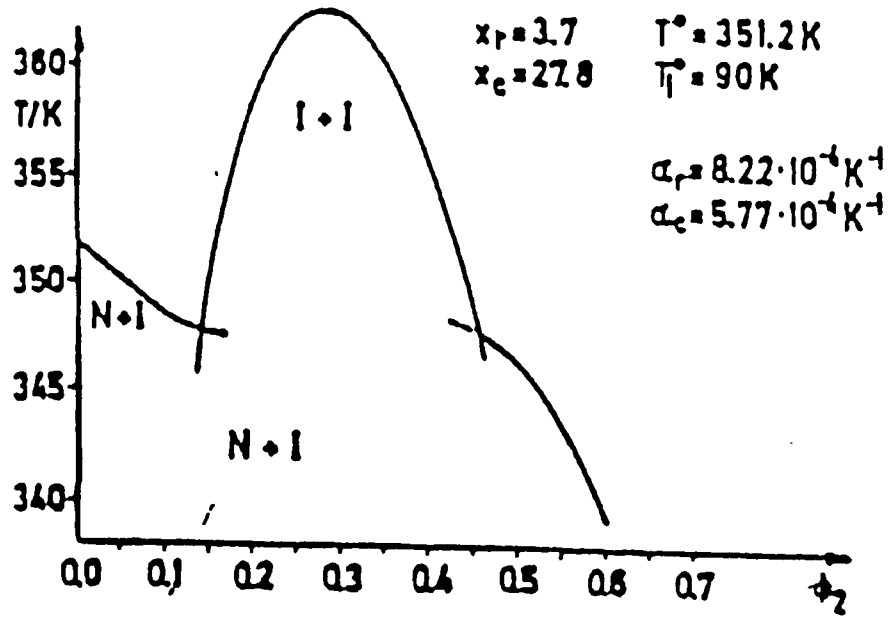

Fig. 1.5 : Phase diagram for a mixture of EBBA and PS. T_I - Temperature for isotropic interaction, χ_2 - Segment fraction of the dissolved polymer (Ref. 36).

and a polymer poor nematic phase. It has been observed that increasing the molar mass of the polymer in such systems tends to increase the width of the miscibility gap[37]. This also leads to an hysteresis in nematic-isotropic transition point between heating and cooling scans. In some instances[38] a homogeneous nematic phase was not observed when the M_W of the polymer was greater than 10,000. Viscosity coefficient measurement of solutions of polystyrene in EBBA, done by Matinoty et al.[39] using ultrasonic impedometric techniques, showed a considerable increase in the LC viscosity upon addition of small amounts of PS. This study also showed that an increase of solution viscosity with decreasing temperature was found to be more rapid than expected from the classical Arhenius dependence which is necessary to describe the solution viscosity of PS in an isotropic solvent.

The interest in the LC polymer-isotropic polymer systems grew rapidly following the recognition that they exhibit low melt viscosities combined with high relaxation times of the mesomorphic phases developed from highly oriented rigid chain conformation. During the past decade a substantial research effort, both industrial and academic , has been directed towards development of suitable thermotropic materials that can be used as effective mechanical reinforcement. Easy deformation of the mechanically dispersed LCP phases under normal shearing encountered during processing can generate anisotropic fillers upon cooling. Processing of these blends from a single phase system to a two phase reinforced solid opens up enormous possibilities for developing cost effective high performance materials. A large number of investigations have been carried out to understand the

interaction between the LCP phase and the isotropic polymer. These studies can be broadly classified into the following areas : 1) Thermodynamics and phase behavior, 2) Rheology and processing and 3) Mechanical properties and morphology.

1.3.1 Thermodynamics and Phase Behavior

Phase behavior of LC polymer/isotropic polymer blends have largely been studied from the point of view of crystallization of the matrix polymer or the LCP in the case of blends of two different types of LCPs. Thermodynamic miscibility of a large number of systems has been investigated from the glass transition analysis, optical and electron microscopy techniques. A theoretical analysis has been presented by Dowell[40] in which she has attempted to describe a mixture of non rigid crystalline solute with a main chain LCP. In this study using a localized mean field, simple cubic lattice theory she has predicted a mixture of two phases in which the anisotropic and isotropic phases coexist. It is also seen that there is a disruption of the orientational order of the LCP in the presence of flexible solute. This also results in a lowering of Nematic-Isotropic transition point.

1.3.1.1 Crystallization Effects

The rate of crystallization and the degree of crystallinity of flexible chain polymers is affected by the addition of an LCP. Joseph et al.[41,42], based on thermal studies, have observed an increase in rate of crystallization and overall crystallinity of PET in a blend with an LCP copolyester of PET and PHB(40 PET/

60 PHB). They attribute this increase in the crystallization rate due to nucleating effects of the added LCP. A similar observation has been made by Misra and coworkers[43,44] when they examined the blends of PET with two different LCP copolyesters, one is a copolymer of HNA and PHB and other a copolymer of PET and PHB. Takayanagi et al.[45] have found a similar nucleating effect of LCP's based on wholly aromatic polyamides when their blends with aliphatic polyamides and polyesters were crystallized from a concentrated solution in a common solvent. Paci and coworkers[46] have investigated the blends of PBT with a LC polymer poly(biphenyl-4,4'-ylene sebacate) prepared by solution blending. Using quantitative differential scanning calorimetry they showed that addition of only 5% LCP increased the degree of crystallinity for PBT significantly. This trend has been shown to reverse for LCP content of beyond 40% w/w possibly due to the presence of a structure that favors the cold crystallization of PBT.

1.3.1.2 Miscibility and Phase Behavior

Miscibility of liquid crystalline thermotropic polymers with different flexible chain polymers has been mainly studied using DSC, scanning electron microscopy and X-ray diffraction measurements[47,48,49,50]. Zhuang et al.[51] investigated blends of a liquid crystalline copolyester of PET and PHB having varying mole ratios of PET/PHB with polystyrene(PS), polycarbonate(PC), and PET homopolymer. A general immiscibility has been shown in the case of PS, though PC and PET show evidence of partial miscibility on the basis of DSC transition temperature data of

respective blends. Nobile et al.[52] supported these findings by proving immiscibility of 40 PET/60 PHB with PC. Partially miscible phases in the blends of PC is shown to be in the region of PET rich phase of the biphasic copolyester of PET/PHB[53]. Kimura and Porter[54] on the basis of a DSC analysis of the blends of PBT showed that the PET rich phase of the copolyester of PET/PHB is miscible with the PBT, and not the PHB rich phase. An attempt to anneal the blends of PC with the copolyester of PET/PHB has been shown to cause transesterification leading to miscible blend showing a single Tg in the DSC analysis[55]. Annealing of blends of PET with this copolyester, however, did not change the Tg of either material. It did, however, reduce the melting temperature of PET in the blend by as much as 42°C.

Transesterification reactions between the LC copolyester and the isotropic polyester is shown to affect the miscibility of the blends made from them. It was found that the blend of PET and a copolyester of PHB , bisphenol-A and terephthalic acid exhibited one phase owing to a ester exchange reaction[56]. It is also shown to be the cause of miscibility between PBT and a liquid crystalline poly(biphenyl-4,4'xylene sebacate) (PB8) in its isotropic state[46]. This blend, however, phase separated upon cooling with increased miscibility between the cold crystallized PBT and the anisotropic LC phase.

Studies by Luise[57] reveal that the miscibility of the melt blends of thermotropic polyester with isotropic polyesters is governed primarily by polymer asymmetry. Blends of crystalline PBT with a thermotropic polymer poly(decamethylene 4,4'-terephthaloyl dioxy dibenzoate)(HTH10) were studied using

DSC[58,59]. Of the double melting endotherm showed by these blends the temperature of the higher melting peak was found independent of the composition. The temperature of lower melting peak however has been shown to decrease with increasing HTH10 content indicating a plasticization effect due to HTH10. Miscibility in the amorphous phase of the two polymers has been concluded on the basis of observation of single Tg intermediate between the two neat polymers after quenching from the melt state. A decrease in the rate of crystallization of PBT has been observed due to a possible interruption in the primary heterogeneous nucleation in the presence of HTH10.

Completely miscible and optically transparent films can be generated from solvent casting of thermotropic polymer and flexible chain polymer. Films of blends of PET and PC with thermotropic copolyester of 40 PET/60 PHB, prepared by solvent casting have been shown to be homogeneous and optically clear[60,61]. Annealing the films at high temperatures, which are characteristic of a lower critical solution temperature, is shown to cause a phase separation in to anisotropic and an isotropic phase via a spinodal decomposition mechanism (Fig. 1.6). A similar phase separation was observed by Chuah et al.[62] in the films made from molecular composites of poly(p-phenylene benzobisthiazole) (PBZT), and Nylon 66.

Seurin, et al.[63] constructed the phase diagram of a mixture of hydroxypropyl cellulose(HPC) and a flexible polymer polyethylene glycol(PEG). Using polarized microscopy they were able to assess the intermolecular interactions decreasing with increasing molecular weight of PEG before eventual phase separation sets in.

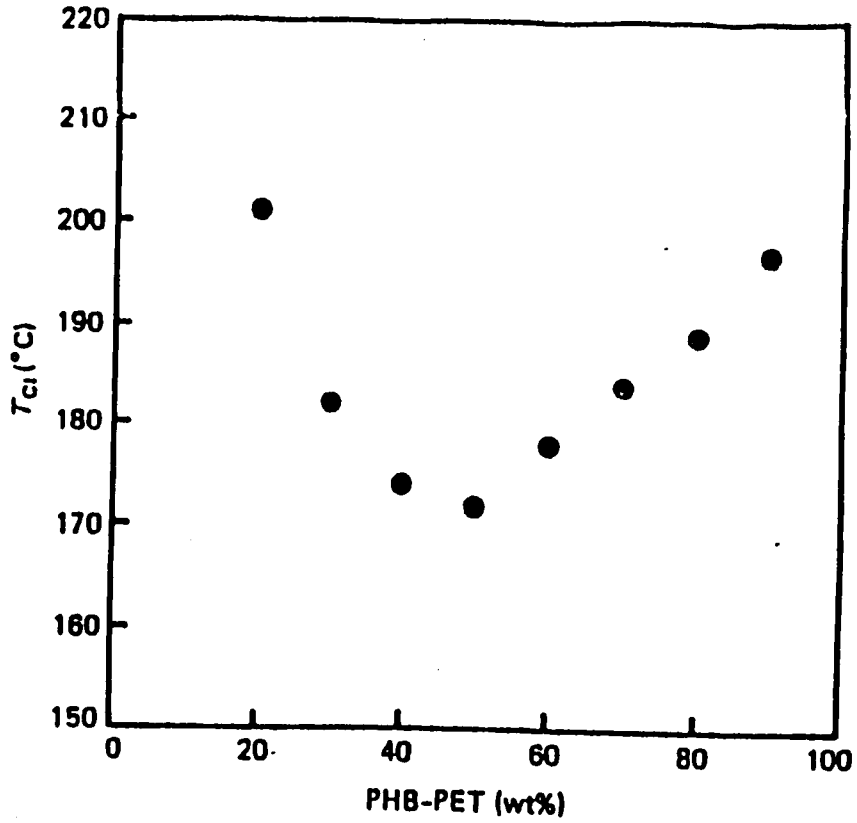

Fig. 1.6 : Phase diagram of PC/PHB-PET blends from cloud point determination at 2°C/min (Ref. 60)

Increasing the molar mass of HPC simply shifted the mesophase-isotropic transition to higher temperatures. Similar phase diagrams have been drawn using polarized microscopy for mixtures of cholesteric and nematic thermotropic liquid crystal materials[64].

Partial compatibility of PC in the blends with the thermotropic copolyester based on HBA and HNA has been reported on the basis of thermal measurements of T_g[65]. DSC thermograms obtained for the blends of PC and an LCP based on 52HBA/28HNA/10TA/10HQ indicate about 2% miscibilty in the PC matrix[66]. Blends of PC with a LCP based on fully aromatic copolyester containing flexible polymethylene chains between the mesogens has been shown to improve the miscibility of the components. This is indicated by a shift in the T_g of the matrix polymer in the DSC scans obtained for various compositions and using LCPs of varying flexible chain lengths[67]. The blends of PPO[68] and PEEK[69] with LCP based on HBA/HNA, however, show immiscible phases largely on the basis of DSC analysis coupled with DMTA measurements.

1.3.2 Rheology and Processing

Thermotropic liquid crystalline polymers have been recognized as potential processing aid materials when used as blends with many of the existing thermoplastic polymers. Investigation with a range of different polymers as matrix materials has shown that the extensional flow at the entrance of the capillary and during shear while in the capillary causes preferential orientation of the mesophase domains in the

direction of the flow[70,71,72]. Relatively much lower viscosity of these mesophase domains cause the matrix phase around them to glide past easily, often deforming the embedded domains, thus lubricating the polymer melt. These physical interactions lead to a lowering of the melt viscosity of the blend system. These investigations have been largely done using capillary rheometers but some investigators used cone and plate or parallel plate rheometers to emphasize the low shear rate viscosities of such systems.

The primary criterion for the processing of such melt blends has been setup from an exhaustive work carried out by Cogswell et al.[25,73,74]. This work produced dynamic viscosity data for a large number of polymers measured at different shear rates. On comparison of data for neat materials with those of the blends using various different LCP's, it was concluded that the temperature range used for conventional melt processing of the thermoplastic materials should overlap with the temperature range in which the LCP forms an anisotropic melt. This study revealed some data on viscosity of the blends of thermotropic polymers with polypropylene, LD polyethylene, polycarbonate, PMMA, nylon 66, PET, PPO/PS blend at uniform level of loading (10% w/w). They observed a decrease in viscosity at all shear rates with maximum effect obtained at 1000 sec^{-1}. Effective reduction in the melt viscosities were reported at 3% LCP compositions for blends of polyethersulfone. This study also showed that these blends could be processed at significantly lower temperatures compared to the neat polymer with improved surface finish and retention of useful mechanical strength. They have also reported varying levels of

viscosity reduction using structurally different thermotropic polymers. Apparently the interaction between the isotropic and anisotropic polymer seems to influence the rheological response of the blends. This phenomenon is particularly apparent in one set of Cogswell's data where the same LC polymer at 10% loading lowers the viscosity of nylon 66 system by a factor of sixteen while actually slightly raising the viscosity of polycarbonate material with similar loadings at the same shear rate of 100 sec^{-1} and a temperature of 285 ° C. This observation though significant has not been explained by the author in this patent.

A large number of investigations of melt rheology has been done on blends containing copolyester of 40 PET/60 PHB. Blizard and Baird[75] reported their studies on blends of this LCP with PC and Nylon 66. Their results obtained from measurements on cone and plate rheometer and capillary rheometer indicate significant reduction in the viscosity of the blends at 10% LCP compositions for nylon 66. In the case of blends of polycarbonate the viscosities are shown to decrease with LCP compositions continuously until a level of 70%LCP as indicated both by dynamic oscillatory and steady shear data obtained at 10 and 100 sec^{-1}. Similar results have been reported by Zhuang et al.[51], while they were studying the blends of this LCP with PS, PC, and PET. Complex viscosities measured at low shear rates of below 0.3 sec^{-1}, however, have been shown to increase with the increasing LCP content for the blends of 40 PET/60 PHB and PC[52]. At high shear rates the complex viscosities decreased with the increasing LCP concentration as had been reported earlier by Acierno et al.[76] for the same blend system. Viscoelastic behavior of

blends of chlorinated PVC with this copolyester were studied by Lee[77]. These blends showed a decrease in the extrudate swell and an increase in the spiral mold flow at low LCP concentrations. Lorenzo et al.[78] investigated the viscoelastic properties of blends of this copolyester with a styrene-butadiene copolymer. They observed that when the extrusion was done below the mesophase transition temperature of the LCP, complex viscosity measured was independent of the LCP concentration. However, when the extrusion was done above the mesophase transition of LCP both Melt Flow Index(MFI) and complex viscosity measured exhibited a maximum and minimum respectively at 10% LCP concentration.

Another widely studied thermotropic liquid crystalline polymer consists of a copolyester of 6-hydroxy-2-naphthoic acid (HNA) and PHB[79,80]. Several grades of this copolyester with varying ratios of comonomers have been commercialized by Hoechst-Celanese Corp. under the trade name of Vectra^{R} and by Imperial Chemical Industries, Ltd. under the trade name of Vitrex^{R}. Some of these polymer composition may also incorporate ester linkage derived from terephthalic acid (TA) and hydroquinone (HQ).

Large shear thinning behavior of the polymer blends incorporating HBA/HNA copolyester have been reported by various studies. Siegmann et al.[81] measured the dynamic shear viscosities of the blends of this copolyester with an amorphous polyamide. Dynamic and steady shear viscosities of the blends were much lower than that of the neat thermoplastic polymer. A large decrease in the viscosities of the polyamide/LCP blend having as low as 5% w/w LCP was reported.

They observed a large non-Newtonian behavior of the melts having different LCP compositions in the blend. Blends of this copolyester with poly(ether amide)[82] and with polyether sulfone (PES)[83,84] have been reported with large reduction in viscosities as compared to the neat resins. About a four fold drop in the viscosity of PES melt was observed with the addition of only 2 weight percent of LCP. In the case of blends of PBT with LC copolyester 40PET/60PHB, the shear viscosities starts to decrease only at an LCP content of 40% or more[85]. The shape of the dynamic viscosity vs. shear rate were reported as Newtonian up to a shear rate of 16 sec^{-1} and they resembled that of the pure PES melts up to 20 weight percent of LCP. Viscosity curves of the blends, however, resembled shear thinning characteristic of pure LCP after 50 weight percent of LCP. Chung[86,87] analyzed the rheology of blends of HBA/HNA copolyesters with nylon 12. He has observed a minimum in viscosity of the blends at a concentration of 10% and a maximum at 20% w/w of LCP. The author believed that below 10% of LCP in the blend, LCP domains were well dispersed in the nylon 12 matrix and acted as lubricant , thereby reducing viscosity. At 20% LCP, it is thought to result in an interlocking morphology with a sharp increase in the viscosity.

Kohli, et al.[66] in their study of blends of PC with a lower melting copolyester based on HNA/HBA/TA/HQ found reductions in viscosities to an extent of 68% below that of neat resin with only 5% of LCP. They observed that the general shape of the viscosity was dominated by the continuous phase of the blend when there is a monotonic decrease in the viscosity with the LCP content over the entire

concentration range.

Several investigations of the rheology of blends of polycarbonate with HBA/HNA copolyester reveal melt viscosities that are similar to the neat PC with more shear thinning that increased with the LCP composition[65]. Cross over points in the viscosity vs shear rate curves of PC and HBA/HNA copolyester melts have been associated with the maximum fibrillation of the dispersed phase[88]. Time dependence behavior of the these blends by solid state relaxation measurements reveal an increased relaxation modulus of the blends as compared to that of the neat resin.

A continuous decrease in the shear viscosity is generally observed with many of these thermoplastic/LCP blends over the entire range of composition[52,65]. Weiss et al.[89], however, reported that the addition of thermotropic LCP based on 4,4'-dihydroxy,α,α'-dimethylbenzalazine to PS raised both the steady shear and dynamic viscosities at low shear rate range ($< 1\ s^{-1}$) or frequencies. This increase in viscosity has been attributed to the tumbling and rotation of the phase separated LCP domains. At high shear rates the viscosities are found to decrease as usual. This has been found more often the case with other blend systems as well when the data at low shear rates were collected using a cone and plate viscometer. The increase in the viscosity under these conditions was consistent with the theoretical predictions of the simple shear flow of two phase liquids. For high shear rate data obtained using capillary rheometers, the simple shear flow in the capillary is preceded by an extensional flow in the entrance region. This extensional flow can deform and align

the LCP domains in the flow direction. This deformed melt morphology is largely responsible for the decrease in the blend viscosity. In the blends of PPO and an LCP based on HBA/HNA copolyester shear dependence of the viscosity is shown to be intermediate between those of the component polymers for the entire range of composition[68].

It is generally observed that the dynamic shear viscosities of the isotropic polymer-LCP blends vary in a complex manner with the composition of LCP and with the shear rates. Blends of PPS with the LCP based on copolyester of HBA/HNA, exhibit shear viscosities that tend to increase with LCP concentration up to 25%, showing values greater than that of pure LCP melts[90]. At low concentrations of LCP, however, it leads to intermediate values of viscosities. At high concentrations, they observed two maximas in the viscosity vs composition curves with each centered around 25% and 85% LCP in the blend. Similar observations have also been made on PEEK/LCP blends[69,91] where a high viscosity LCP was blended with a low viscosity thermoplastic polymer.

The dimensional stability of some blends of liquid crystalline polymers with thermoplastic resins was shown to improve greatly over that of the neat resins. Two different melt processible LCP materials were prepared and examined by Apicella et al.[92] for their effect in improving the shrinkage after blending with polystyrene resin. On the basis of measurement of recoil kinetics of the blend films prepared by extrusion and hot drawing, they were able to prove large reduction in shrinkage of unfilled polystyrene at LCP levels ranging from 4 to 5 weight percent. They suggest

that the non-compatible LCP fibrils put a constraint on the surrounding polymer allowing them to stress relax and not creep when exposed to high temperatures. Similar studies carried out on blends of 40 PHB/60 PET with PBT yield large reduction in shrinkage measured with time with 5% level of LCP in the blend and the values actually closely approached that of pure LCP[93]. They attribute the shrinkage behavior to the high elongational viscosity of the blends as compared to PBT. Morphological, the presence of LCP polydomains in the blend make the flow difficult at low shear rates encountered in shrinkage experiments.

1.3.3 Mechanical Properties and Morphology

Thermotropic polymers are produced by careful modification of a rigid chain homopolymer by copolymerization with controlled amounts of flexible moieties, bent and crankshaft monomers and the incorporation of bulky side groups. The quiescent mesomorphic state of these thermotropic polymers can be pictured as an aggregate of domains, each characterized by a preferred chain orientation indicated by the director[94,95,96]. In the presence of a flow field, the domain texture (size and orientation) may change and under ideal conditions may transform into a monodomain, in which all the molecules assume the same preferred orientation (Fig. 1.7). The intrinsic chain stiffness of the LCP's is consequently reflected in excellent mechanical strength and stiffness in the direction of orientation. Due to a weak interchain interaction, the transverse and shear mechanical properties of highly oriented LCP's are low, limiting the potential of thermotropic polymers as high

performance thermoplastics. Several special processing technologies have been proposed for the production of morphologies with reduced anisotropy. These are generally based on a combination of different flow fields and the specific examples include rotational compression molding and rotational extrusion[97,98] (Fig. 1.8). The incorporation of anisotropic fillers has been found to favor biaxial balancing of properties without a large influence on the LCP orientability and melt viscosity[99]. Mechanical properties of the neat thermotrotropic polymers based on copolymer of HBA with various different monomers are summarized in the Table 1.1. Processing techniques employed for producing these LCP materials influence their morphology and the resulting mechanical performance to a great extent[100].

Low shear stresses of the LCP melts in producing a facial chain orientation in the direction of shear can be visualized to impart high mechanical properties to conventinal thermoplastics when their blends are processed under anisotropic forces[101,102]. An indication of this possibility of reinforcing thermoplastics was given by Cogswell during the course of his investigation of the processibility of such blends. A comprehensive study on the mechanical properties and morphological examination of this type of blend using commercially produced LC polymers was given by Kiss[103]. They observed extremely fine fibrillar morphology of the dispersed LCP with a high degree of orientation, concentrated mostly towards the center for the extruded strands processed at different shear rates and with a finite melt draw ratio. The fracture surface of injection molded tensile bars on the other hand shows a gnarled appearance of the reinforcing LCP fibrils with a range of

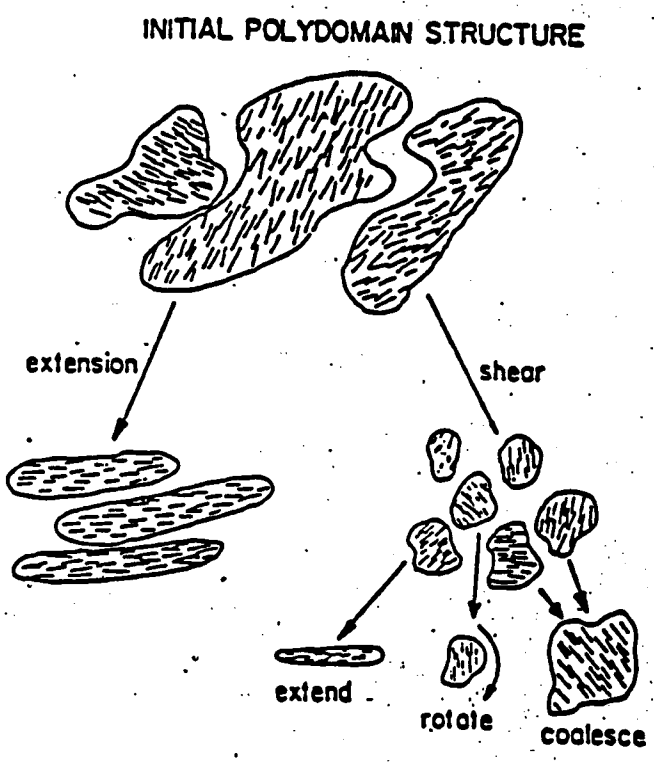

Fig. 1.7 : Polydomain representation of the mesomorphic state and the effect of flow (Ref. 95).

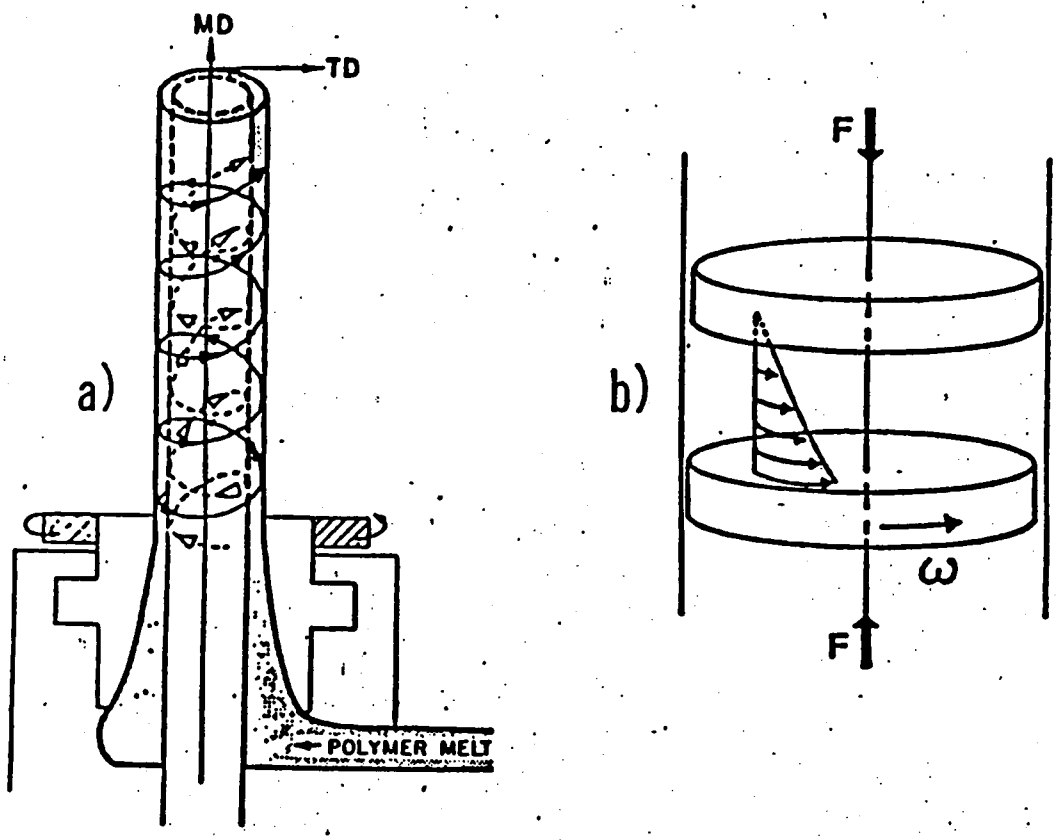

Fig. 1.8 : Schematic of a) the Rotational Annular Die (Ref. 98) and b) the Squeezing Flow Apparatus (Ref. 97).

Table 1.1 : **Typical properties of Poly(p-hydroxy benzoic acid) (HBA) and Liquid crystalline copolyesters of HBA.**

	HBA[a] (CS)	HBA/BPT[a] 2/1 (IM)	HBA/NDA/TPA[b] (60/20/20) (IM)	HBA/PET[c] (60/40)	HBA/HNA[d] (58/42) (IM)
Modulus (GPa)			18		10–40
Streng. (MPa)			150–200		140–240
Elong. (%)			1.5		1.2–6.9
Flex Mod.,GPa	6.9	4.8 1.6*	15 (IM) 5–35 (E)	12.4	10–35
Flex Str,GPa	7.4	117 27.5*	180 (IM) 50–700 (E)	232	150–300
Flex. Elong(%)				20	1.6–7.0
Notched Izod (J/m)				416	53–530
Unotched Izod (J/m)				1476	
HDT (°C)				64	180–240

(CS) Compression sintered, (IM) Injection molded, (E) Extruded

(a) J. Economy, *J. Macromol. Sci., (Chem.)*, A21, 1705 (1984).
(b) H. Thaper and M. Bevis, *J. Mater. Sci., Letters*, 2, 733 (1983).
(c) Y. Takeuchi, Y. Shuto and Yamamoto, *Polymer*, 29, 605 (1988).
(d) Celanese, VECTRA, High Performance Resins, *Mater. Bull.* Publ. No. 106-A.

diameters from 0.1 μm to as high as 5 μm. Mechanical properties such as tensile modulus and tensile strength are improved to different levels depending on the thermoplastic polymer (see Table 1 in appendix A). In some cases, there is a decrease in tensile strength due to apparent lack of reinforcement of the matrix at particularly high strains. In all the blends analyzed in this study there is, however, a drastic drop in the breaking elongations as compared to the neat materials. High shear rates of the extruded strands is shown to improve the mechanical properties for the case of PES blends.

In many ways, properties and microstructure generated in the blends of rod like polymers with the flexible chain amorphous polymers can be compared with blends containing thermotropic LCP. In the blends of ABPBI, an amorphous polymer, with PPBT, it was found that high content of PPBT made it difficult to control the morphology and failed to improve the orientation of the domains[104]. This and other studies[105,106] on blends of flexible amorphous polymers with a range of rod like polymers containing heterocyclic rings showed that the modulus of the cast films increased upon stretching when the rod like polymer is present as a minor component. Takayanagi et al.[52,45,107] studied blends of wholly aromatic polyamides such as PPTA and PBA with aliphatic nylons, PVC, NBR, and ABS. Initial modulii and the yield stress of the blends have been found to increase with the content of the rigid aromatic polyamide dispersed in the flexible polyamide[108]. Improvements in ultimate elongation were, however, achieved by the use of blends of block copolymers of a wholly aromatic polyamide and a aliphatic polyamide.

Outstanding reinforcement at a concentration less than 5% of the rigid component was achieved. This was attributed to the formation of a microfibrillar network. The network was characterized as anisotropic and a quasi three dimensional lattice model was proposed by Takyanagi[109] to explain the anisotropy.

Investigations of the phase structure of LCP-isotropic polymer blends recognize that the size, shape, and distribution of the LCP phase depended on many factors such as composition, processing conditions, viscosity ratio of the component polymers, and the rheological nature of the matrix polymer. The widely used technique to study the dispersed phase morphology of these immiscible LCP domains has been scanning electron microscopy (SEM). Some studies have, however, made use of XRD and SAXS[80,53,110,111] to find the degree of order of LCP phase in the blend. Injection molded and extruded blends of PC and HBA/HNA copolyester containing greater than 25 % by weight of LCP showed spherical LCP domains dispersed in the PC matrix[90]. But the blends with less than 10% LCP had a fibrillar LCP morphology. A similar observation has been made during a study on blends of PBT and a liquid crystalline polyester, decamethylene 4,4'-terephthaloyldioxy dibenzoate, obtained by quenching from melt[59]. In this case, however, up to 50 % by weight of LCP oriented fibrillar structures protruding up from the fracture surface were observed. Above 50 % composition, however, the morphology was homogeneous, and no visible fibrillar features of LCP domains were obtained. Mechanical properties of the blends containing LCP were seen to vary with the LCP content for different systems depending upon the thermorheological and viscoelastic

nature of the LCP. In some cases chemical interaction between the dispersed LCP and the matrix polymer improve the adhesion between the two phases such that even low aspect ratio fibrils contribute significantly to the reinforcement of the matrix[103]. PET blended with copolyester of HBA/HNA did not improve the modulus until 80% level of LCP in the blend[80]. But the copolyester based on HBA/PET when blended with PET homopolymer did produce improvement in the initial modulus and tenacity of the resulting fibers with the effect increasing with increased LCP content[60]. Elongation-at-break of the blend fibers were, however, found to decrease with the LCP content and the mode of failure changed from ductile to brittle. Isotropic interaction from a long flexible spacer of LCP has been shown to improve the mechanical properties of the blends[67]. A large increase in the elongation-at-break has been reported for the blends of PC and LCP with long flexible spacers. Blending of LC polyester based on HBA/HNA with an amorphous polyamide improved the mechanical properties, which increased with the increasing LCP content[81]. Similar improvements in tensile modulus and tensile strength of compression molded films, extrudates and melt spun filaments have been reported for the blends of PET, PC and PS with copolyester based on 40 PET/60 PHB, especially at low compositions of LCP[51].

High extrusion temperatures tend to promote spherical shape of the dispersed LCP phase[52,76]. This can be attributed to reduced differences in viscosity between the LCP and the matrix at high temperatures. A decrease in the tensile modulus with extrusion temperature has been correlated with a corresponding increase in the fibril

diameters and a decrease in the number of fibrils[80]. For the blends of 40PET/60PHB with PC, it was observed that the tensile modulus increased with the draw ratio for the fibers drawn at 220°C, but had a very little effect on the fibers drawn at 260°C[52]. Microfibrillar structures oriented in the direction of flow are formed due to the deformation of the dispersed LCP when the blends containing them are extruded and drawn in the melt state[112,113]. Increased orientation of the LCP microfibrils upon drawing can greatly improve the mechanical properties of the resulting fibers or films. Weiss et al.[114] in their study of blends of PC with a copolyester of HNA/PHB/HQ/TA found that an increase in the draw ratio of the extruded fibers from 1 to 1000 leads to a six fold increase in the modulus with 20% LCP in the blend. Increased molecular orientation within the LCP domains were also confirmed for the drawn samples. Similar studies with extruded sheets of blends of PPS with 40PET/60PHB, and of PEI with HBA/HNA have found that the modulus of the fibers increased with drawing[113]. This study also reports an oriented fibrillar morphology with a high degree of molecular orientation within the LCP domains. Drawing characteristics of the blends of PET and the same copolymer has been investigated for conventional and microwave heating[115]. The results of this study established optimum drawing tension, temperature, and draw ratio necessary for obtaining an optimum modulus, which decreased with increasing LCP content. According to one study on blends of PPS with a range of LCP copolyesters, fibril formation in the extrudates depends on the composition and not on the draw ratio[116].

Skin-core morphology is reportedly shown by some of the blends of LCP with thermoplastic polymers. This feature is caused by having a higher degree of orientation of LCP phase in the skin rather than in the core when these blended are extruded or injection molded. The blends of nylon 66 with HBA/HNA and two different copolyesters based on PHB/PET[75,117] were shown to possess this discreet feature. In both the systems more LCP fibrils were observed in the skin rather than in the core. A similar shell-core structure was observed in the fracture surface of an injection molded blend of polyetherimide and HNA/HBA copolyester[82]. Skin- core structure of the extruded strands is shown to disappear completely at high draw ratios due to the greater influence of elongational forces in the post die deformations[118]. Another study on the blends of PS and LCP based on 4,4'-dihydroxy-α,α'-dimethylbenzalzine, however, showed a higher concentration of LCP microfibrils near the core[89,112]. According to the author, it is caused by a two way migration of the LCP droplets. Under the effect of shear inside the tube, the inward migration dominates and the equilibrium shifts towards the axis. This observation was supported by studies on blends of nylon 12 with different LC copolyesters[86,87].

Melt shear rate in the capillary flow conditions has been shown to influence the morphology developed in blends of PC and an LCP based on 60PHB/40PET[75]. It was observed that increasing the shear rates from 45 to 457 sec^{-1} apparently reduced the diameter of the fibrils and a phase inversion could be seen at the periphery of the extrudates. Fibrillar morphology of the extruded strands from 30% LCP composition is shown to disappear by the use of longer dies due to relaxation

of the structure in the shear field. This result is supported by similar finding on blends of PC and HBA/HNA copolyester system[66]. Malik et al.[65] while studying the blends of HBA/HNA with PC found that the modulus of pure LCP extruded through a capillary increased up to a shear rate of 150 sec^{-1}, but it decreased at high shear rates.

The reinforcing nature of the various LCP's in different blends examined so far has led some of the investigators to test the validity of composite theories. Blends of PC and copolyester based on HNA/HBA have been treated as unidirectional fiber reinforced composites and a reasonable agreement with the conventional composite theory was obtained[81]. Another study on blends of PC with copolymer of HBA/HNA/HQ/TA showed that the moduli of the highly drawn melts could be modelled by a simple rule of mixtures[66],

$$E_c = E_1 V_1 + E_2 V_2$$

where E_c is the composite modulus, E_1 and E_2 are the moduli of the reinforcing LCP and the matrix, respectively, and V_1 and V_2 are the volume fractions. One of the major reasons for agreement with this model was the high alignment of the LCP microfibril phases in the draw direction and their high aspect ratios.

Tensile modulus and tenacity data for blends of PPE/PS and PS with HBA/HNA and thermotropic polyesteramide material have been compared and modelled using the Helpin-Tsai equation for transversely isotropic and uniaxially oriented short fiber reinforced composites[118]. They report increased deformation by fibrillation of LCP phase in the extruded strands that is simultaneously drawn into fibers, as opposed to the injection molded specimens. They also emphasize that the elongational viscosity is more efficient in producing fibrillar deformation compared

to a weak shear and local extensional forces operating during injection molding. Rule of mixtures for the prediction of modulus has been given as an extreme case where the aspect ratio for the filler LCP reaches a value of 100 or more with compositions of 10% or more of LCP in the blend. Initial decrease in the modulus and the tenacity of the fibers at low compositions has been modelled qualitatively in terms of the contribution of reinforcements of voids created by delamination of low aspect ratio LCP fibrils. A reasonable correlation between the calculated and experimentally measured quantities were achieved.

A quantitative morphological analysis in terms of number and aspect ratios of the LCP fibrils present in the fibers from the blends of PC and polyetherimide and two different thermotropic polymers has been presented[119]. In this analysis they have tried to combine rheological and heat transfer equations for the post die processing of the spun fibers to predict the extrudate morphology. It reveals that the post extrusion extensional strain imparted to the dispersed LCP phase is critical for the formation of an optimal fibrillar morphology.

1.4 Over View of the Present Work

Blends of a main chain thermotropic polymer (Vectra^R A910RX) and an amorphous thermoplastic polyarylate (Durel^R 100) were investigated. The focus of this work mainly rests on the effects of processing conditions (mainly extrusion) on the mechanical properties and morphology of the resulting strands and fibers. Neat materials and blends have been processed by extrusion, generating filaments about

0.1 to 0.5 mm in diameter. The influence of composition, temperature and draw ratio on the biphasic structure of the fibers and the resulting mechanical properties were examined. Simple concepts of composite mechanics were used to establish morphology-property correlations. The glass transition behavior of the blends of varying composition have been analyzed to assess the miscibility. Rheology of the blends has been studied for capillary flow conditions to determine the effects of composition, shear rates and melt temperatures.

Thermal characterization of the pure materials was performed to draw information on their main transitions using differential scanning calorimetry. Information on their molecular weight and their degradation behavior has been derived from the available literature. Results have been used to identify proper processing conditions.

CHAPTER 2

EXPERIMENTAL

2.1 Materials

Polyarylate (Durel^{R},Natural DKX 066) used for blending was kindly provided by the Hoechst-Celanese Corporation. This material is a wholly aromatic polyester derived from Bisphenol-A and a mixture of o- and p-benzenedicarboxylic acid. It is an engineering thermoplastic resin with a glass transition temperature of 193°C. Thermotropic LC polymer, Vectra^{R} A910RX, used in this study has also been provided by the Hoechst-Celanese Corporation. It is a copolymer with a molar ratio of 70% p-hydroxybenzoic acid (HBA) and 30% 2,6-hydroxynaphthoic acid (HNA). It exhibits a strong endothermic crystalline transition to a liquid like nematic phase at a temperature of 287°C. These transitions have been confirmed through DSC measurements of as received materials and from dynamic mechanical measurements of compression molded films. DSC measurements on Durel^{R} yielded a glass transition of 183°C, which is about 10°C less than that obtained using DMA at a frequency of 0.1 Hz.. All materials were used after vacuum drying at 130°C for at least 6 hours.

2.2 Processing

Blends of the two materials were prepared by compounding in a single screw Brabender extruder at a temperature ranging from 290 to 310°C. Various

compositions ranging from 1 to 20 %w/w of the LCP were extruded through a 2 mm die (L/D =10). Extruding strands leaving the die exit were quenched in a water bath, air dried and chopped into pellets.

Blends of different compositions, prepared by compounding, were then reextruded and spun into filaments at a melt temperature of 290°C. Extruding filaments were quenched in a water bath and then wound onto a take-up bobbin rotating at a constant speed. A constant screw speed yielding a melt throughput of 7.7 cc/min was used in the spinning of all compositions. A take-up speed corresponding to an overall draw ratio of 30.6 was maintained. A straight capillary die with L/D ratio of 10 and a diameter of 2 mm attached to the exit of extruder was used for spinning filaments of all compositions. A melt shear rate of 164 sec^{-1} was maintained during the spinning of different blend compositions.

Filaments were also prepared at various shear rates, temperatures and melt draw ratios. A fixed composition of 10 %w/w of LCP was used for spinning under varying conditions. Different shear rates were obtained by employing dies of different diameters ranging from 1 to 3 mm, all having an L/D ratio of 10. Melt draw ratios during spinning were controlled by altering the take-up speed for the same melt shear and temperature conditions. Pure filaments were also obtained using neat polyarylate resin under an identical set of conditions. Filaments from neat Vectra resin were obtained corresponding to different melt draw ratios. Extrusion was done at a melt temperature of 300°C and a shear rate of 164 sec^{-1} for this spinning experiment.

2.3 Characterization

2.3.1 Differential Scanning Calorimetry

Perkin-Elmer DSC 7 model equipped with a dual cell calorimeter was used for the thermal analysis of the materials. DSC scans were obtained for pure materials both under as received state, after vacuum drying and after melt quenching from a high temperature. Heating runs were made under N_2 in the temperature range from 30 to 350°C. All blend compositions were analyzed before and after drying in vacuum for at least 6 hours at 130°C. A heating rate of 10°C/min was used for all the blends and the pure materials unless stated otherwise. Pure Vectra material was melt quenched from 300°C assuming no degradation of the transformed liquid crystalline phase. Cyclic runs have been carried out for neat polyarylate after quenching the melt from a temperature of 350°C under N_2 inside the DSC cell.

2.3.2 Dynamic Mechanical Thermal Analsis

Rheovibron model DDV -II-C manufactured by Toyo Baldwin Company was used to measure the dynamic mechanical properties under controlled cyclic strains. Thin film specimens of 0.4 cm width and 3 cm length were oscillated along the length under different frequencies of 1.1, 11 and 110 Hz. Load response of the specimens were recorded by a computer at an interval of 2°C. Specimens for testing were prepared out of the blends and unblended polymers by compression molding at temperatures in the range of 290 to 320°C. Samples were heated at rate of 2°C/min under N_2 in the Rheovibron chamber. Strip samples were put under a constant tension of 20 gm during the cyclic deformation in the range of 25 to 210°C.

2.3.3 Polarized Optical Microscopy

Optical microscopy of the extrudates was carried out under transmitted light using a Nikon instrument. Thin sections of about 2-3 micron thickness were obtained by microtoming using a glass knife. Specimens were cut both along and across the long direction of extruding filaments. Pictures of the viewed specimens were obtained under different orientation of the polarizer and analyzer. Birefringence of the dispersed LCP phase was recorded in the micrographs obtained under cross polar position of the analyzer and polarizer. However, for assessing the general phase morphology pictures were taken under corresponding parallel positions. Some micrographs were taken of the similar sections obtained from melt drawn fibers as well. Magnifications of 400 and 1000 were used for recording the images.

2.3.4 Scanning Electron Microscopy (SEM)

A Cambridge stereoscan S-360 was used in the scanning mode for studying the fracture surface. Samples for the study were prepared by performing fracture at room temperature of the individual fibers in the Instron tensile tester under a strain rate of 20 mm/min (80 %/min). Fiber specimens of approximately 1 cm in length from the fracture surface were cut. These were then mounted vertically up supported by the holes drilled on the periphery of conventional specimen stub and glued at the bottom. The fracture surface was then sputter coated with 150 to 200 A° of Au metal on a low vacuum. Specimens thus prepared were viewed immediately in the microscope. All micrographs were recorded normally at a magnification of 10^4 to

read the features at the base of the surface and the protruded structures. Some pictures were also taken at low magnifications to study the uniformity of the overall features present.

2.3.5 Mechanical Properties

Mechanical properties of the fibers were measured under tension using an Instron^{R} tensile tester. ASTM D-3822 method was followed to measure the tensile properties. A uniform gauge length of 25.4 mm with strain rate of 20 mm/min (80 %/min) was used with all the different compositions of fibers. Different tensile properties measured were reported as an average value from a minimum of 10 specimens each. A load cell of 200 lbs maximum capacity was used to measure the loads during tensile stretching in the machine. A grip pressure of 15-20 lbs was used to hold specimen between the clamps.

2.3.6 Rheometry Measurements

Dynamic shear viscosities of different blend compositions and pure polymers were measured using an Instron^{R} capillary rheometer. A melt temperature of 300 °C was used to compare the data at various blend compositions. Blends containing 1 to 20 % LCP were analyzed over the shear rate range of 0.1 to 1000 sec^{-1}. A straight capillary die of diameter 0.031 inches with a L/D ratio of 30 was used for all the measurements. The load cell used in the measurement had a maximum capacity of 1000 lbs. Shear viscosity data was also obtained at different melt temperatures ranging from 290 to 325 °C for a fixed blend composition of 10 %LCP.

CHAPTER 3

RESULTS

3.1 Differential Scanning Calorimetry

Neat polyarylate (Durel^{R}) and the copolymer P(HBA/HNA) (Vectra^{R} A910) were analyzed using DSC in the as received condition to determine their transition behavior. The DSC traces for polyarylate are shown in Fig. 3.1. All transition temperatures were obtained using the commercial software from Perkin-Elmer. All transitions were measured at a heating rate of 10°C/min. unless specified otherwise. The glass transition behavior of polyarylate showed an erratic response in the range of about 175 to 200°C (curves 1, 2 & 3). Of several first heating runs made for the as received polyarylate one sample showed in addition an exotherm at a peak temperature of about 190°C, following a sharp glass transition observed at about 178°C (curve 3). This sample was then quenched from the melt at 250°C and reheated in the DSC. It then showed a broad glass transition at 183°C followed by a small melting endotherm at 370°C (curve 4). This melting endotherm had a heat of fusion that was approximately equal to the heat of crystallization observed for the exotherm in curve 3, indicating that it was due to the melting of the crystals formed in curve 3. The melt from 375°C (curve 4) was quenched once again to prepare a new sample with a different thermal history. This quenched sample on subsequent heating showed only a sharp glass transition at about 178°C (curve 5). Since the

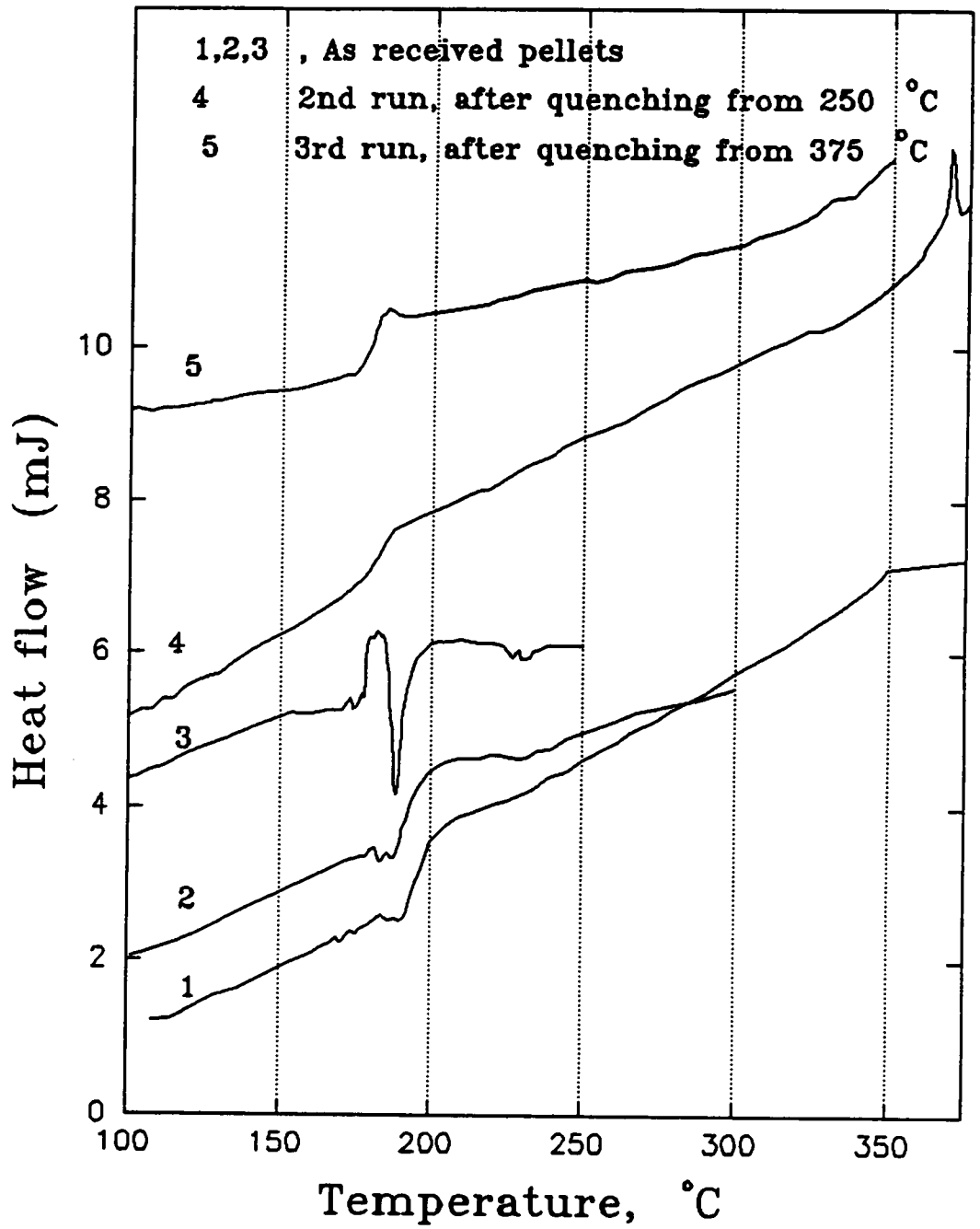

Fig. 3.1: DSC traces for neat polyarylate under different thermal histories. Curves displayed vertically for clarity.

exotherm observed in curve 3 was obtained in only one case and was not repeatable, it probably indicated the presence of a small impurity in the bulk produced commercial polyarylate. Since the first heating runs of as-received materials showed an erratic T_g, it was considered useful to melt the samples by heating them to 250°C. These were then quenched to room temperature at a fixed programmed cooling rate of about 300°C/min in the DSC cell. Samples quenched in this way showed a reproducible T_g at about 183°C as was observed in curve 4 (Fig. 3.1). The T_g determined in this way was apparently free from any effects of previous thermal and mechanical history that tend to obscure the reproducible and clear appearance of the glass transition temperature. Previous measurements done on polyarylate derived from bisphenol-A and a mixture of 50% isophthaloyal and 50% terephthaloyal units(Ardel^R D100) has reported a T_g of 185°C at a heating rate of 20°C/min[120]. This result can be compared with those obtained here for polyarylate (Durel^R) after allowing for an increased heating rate.

Thermo-mechanical properties of polyarylate, like any other aromatic polyester are considered sensitive to the presence of moisture during its storage and processing. To study the effect of humidity on T_g of the material, two sets of polyarylate samples were prepared by quenching the melt from a temperature of 250°C and a cooling rate of 300°C/min. These were then stored at room temperature with one set exposed under dehumidified air (drierite in a dessicator) and the other kept at ambient room conditions, respectively. The T_g of this prequenched material was determined from a second heating run in the DSC

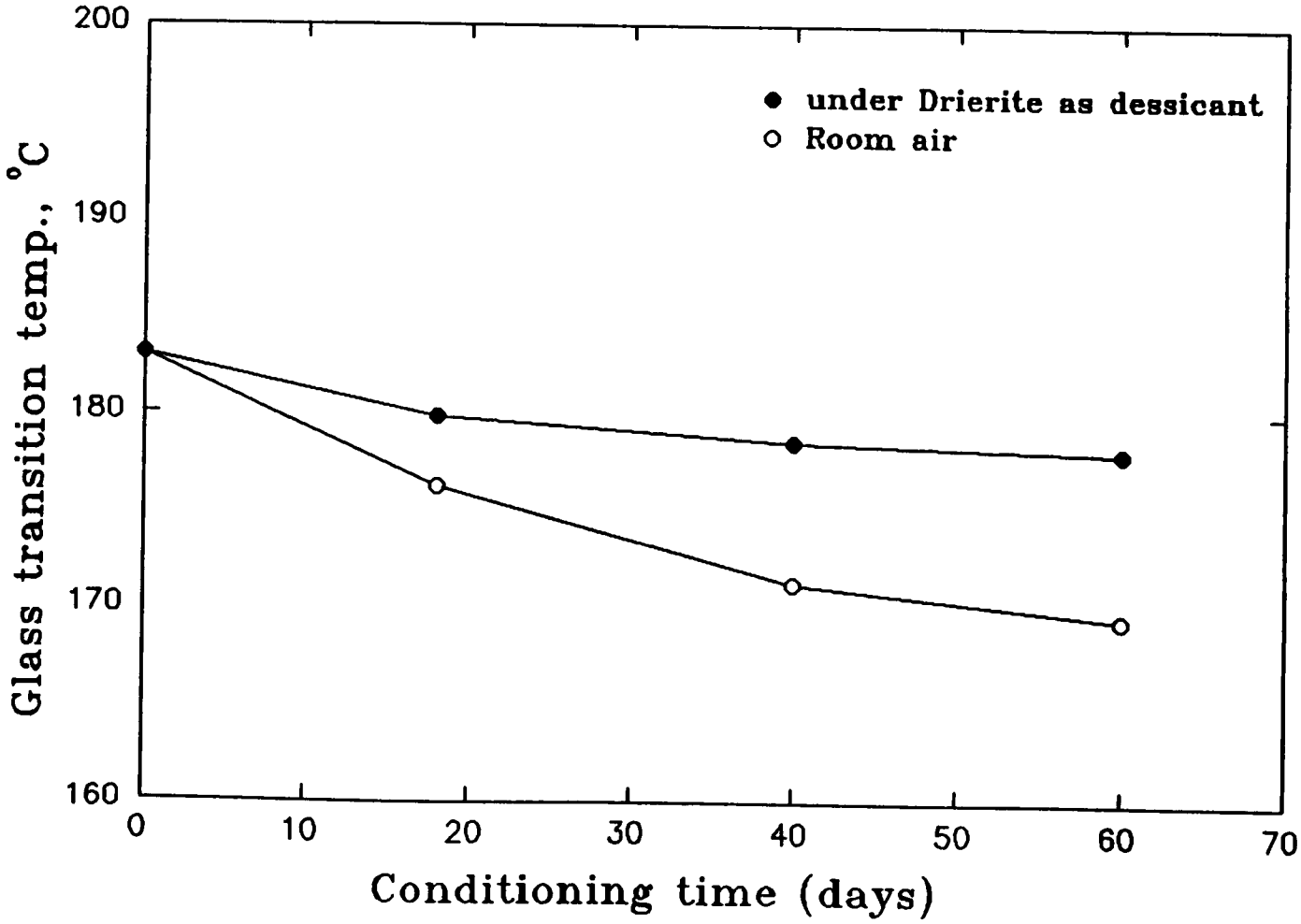

Fig. 3.2 : Glass transition temperature of polyarylate stored under different moisture conditions (as obtained using DSC).

taken after suitable intervals of time. The data obtained are shown in Fig. 3.2. These indicate that polyarylate was very sensitive to moisture. The T_g of polyarylate decreased from a temperature of 183°C to 171°C in the case of humid air equilibrated samples while those kept in nearly anhydrous conditions showed a decrease of only about 5°C. This small decrease in the glass transition from 183°C may be associated with a low humidity environment created even with the drierite material.

DSC traces for Vectra taken under different conditions of thermal history are shown in Fig. 3.3. These show a broad glass transition centered around 92°C. This is obscured slightly by the slope of the trace. In addition, these showed an endothermic transition having a broad beginning, and a peak temperature at about 279°C. The second heating (curve 2) of the samples quenched from the anisotropic melt at 375°C showed a slight sharpening of this endothermic transition that appeared at about the same temperature (279°C). The broad beginning observed in curve 1 remained almost unaffected. The as-received vectra sample was, in addition, annealed at 260°C for 30 minutes in the DSC cell and then quenched to room temperature. On subsequent heating run in DSC, this annealed sample showed a broad endotherm centered around 240°C (curve 3). The heat of transition of the previously observed endotherm was found doubled from its value in curve 2 and the peak temperature shifted to 287°C from 279°C.

Phase behavior of the blends of polyarylate with the thermotropic copolymer of HBA/HNA have been analyzed using the DSC. The T_g due to the polyarylate

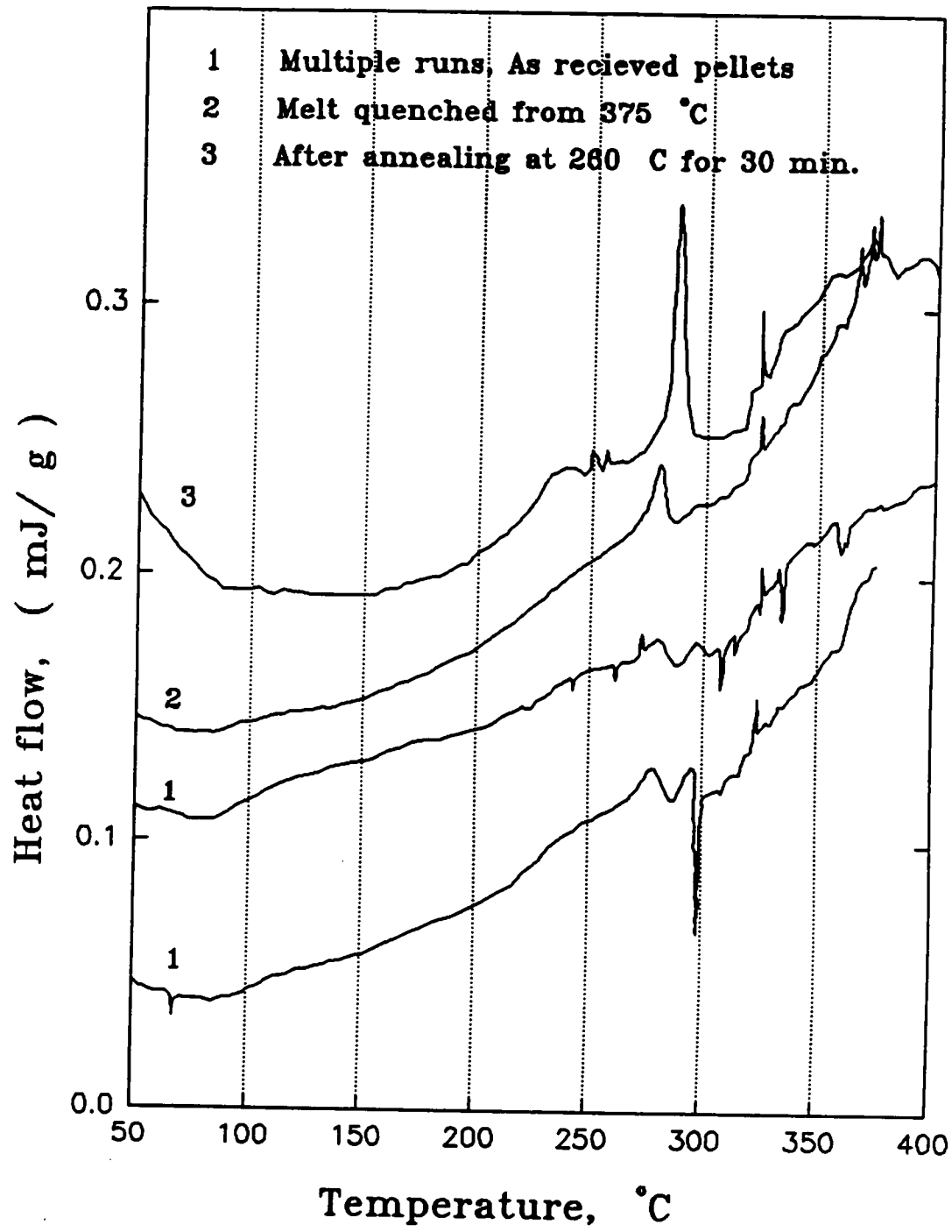

Fig. 3.3: DSC traces of Vectra A910 under different thermal histories. Curves shifted vertically for clarity.

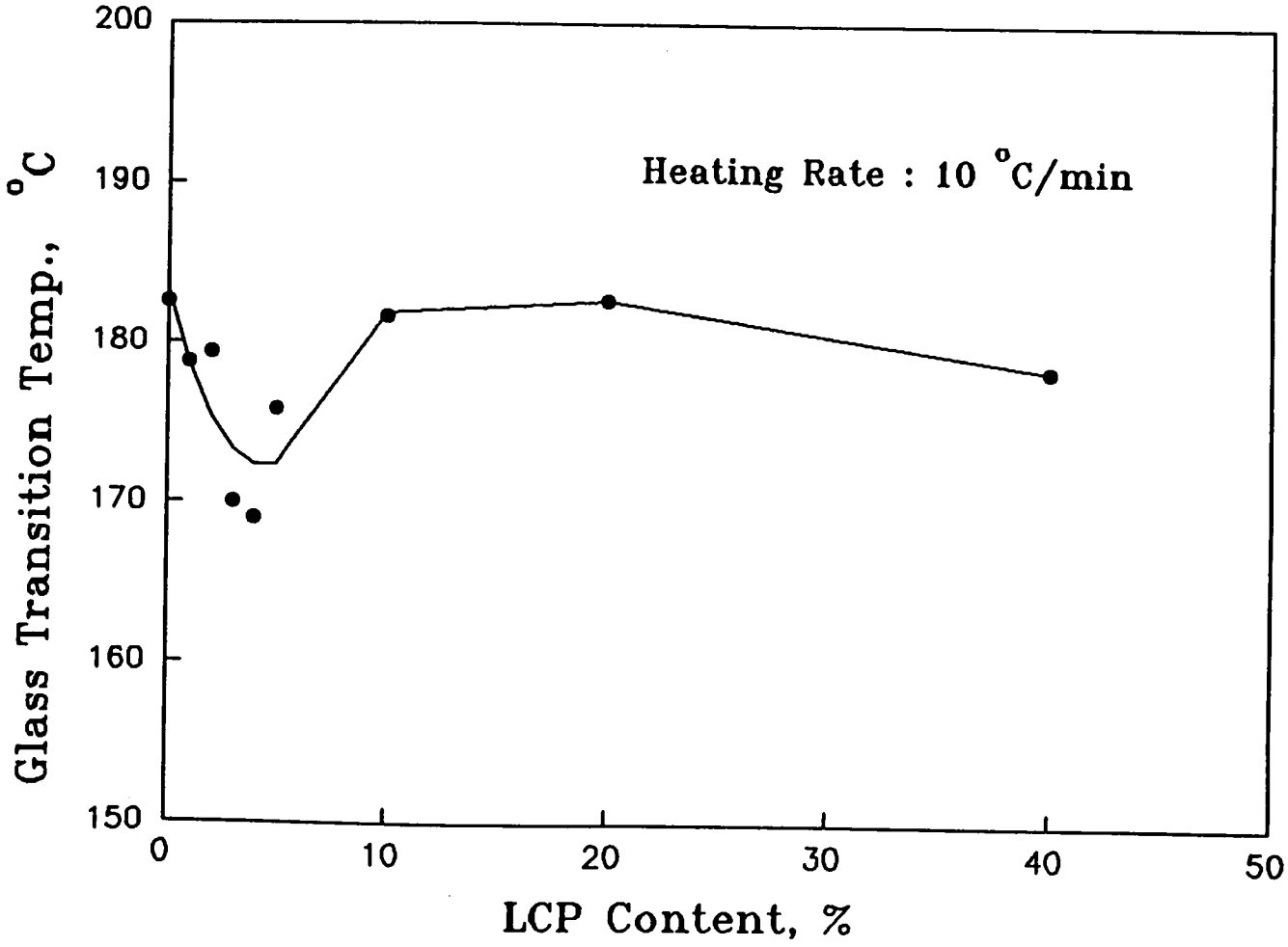

Fig. 3.4 : T_g of the polyarylate rich phase of the blends (as obtained using DSC).

rich phase of the blends, containing up to 40% by weight of LCP, has been plotted in Figure 3.4. Single T_g of neat polyarylate component of the blends have been observed except for the low composition region. No detectable glass transition was observed corresponding to the dispersed LCP phase. The T_g of the polyarylate rich phase is shown to decrease sharply on addition of a small amount of LCP. A lower T_g of about 170°C for the polyarylate rich phase is maintained in the range of about 3 to 4% LCP in the blend. T_g of the polyarylate rich phase in these blends has been found to be reproducible during up to five repeated cyclic heating runs performed after cooling of the melt from 250°C at a rate of 10°C/min. The blend, however, showed a single T_g of the immiscible polyarylate phase in the range of 10-40% LCP composition. A similar trend has also been obtained for the temperatures of tan δ loss peaks recorded in the dynamic mechanical scans at an oscillation frequecy of 1.1 Hz. A comparison of tan δ loss scans for different blend compositions upto 10% LCP has been presented in Figure 1 of appendix B. The temperatures of tan δ loss peaks recorded for different blend compositions and pure polyarylate, however, do not compare with the corresponding T_g of the materials recorded through DSC.

3.2 Polarized Optical Microscopy

Optical microscopy of the extruded strands from the blends of different composition was done to look into the biphasic nature of the blends. This study will be used to determine the microstructure of the immiscible LCP phase. In addition, an estimate can also be obtained of the shape and size distribution of the dispersed

particles. Microtomed sections about 3 micron thick were cut using a smooth glass knife from the extrudates of different LCP compositions. Thin sections were obtained by slicing along the flow directions mainly from the core regions. Strong birefringence due to the dispersed LCP regions is observed against a dark background of isotropic matrix when the analyzer is placed at the crosspolar position with respect to the polarizer (Fig. 3.5 and 3.6). Sclereon textures characteristic of the nematic morphology of the cooled LCP phase can be seen in one of the poorly dispersed blends prepared by extruding the materials from a straight screw channel (Fig. 3.5b). More uniform and fine dispersion of the LCP phase resulted when the extrusion was done through a screw having vertical pins mounted intermittently over small regions in the flow channel (Fig 3.5a). Sections from these extrudates reveal spherical droplets of LCP dispersed uniformly in the core region of the extrudates as shown in Figure 3.5a and 3.6. Dispersed particles of LCP are shown to have a distribution of sizes ranging from 0.5 to 2 microns. Distribution of particle size is apparently seen to get narrower as the LCP content in the blend is increased from 2% to 20% as shown in figures 3.5a and 3.6. Dispersed LCP particles do not seem to deform appreciably in the flow direction as a result of shear forces in the capillary; this can be seen through a comparison of the Figures 3.7(a) and (b) for the blend containing 10% LCP. These pictures were observed under a bright field of view through thin sections of the extruded filaments with no external pull applied on the melt. Sections were cut along the flow direction and across the flow direction, respectively.

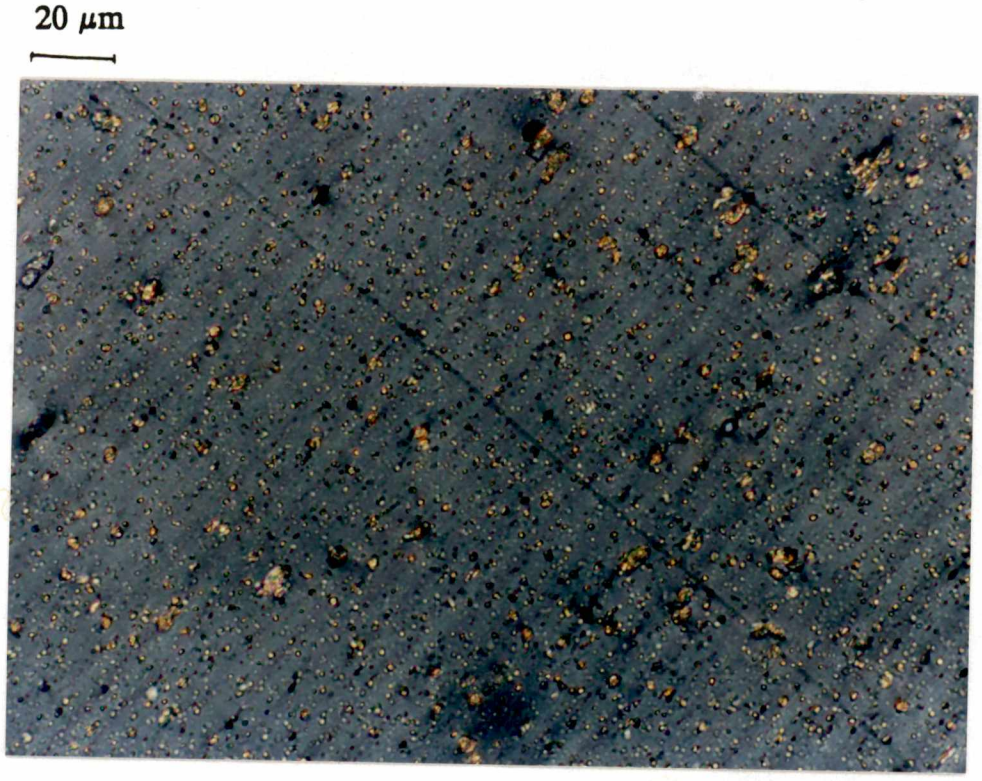

(a)

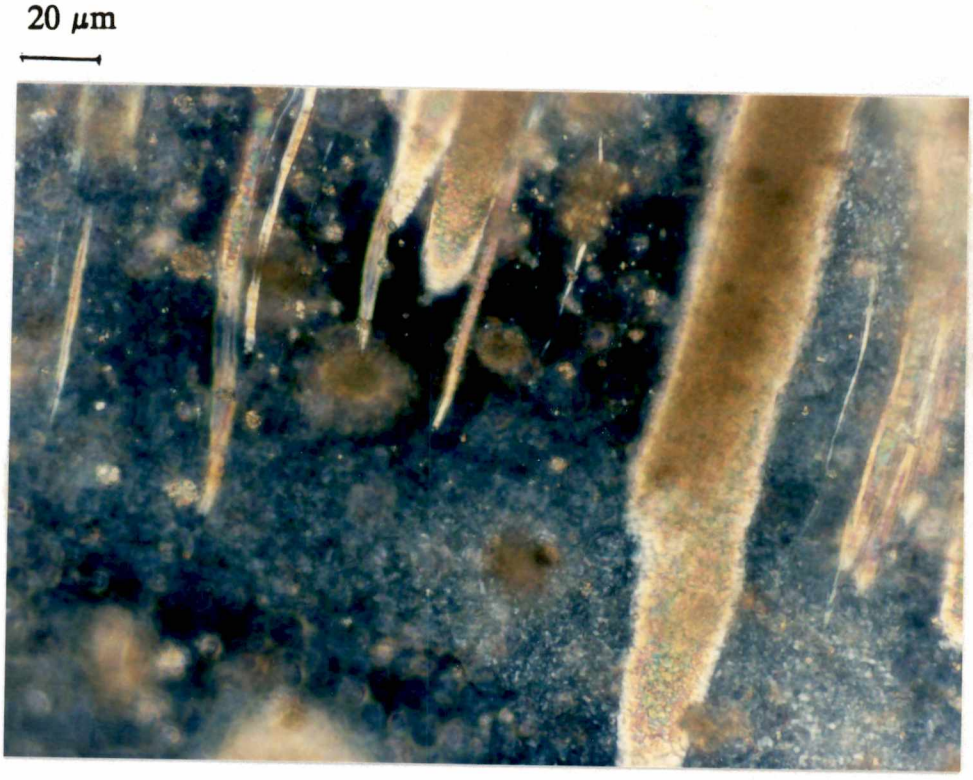

(b)

Fig. 3.5 : Microscope view of 90/10 blends (extrudates) from transmitted light and under cross polars. a) Finely dispersed b) Poorly dispersed.

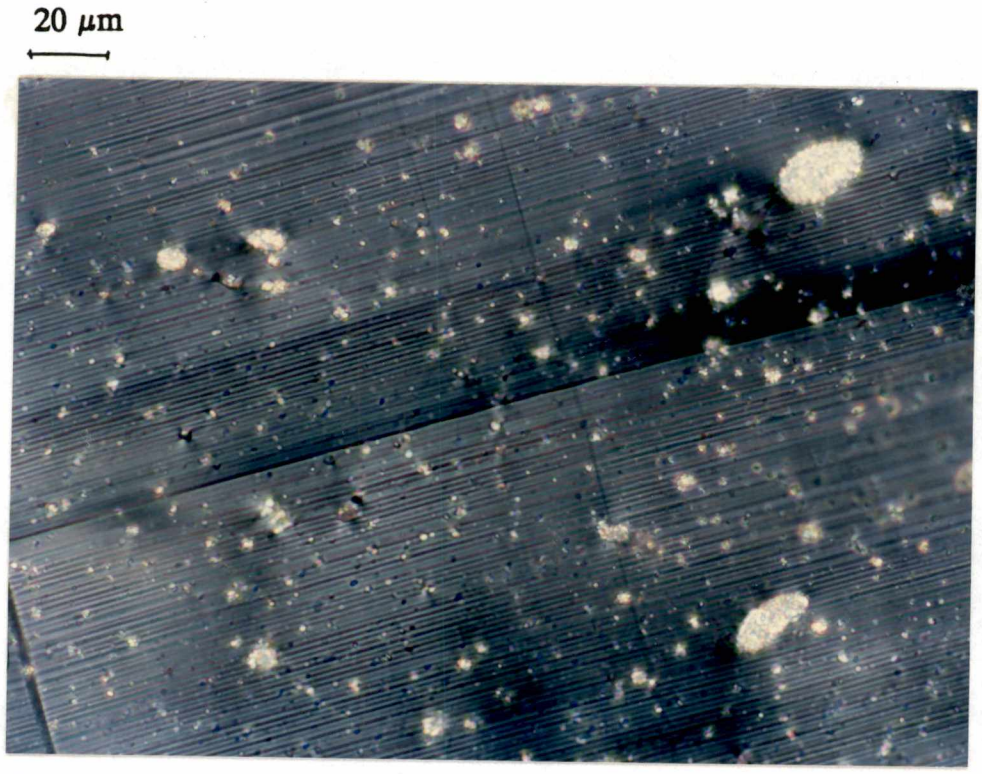

(a)

(b)

Fig. 3.6 : Microscope view of blends (extrudates) from transmitted light and under cross polars. a) 95/5 b) 80/20.

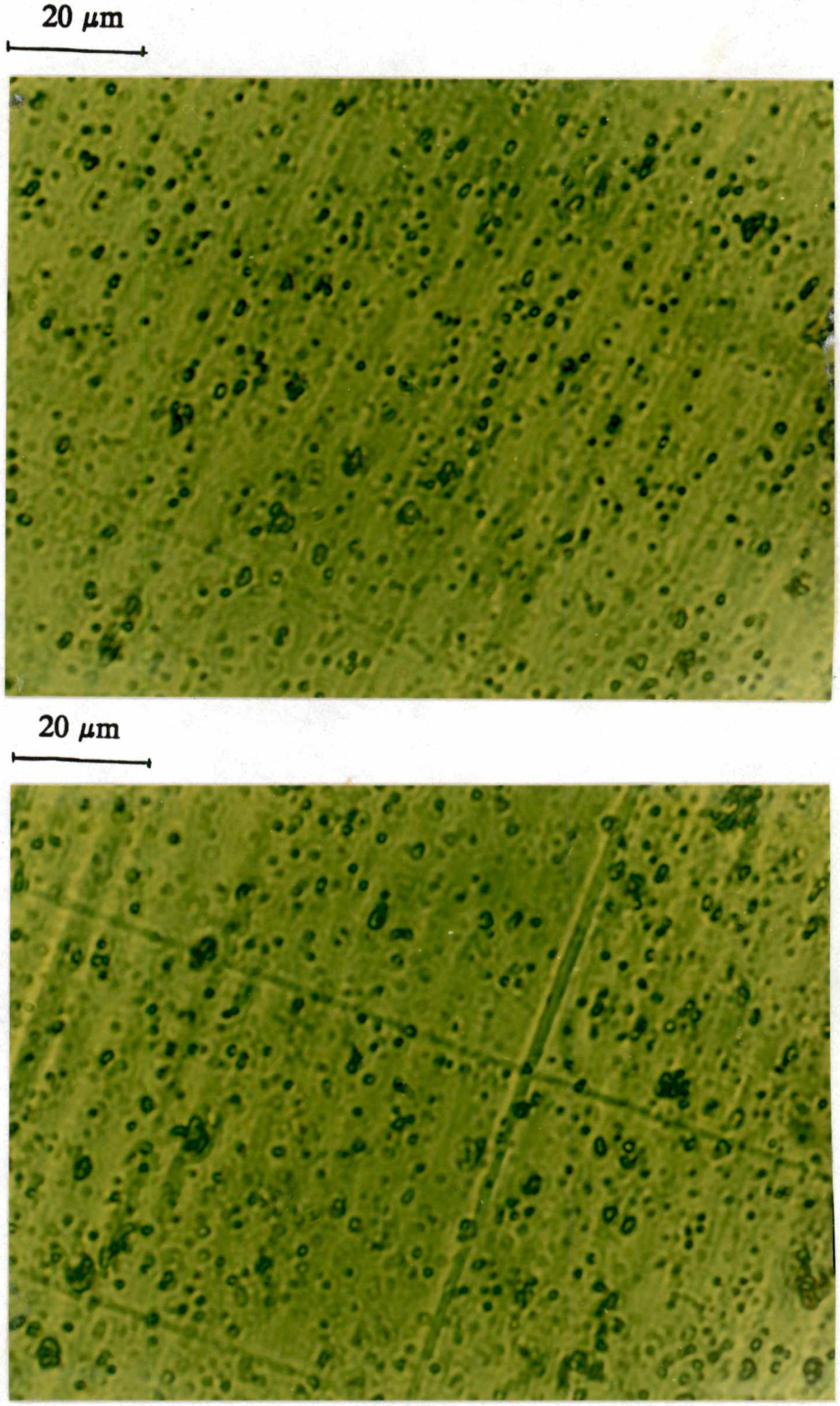

Fig. 3.7 : Microscope view of blends (extrudates) from transmitted light and under bright field. a) cross sectional view b) Along the flow direction.

3.3 Scanning Electron Microscopy Studies

The fracture surfaces obtained from the breaking of the fibers during tensile extension has been investigated for the nature of the biphasic morphology obtained due to the blend components. The shape and adhesion behavior of the dispersed phase were examined for its formation and consequent reinforcing effects. Fibers were ruptured at room temperature and a fixed extension rate of 20 mm/min in Instron. The fracture surfaces created were viewed at an angle of about 5° with respect to the fiber axis. All the specimens electron micrographed for the study revealed long fibrillar structures of dispersed LCP domains. The origin of these fibrillar phases has been investigated further from the observation of fracture surface of the as extruded filament with no external draw-down. The presence of spherically shaped dispersed LCP particles is clearly evident in the photomicrograph shown in Fig. 3.8a. Apparently, the dispersed fibrillar morphology for the LCP phase seems to have been generated during the melt drawing process following the extrusion through the capillary die. The dispersed LCP fibrils seen in the micrographs have also been separated by soxhlet extraction of the matrix polyarylate using chloroform as a solvent. The residue obtained from the melt drawn fibers for the 90/10 blend was then sputter coated with metallic gold. The SEM images taken of this material then revealed fine fibrils of the dispersed LCP with aspect ratios of the order of several hundred (Fig. 3.8b). These fibrils, formed during the capillary extrusion and drawing process, are seen to have a range of diameters (0.1 to 0.5 μm). The fracture surface images of these biphasic fibers reveal the sporadic presence of thick fibrils

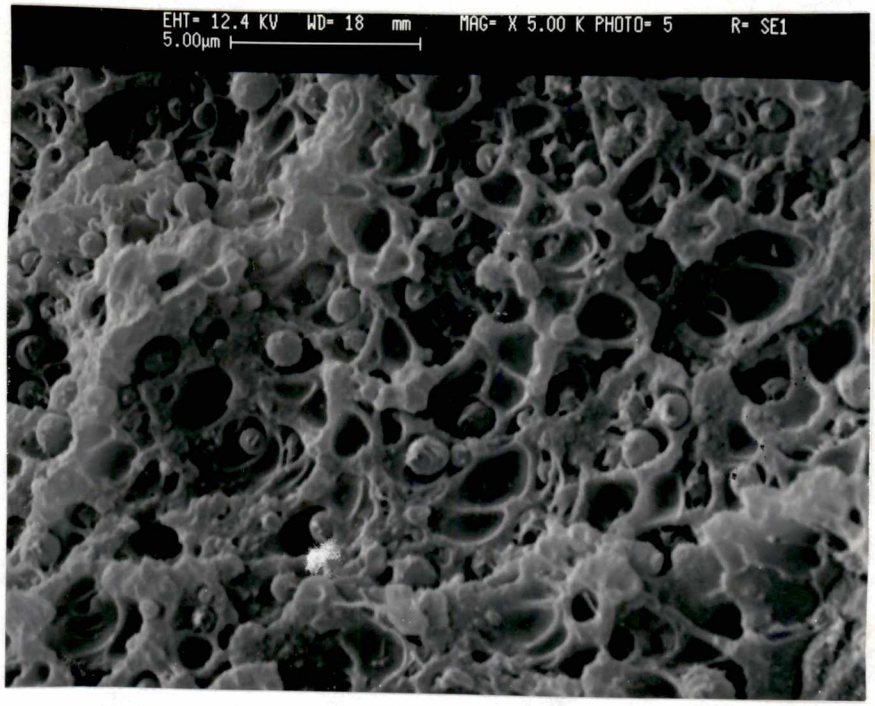

(a)

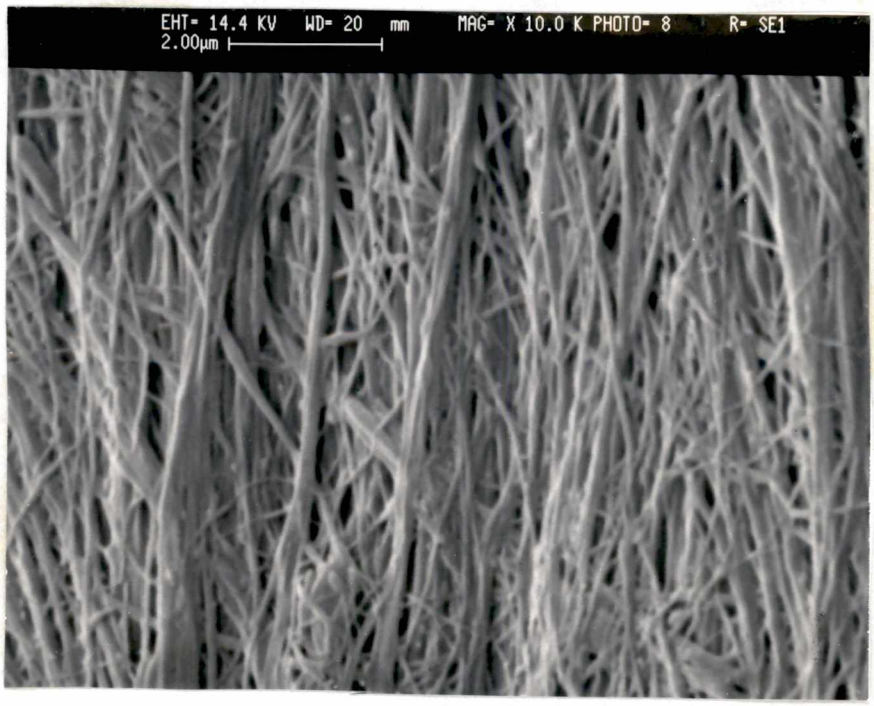

(b)

Fig. 3.8 : a) SEM fracture surface view of extrudates from 90/10 blends.
b) Melt drawn fibers (D.R. 30.6) from 90/10 blend. Residue after removal of the matrix polyarylate by selective extraction with chloroform.

with wide annular spaces around them. These thicker fibrils are shown to have long tapering diameters projecting up from the fracture surface in the direction of melt flow. Existence of a large number of circular holes with distribution of sizes is also shown on these fracture surfaces. These holes have apparently been generated due to pulling out of the embedded LCP fibrils with smooth tapering tips. Such long tapering ends indicate poor adhesion of these fibrils to the matrix polymer. In addition, there is a large number of small diameter fibrils seen in these micrographs. Some of these thin fibrils are also seen to have been pulled out of the matrix due to poor adhesion as shown by the presence of a large number of smaller holes. Sporadic existence of flat broken ends due to breaking of these thin fibrils may also be observed close to the fracture surface particularly in fibers with 5% LCP content (Fig. 3.9d).

An increase of the LCP content in the blend has apparently increased the number of long and tapering fibrils present on the fracture surface (Fig. 3.10). With an LCP content of 15% they still appear to have been pulled out from the matrix due to poor adhesion as revealed by the presence of holes created by it. However, the speckled appearance of surface appears to have changed visibly from 2% LCP to 15% LCP in the blend (Fig. 3.9-3.10). A closer examination of the specific composition (10% LCP) reveal that this speckled appearance was due to a large number of small diameter fibrils rising low on the surface.

Increased draw ratio due to the post die drawing of the melt seems to have changed the appearance of the fracture surface (Fig. 3.11). It shows evidence of an

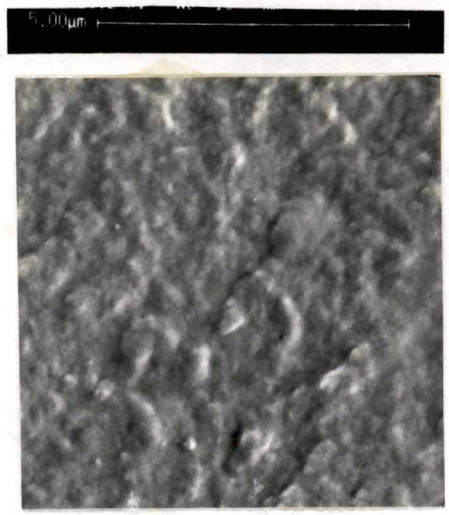

(a)

(b)

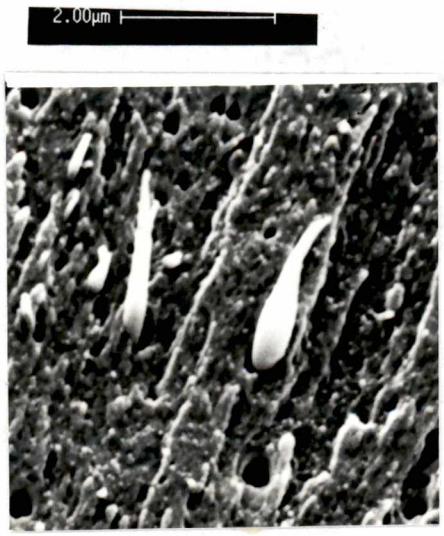

(c)

(d)

Fig. 3.9 : SEM images of fracture surface of the fibers melt drawn from the blends. Blend ratio (% by weight LCP) : a) 0 b) 1 c) 2 d) 5.

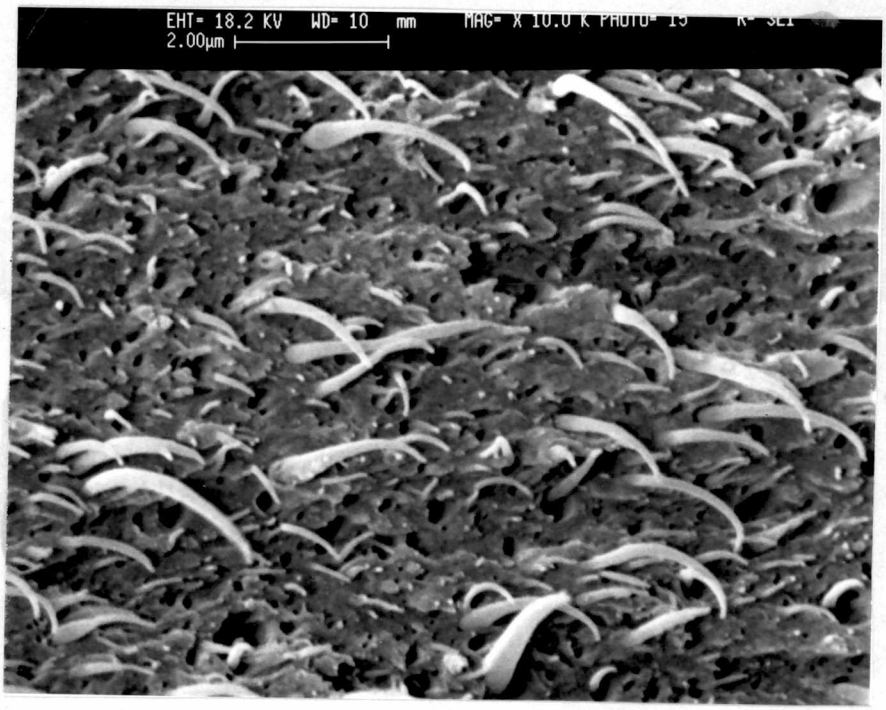

(a)

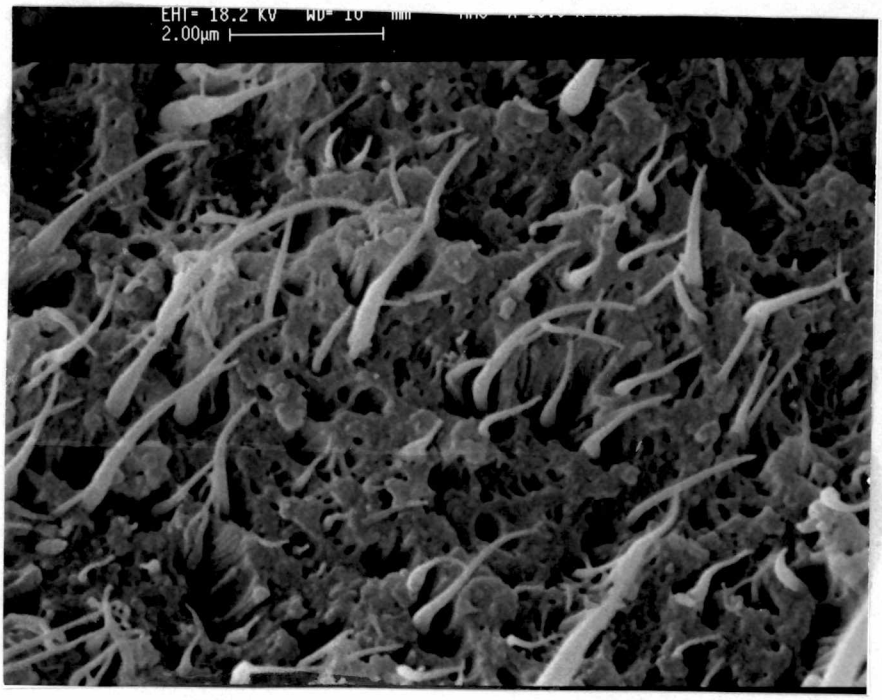

(b)

Fig. 3.10 : SEM images of fracture surface of the fibers melt drawn from the blends. Blend ratio (% by weight of LCP) : a) 10 b) 15.

(a)

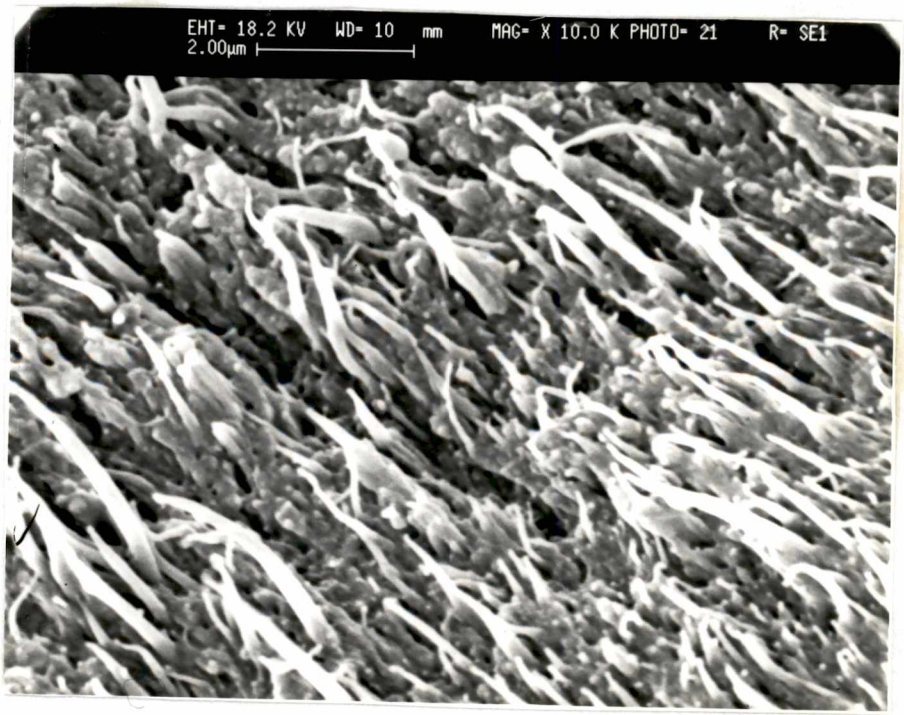

(b)

Fig. 3.11 : SEM images of fracture surface of fibers melt drawn from 90/10 blend. Melt draw ratio : a) 30.6 b) 114.

induced plastic flow of the immiscible polyarylate matrix around the deformed LCP fibrillar phase. The orientation of these fibrils has apparently improved both parallel to each other and along the fiber axis as shown in Fig. 3.11(b) for 10% LCP blend at a draw ratio of 114. A comparison of the blend fibers spun at two different melt temperatures of 300°C and 330 °C is presented in the fracture surface view shown in Fig. 3.12(a & b). It shows that at a high melt temperature of 330 °C, there is a visible reduction in the number of speckled domains. However, the long tapering fibrils have grown thicker in size, i.e. there is an agglomeration of the LCP domains. The number of fibrils is also seen to be reduced significantly as compared to fibers processed at lower temperature. Blends spun at low temperature of 290 °C apparently shows a lesser number of fibrils that have better adhesion to the matrix. This is evident in terms of a greater number of holes due to pulled out fibrils seen in the fracture surface of fiber spun at 300°C as compared to those spun at 290°C.

Fibers formed by extrusion at low shear rates show evidence of crack initiated from a surface flaw, which then propagates across the fiber cross section. Apparently weak adhesion between the elongated LCP fibrils and the polyarylate matrix allows the crack propagation randomly leaving a trail of delaminated smaller regions. A closer examination of the fracture surface reveal an highly striated appearance of the surfaces generated by cracking as shown in Figure 3.13a. The fracture surface from the fiber spun at high shear rates of 1134 s^{-1} apparently does not show such wide spread cracked appearance. However, probably due to some local flaw or some trapped air bubble, a similar striated structure was evident in the core region of the extruded fiber (Figure 3.13b).

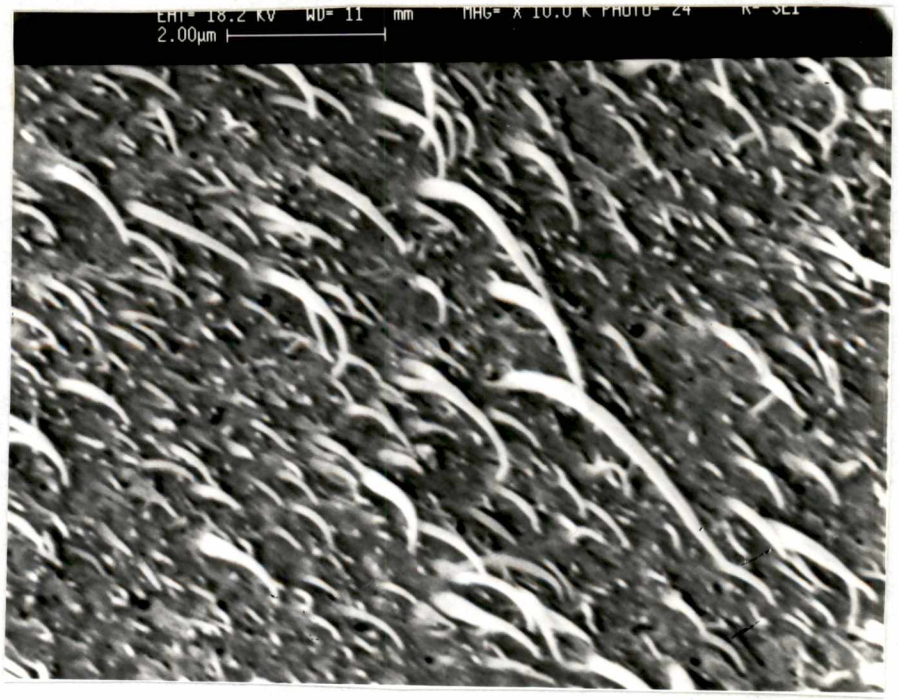

(a)

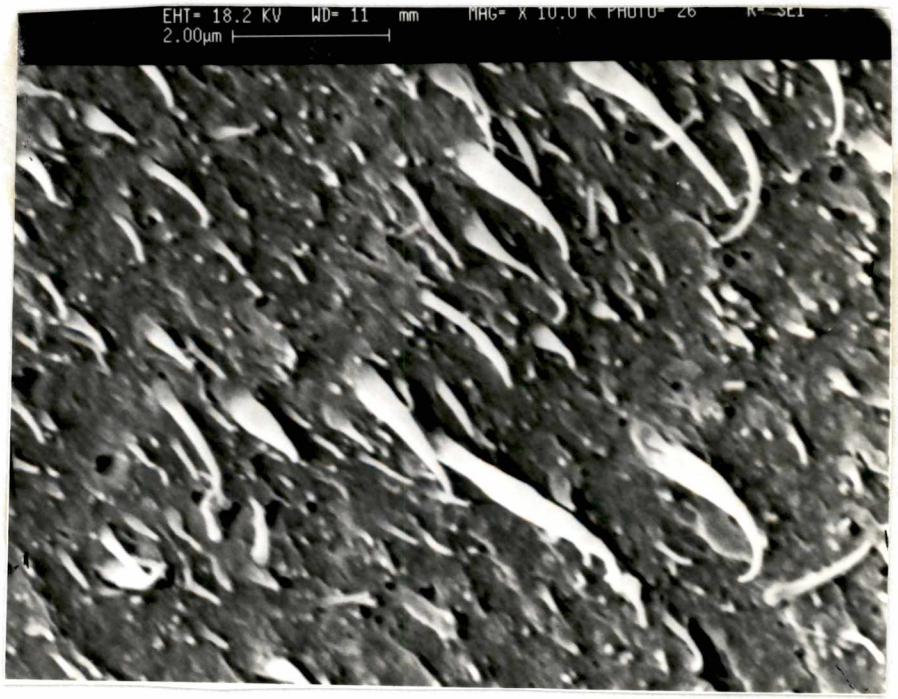

(b)

Fig. 3.12 : SEM images of fracture surface of fibers spun using different melt temperatures. Blend ratio : 90/10 (PAr/LCP). a) 300°C b) 330°C.

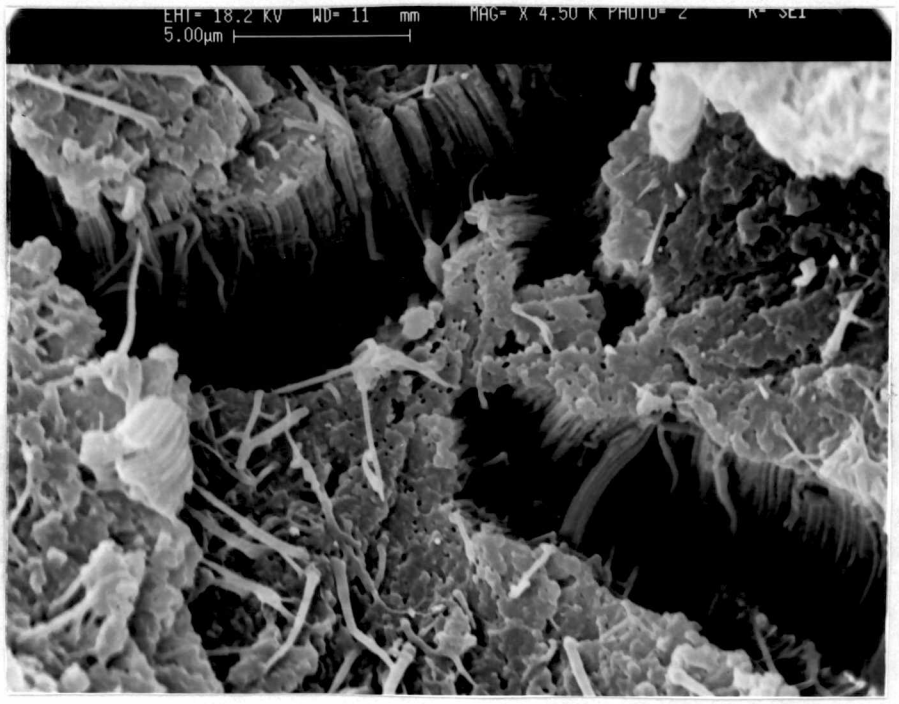

(a)

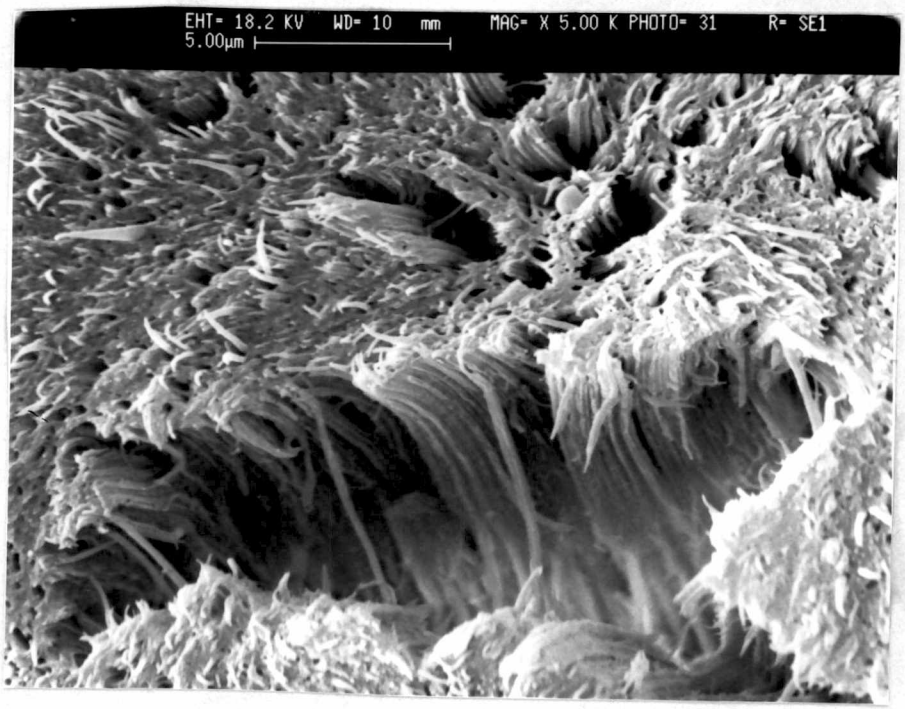

(b)

Fig. 3.13 : SEM images of fracture surface of the fibers melt spun under different shear rates. Blend ratio : 90/10 (PAr/LCP). a) 48 s^{-1} b) 1134 s^{-1}.

3.4 Dynamic Shear Viscosity of the Blends

Processibility of the neat polyarylate has been compared with the blends having various compositions of LCP. Shear viscosity data was obtained for the capillary flow conditions. Results of the measurement taken at a melt temperature of 300°C and a range of shear rates from about 1 sec^{-1} to about 10^3 sec^{-1} have been plotted in figures 3.14 and 3.15. Two broad regions have been identified for observing the trend in the change in the viscosity with composition of the blend. These regions constitute those marked below a shear rate of about 2 to 3 sec^{-1} and the other is the high shear region beyond about 10 sec^{-1}. Shear viscosity of the polyarylate blends was seen to decrease with the increased LCP content with a minimum at 5% level as shown in Figure 3.16. However, beyond the 5% level the dynamic viscosities of the melt shows a slight increase to higher values that does not change with the composition any further. All the blends were shown to follow the Newtonian behavior of the neat polyarylate in the shear rate region of 10 to about 200 sec^{-1}(Fig. 3.14). Blend with 1% by weight of LCP, however showed a shear thinning behavior up to about 100 sec^{-1} followed by a narrow plateau region(Fig. 3.15). Shear viscosity of the melt do not show any definite trend below a shear rate of about 2 to 3 sec^{-1}. At shear rates above 300 sec^{-1}, the melt viscosity of different compositions show a shear thinning behavior with increased shear rate.

The blend with 10% LCP composition was examined for variation of dynamic viscosities with temperature. The data have been presented for 4 different temperatures in figure 3.17 and 3.18. As is apparent from these plots, viscosities at

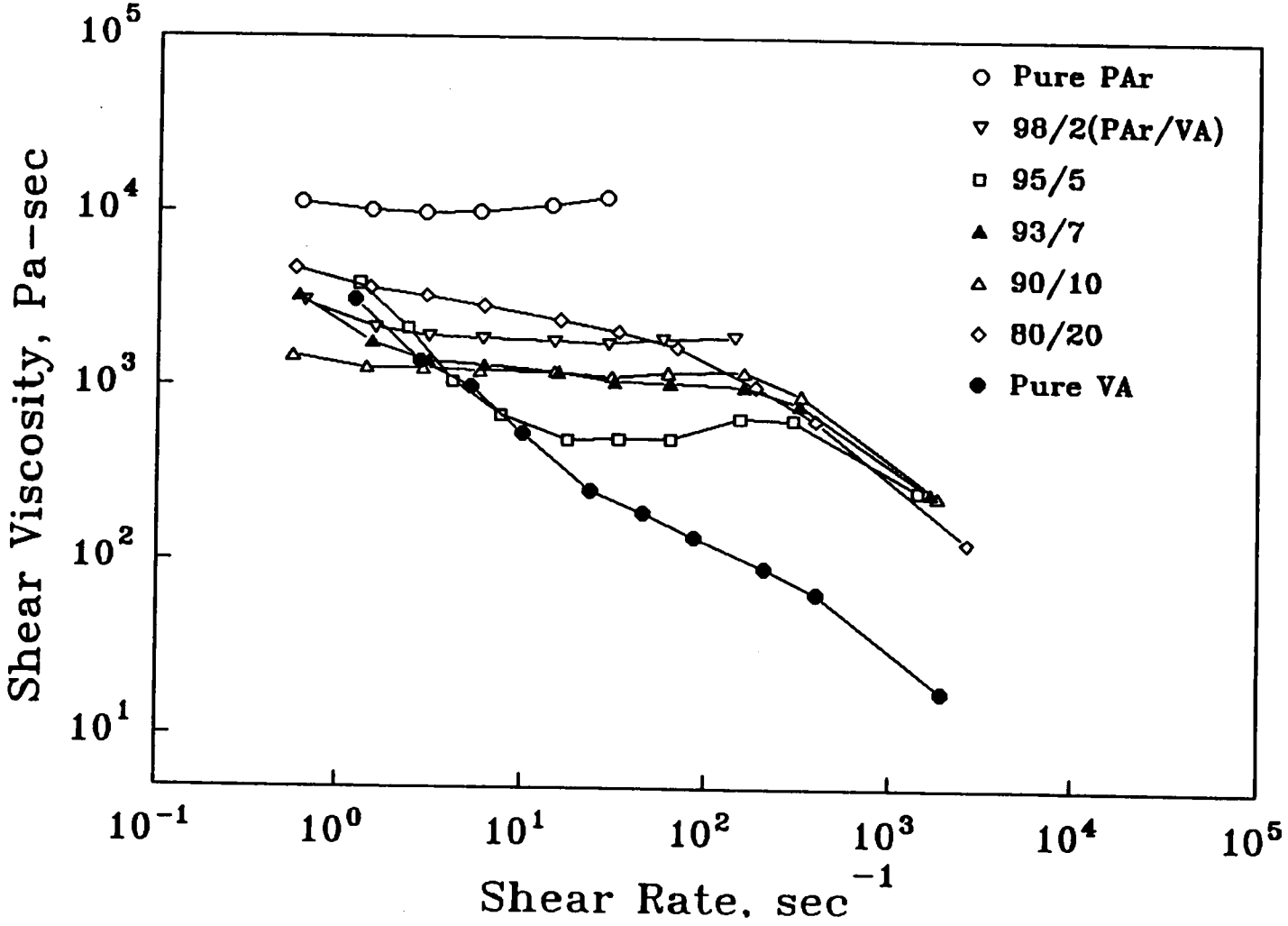

Fig. 3.14: Melt viscosities of the blends for capillary flow measured at 300°C.

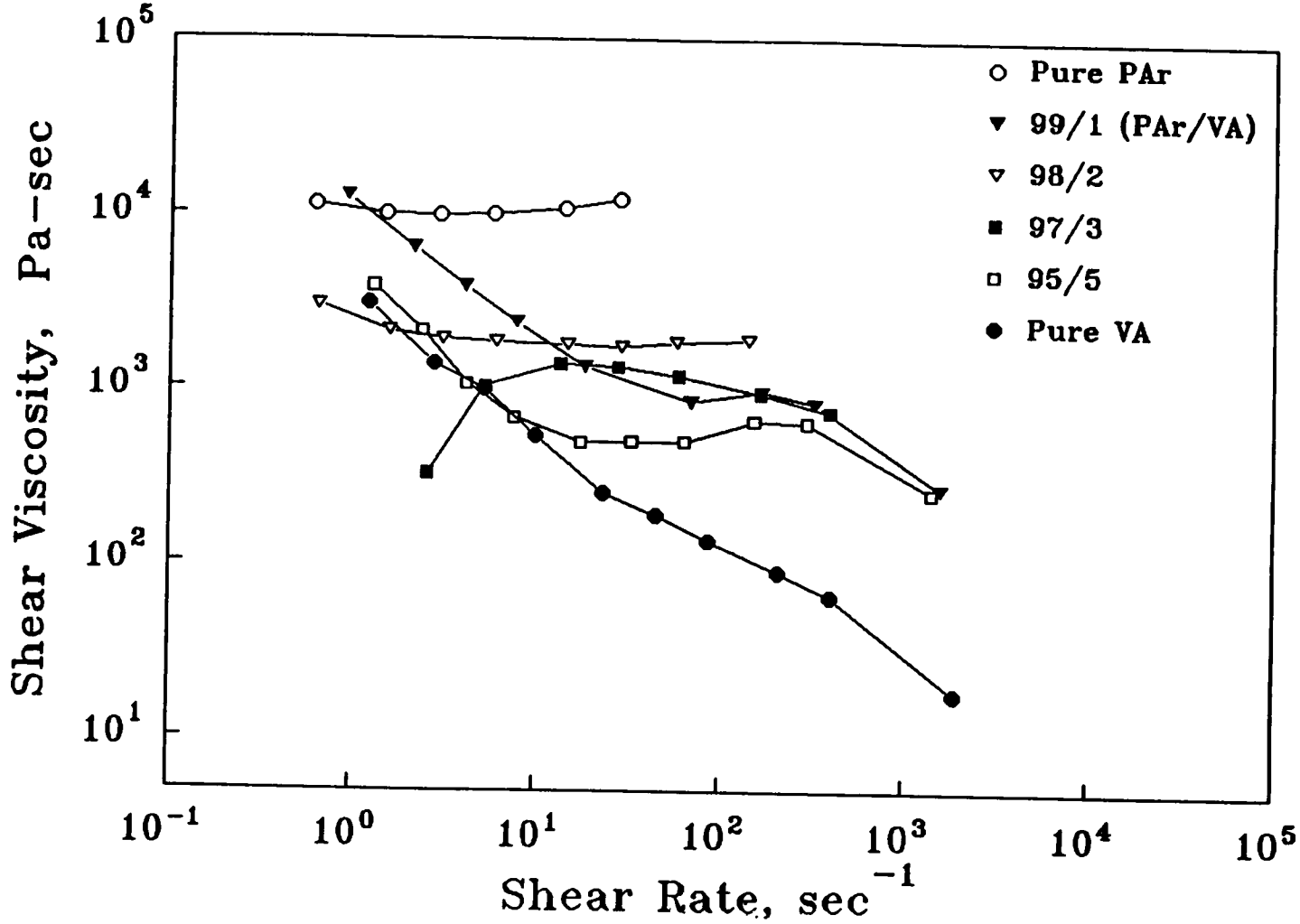

Fig. 3.15: Melt viscosities of the blends for capillary flow measured at 300°C.

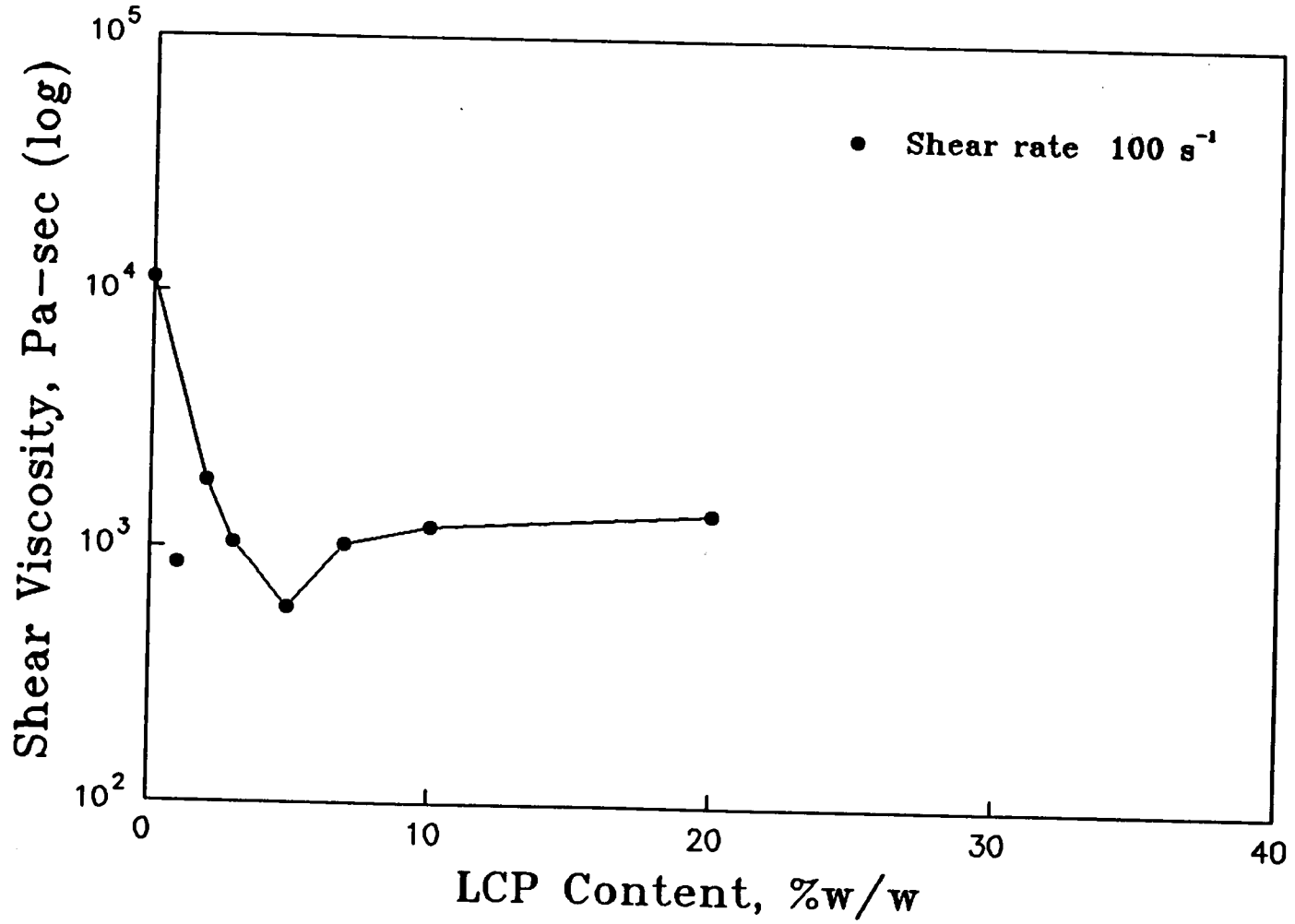

Fig. 3.16: Melt viscosities of PAr / Vectra (V) blends under capillary flow for a steady shear rate.

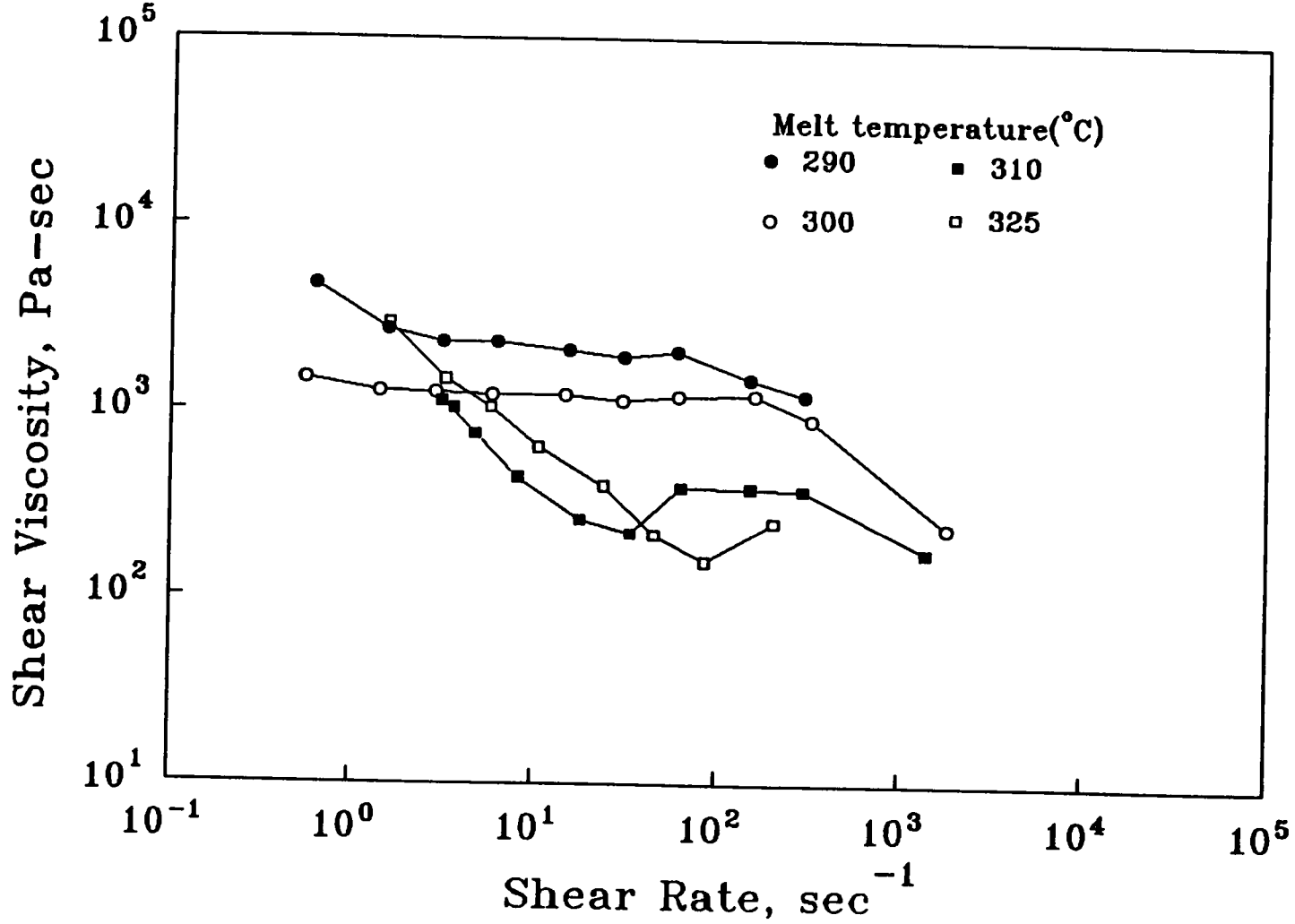

Fig. 3.17: Melt viscosity of PAr / Vectra (V) blend (90/10) at different melt temperatures.

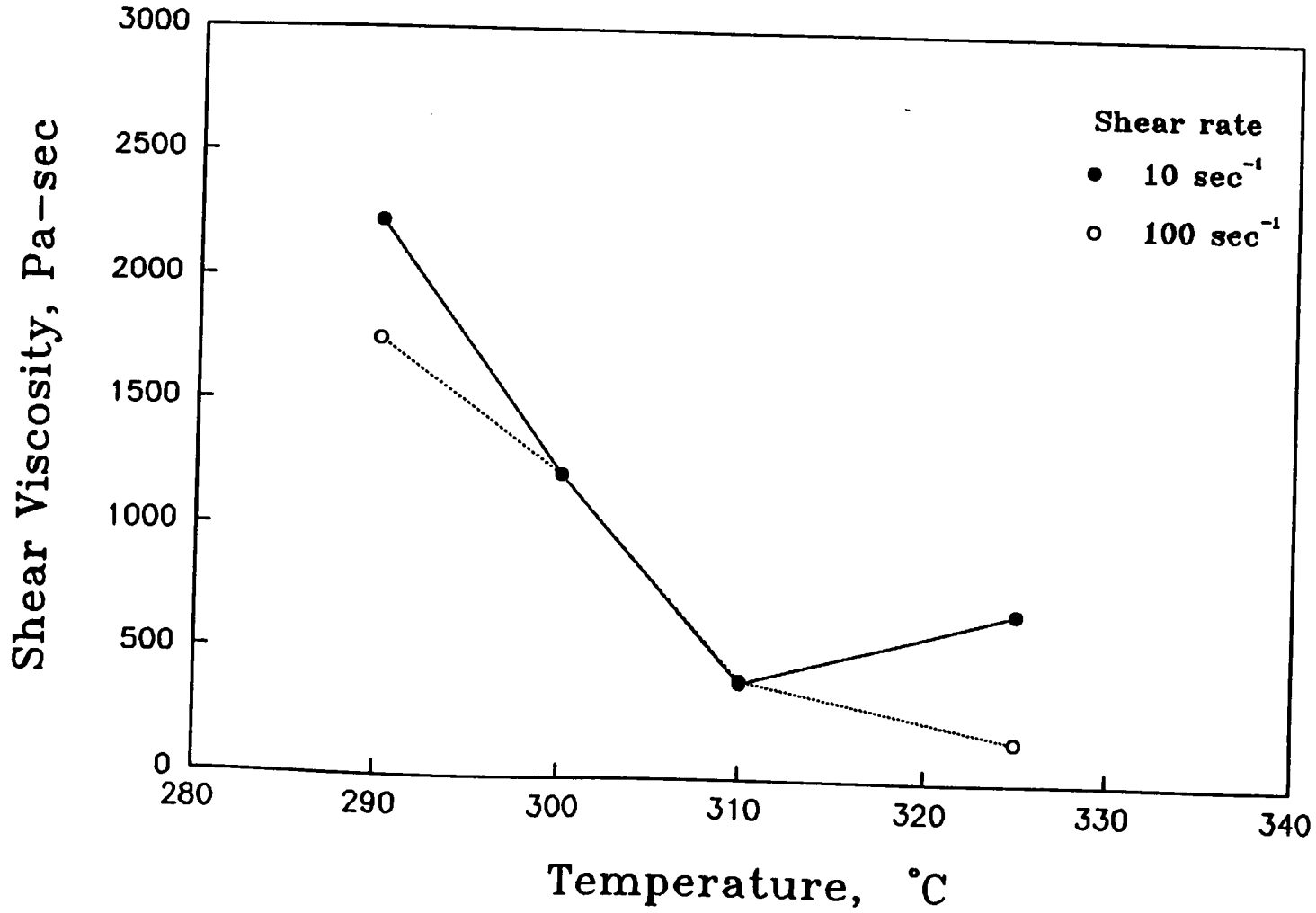

Fig. 3.18: Melt viscosity of PAr / Vectra (V) blend (90/10) at different melt temperatures.

290°C improves moderately to lower value at 300°C both showing a Newtonian plateau region between 10 to 100 sec^{-1} (Fig. 3.17). After about 100 sec^{-1}, viscosities measured at both these temperature decreases with the shear rate with only a small difference between them. At high temperatures, on the contrary, the shear thinning behavior of the melt begins at low shear rates and continues up to about 100 sec^{-1} before a short plateau region is obtained. Activation energies for the melt flow have been estimated using an Arhenius type of relationship in the temperature range of 290 to 310°C. Slopes of the inverse temperature plots shown in Fig. 3.19 gives their values as 138 and 117 kJ/mole at shear rates of 10 and 100 sec^{-1} respectively.

3.5 Mechanical Properties

Fibers spun from different blend compositions and under varying spinning conditions were analyzed for their tensile properties using an Instron tensile tester. These properties will be useful in describing their two phase morphology examined earlier through optical and scanning electron microscopy of the fracture surfaces. Results of modulus of elasticity, breaking strength and the breaking elongation have been plotted as a function of LCP composition for a uniform strain rate of 20 mm/min. (80% /min.) and are presented in the Figures 3.20-3.22. These result show a significant increase in the elastic modulus of the blends beyond a composition of about 10% by weight of LCP. The overall increase at 15% LCP composition is shown to reach a value close to 300% improvement over the neat polyarylate spun under identical conditions. The breaking stress measured for the blends shows a dip

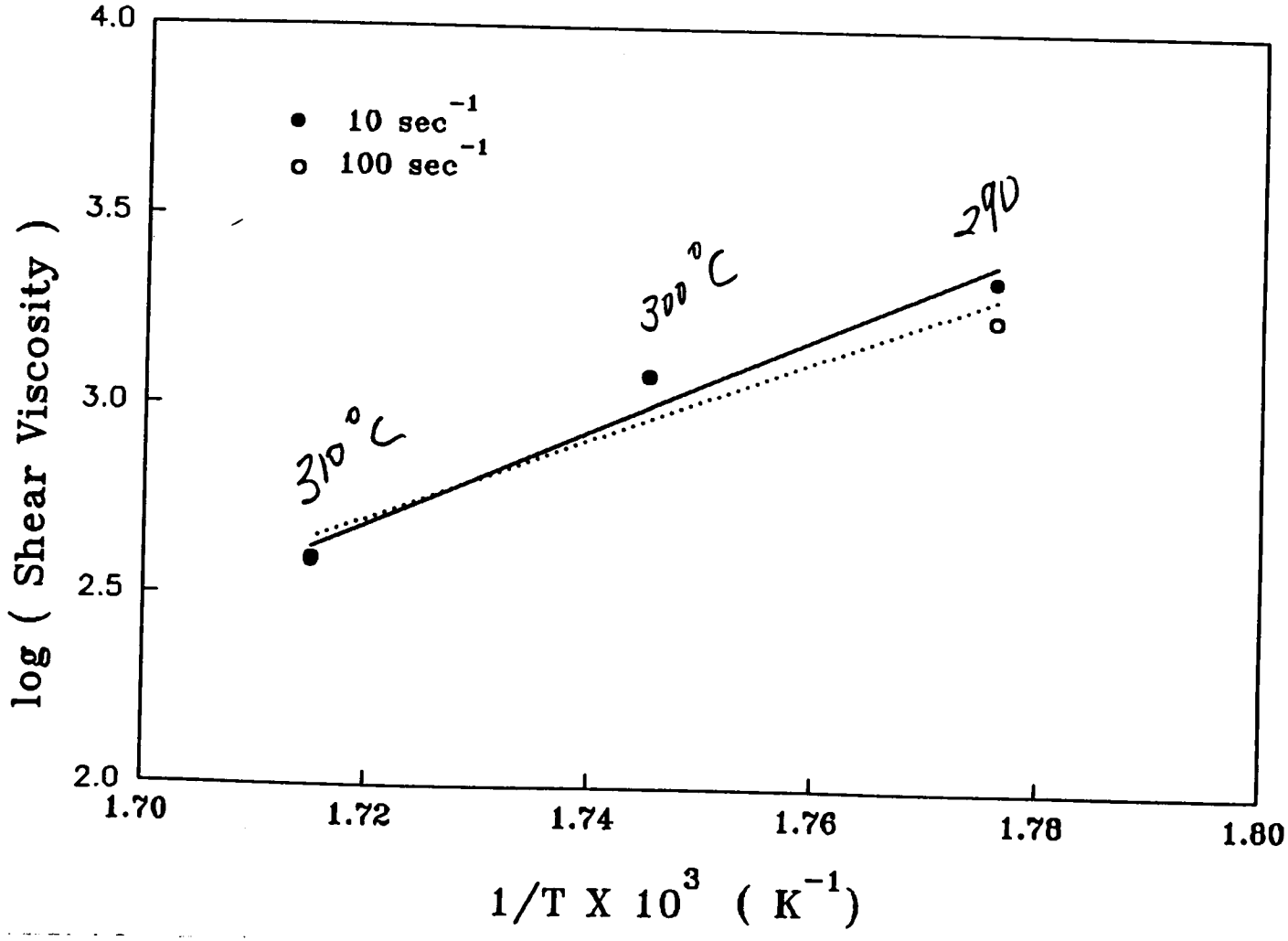

Fig. 3.19: Determination of flow activation energy of PAr / Vectra (V) blend (90/10) using Arhenius type relation.

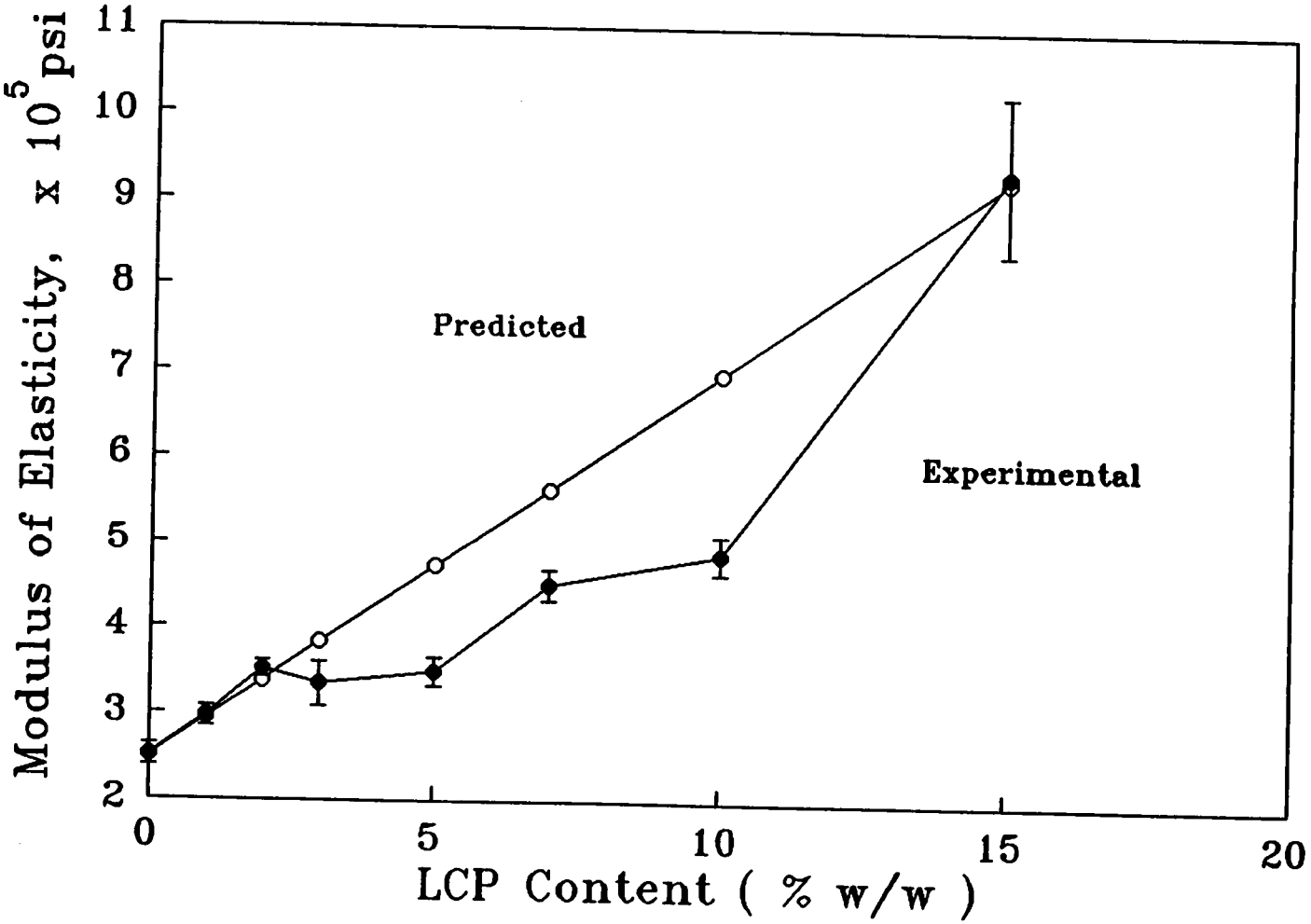

Fig. 3.20: Modulus of elasticity of PAr / Vectra (V) blend fibers of varying composition.

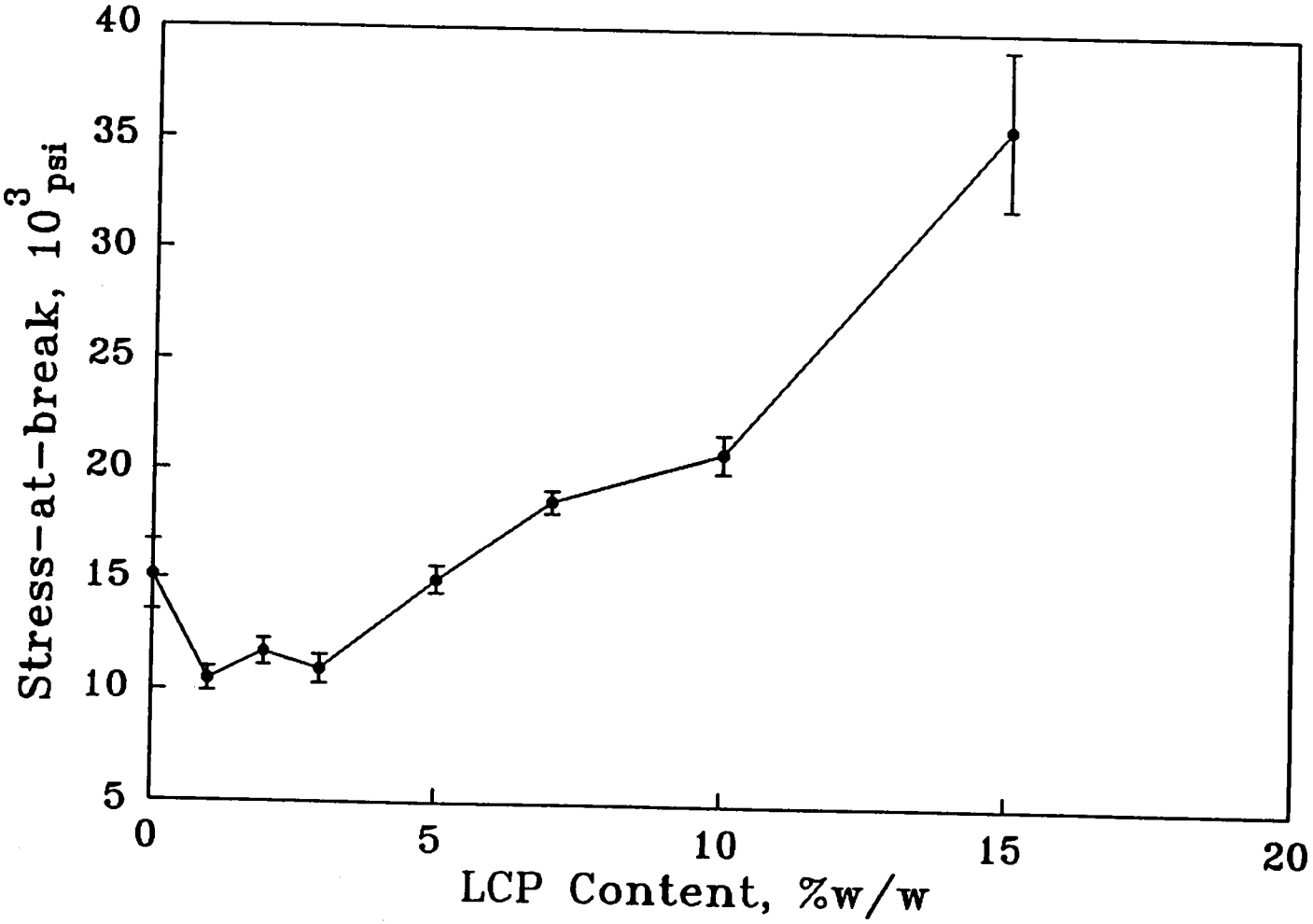

Fig. 3.21: Stress-at-break of PAr / Vectra (V) blend fibers with varying LCP compositions.

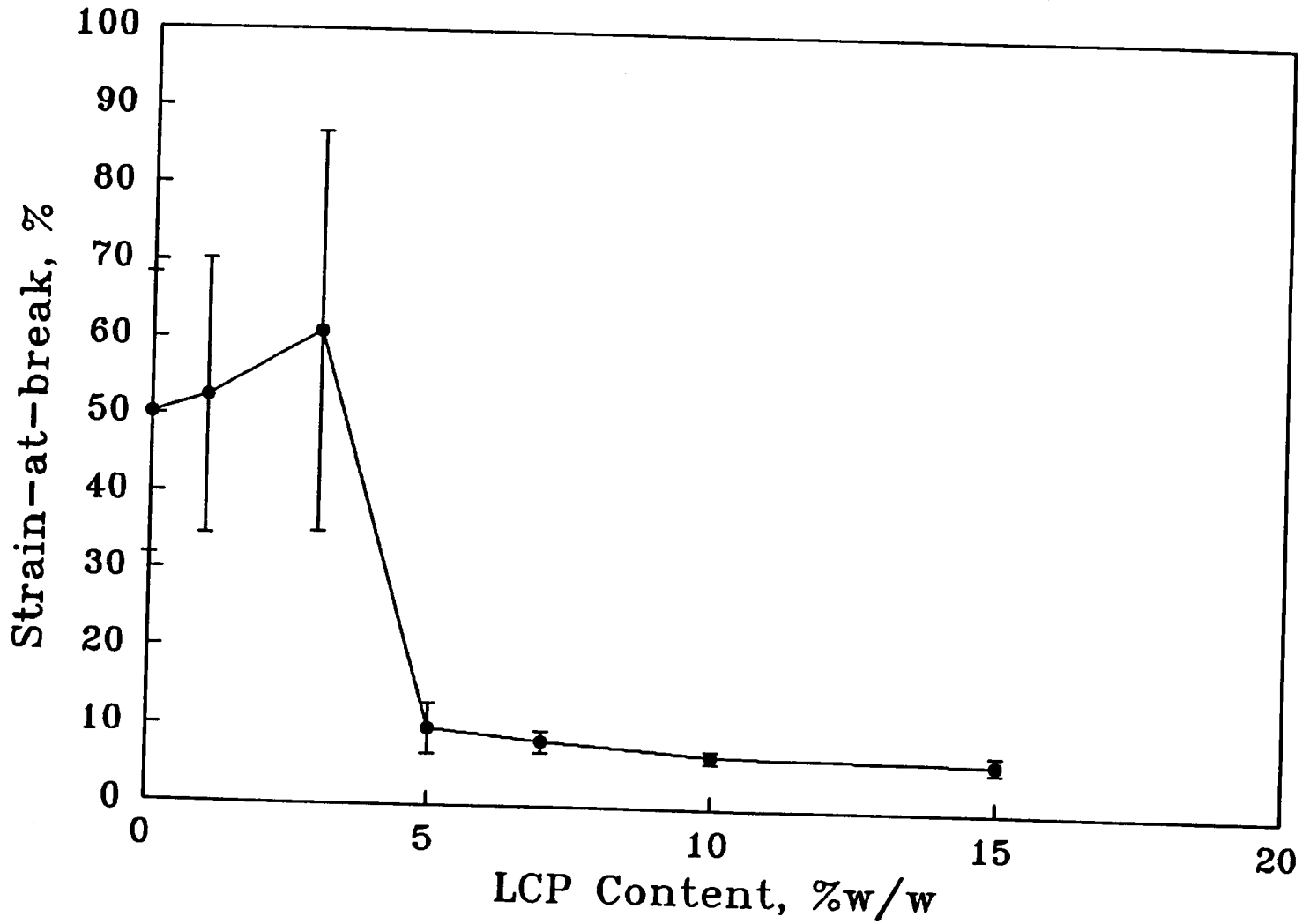

Fig. 3.22: Strain-at-break of PAr / Vectra (V) blend fibers of different LCP compositions.

at low compositions of LCP (1-3% by weight) before monotonically increasing to higher values as the LCP content increases (Fig. 3.21). There is observed to be more than a 100% increase in the breaking strength value at 15% LCP composition. Fig. 3.22 depicts the change in the breaking elongation values for the blends. Breaking elongation of the blends is shown to improve up to 3% LCP. Beyond 3% LCP content the elongation values drop very sharply to less than 10% for all compositions up to 15%. Varying the melt draw ratio during the spinning of these blends is shown to increase the modulus of the resulting fibers significantly. A nearly linear increase in the modulus of the fibers containing 10% LCP by weight was observed upto a draw ratio of 114 as shown in Fig. 3.23. A similar trend has also been observed with the breaking strength data of these fibers. Improvement in breaking strength is shown to be around 50% at high draw ratios (Fig. 3.24). Breaking elongation values have been shown to reduce marginally to about 5% at high draw ratios (Fig. 3.25). Therefore a further reduction in the toughness of the fibers results due to an increase in the melt draw ratios.

Modulus and breaking strength of the fibers spun from 10% LCP blend is shown to reach a maximum value at a melt temperature of 300-310°C as shown in Figures 3.26 and 3.27. At all other temperatures it is, however, shown to decrease to lower values. Breaking elongation of the spun fibers is shown to change slightly to higher values until the a melt temperature of 320°C (Fig. 3.28). Melt shear rate in the capillary die extrusion is shown to influence the mechanical properties of the resulting fibers as shown in figures 3.29-3.31. Once again there is observed to be an optimum shear rate of about 164 sec^{-1}, when all the properties register maximum

values. Improvement in modulus is shown to be significant on increasing the shear rate from 48 sec^{-1} to 164 sec^{-1}. It, however, drops off gradually at high shear rates (Fig. 3.29). Elastic modulus data for the pure LCP fibers spun at a melt temperature of 300 • C shows an initial increase with increase in the melt draw ratio. After a melt draw ratio about 30, the elastic modulus is shown to drop significantly to lower values as shown in Figure 3.32.

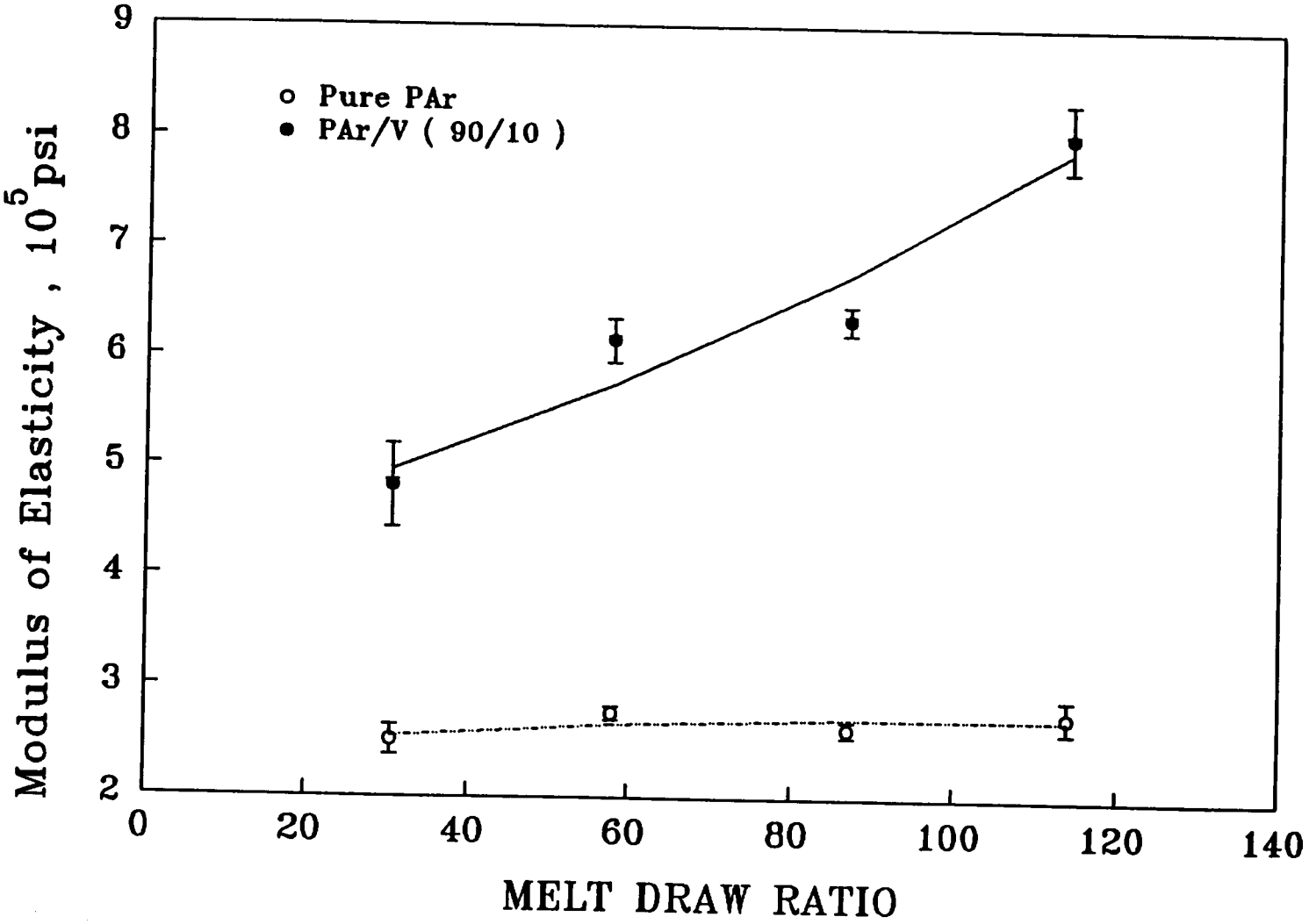

Fig. 3.23: Modulus of elasticity of fibers spun at different melt draw ratios.

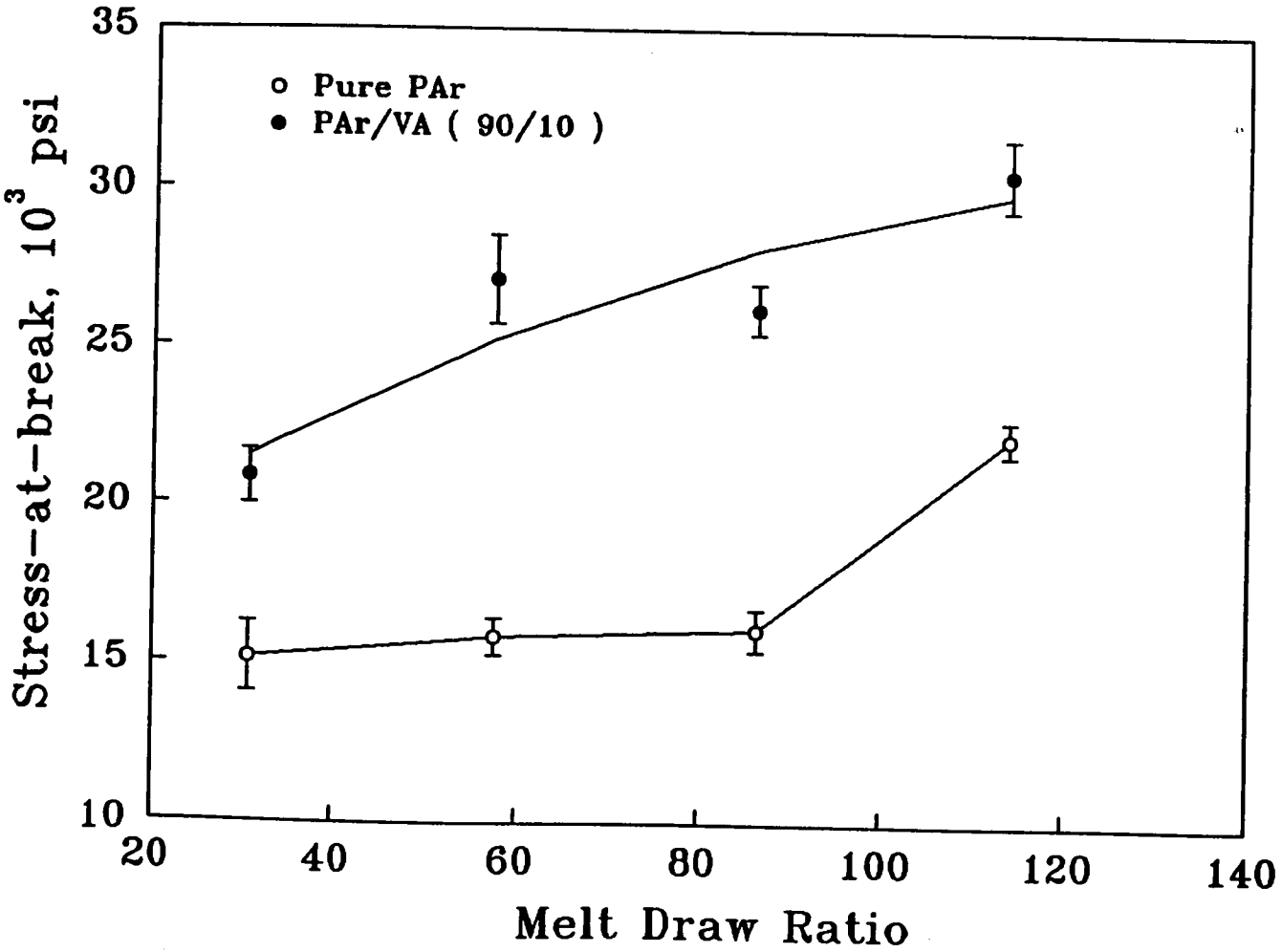

Fig. 3.24: Stress-at-break of fibers spun under different melt draw ratios.

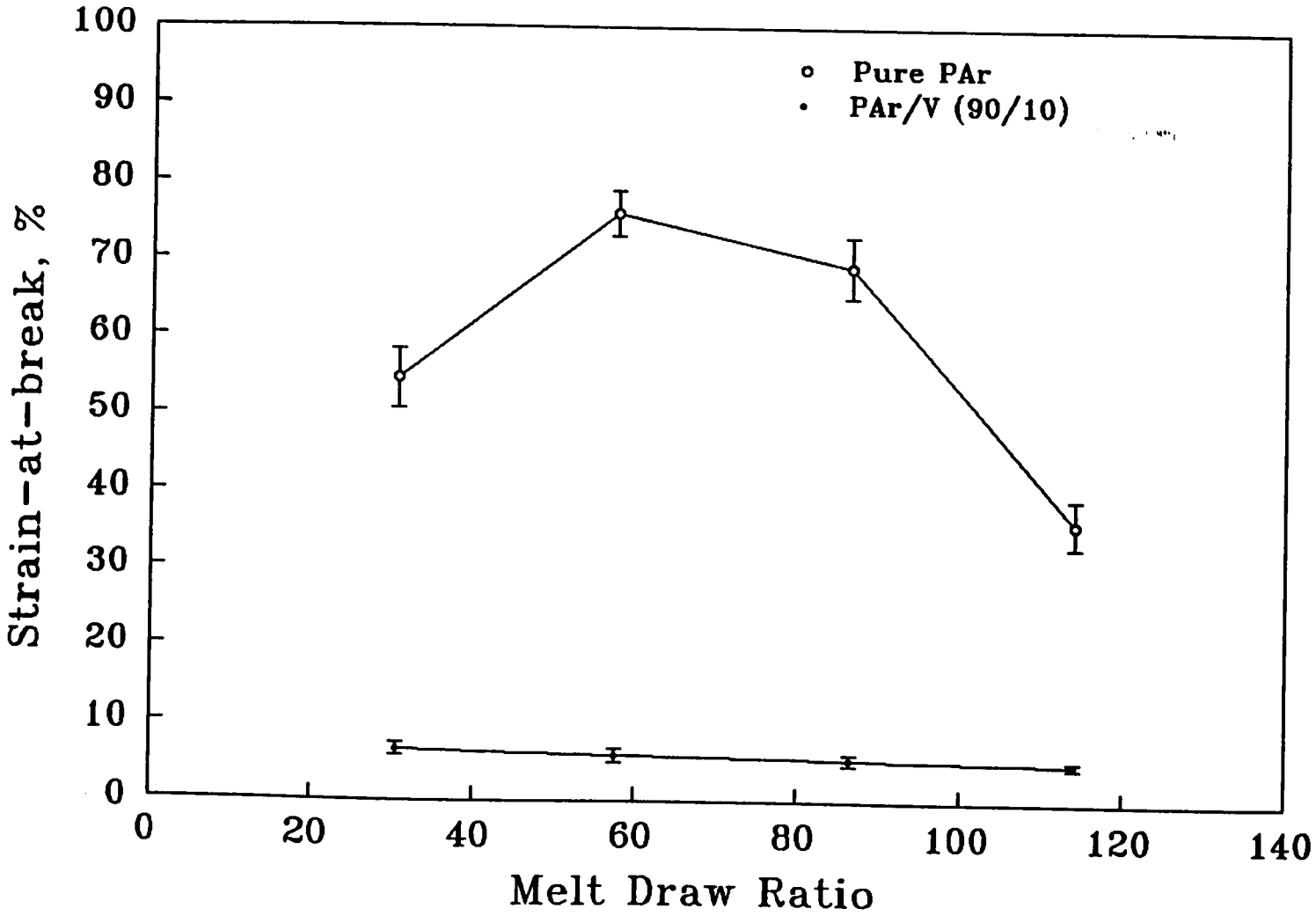

Fig. 3.25: Strain-at-break of fibers spun at different melt draw ratios.

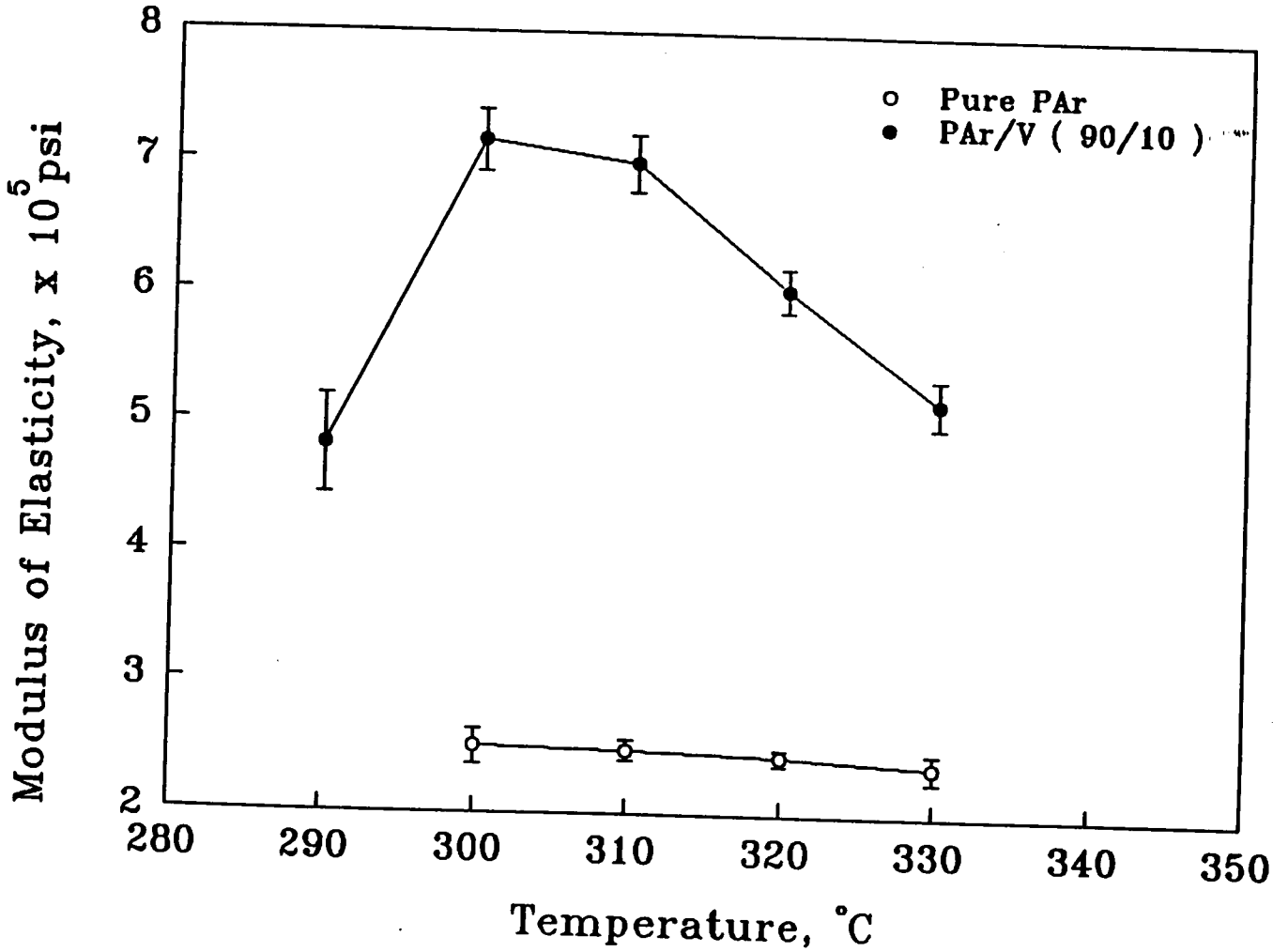

Fig. 3.26: Modulus of elasticity of fibers spun at different melt temperatures.

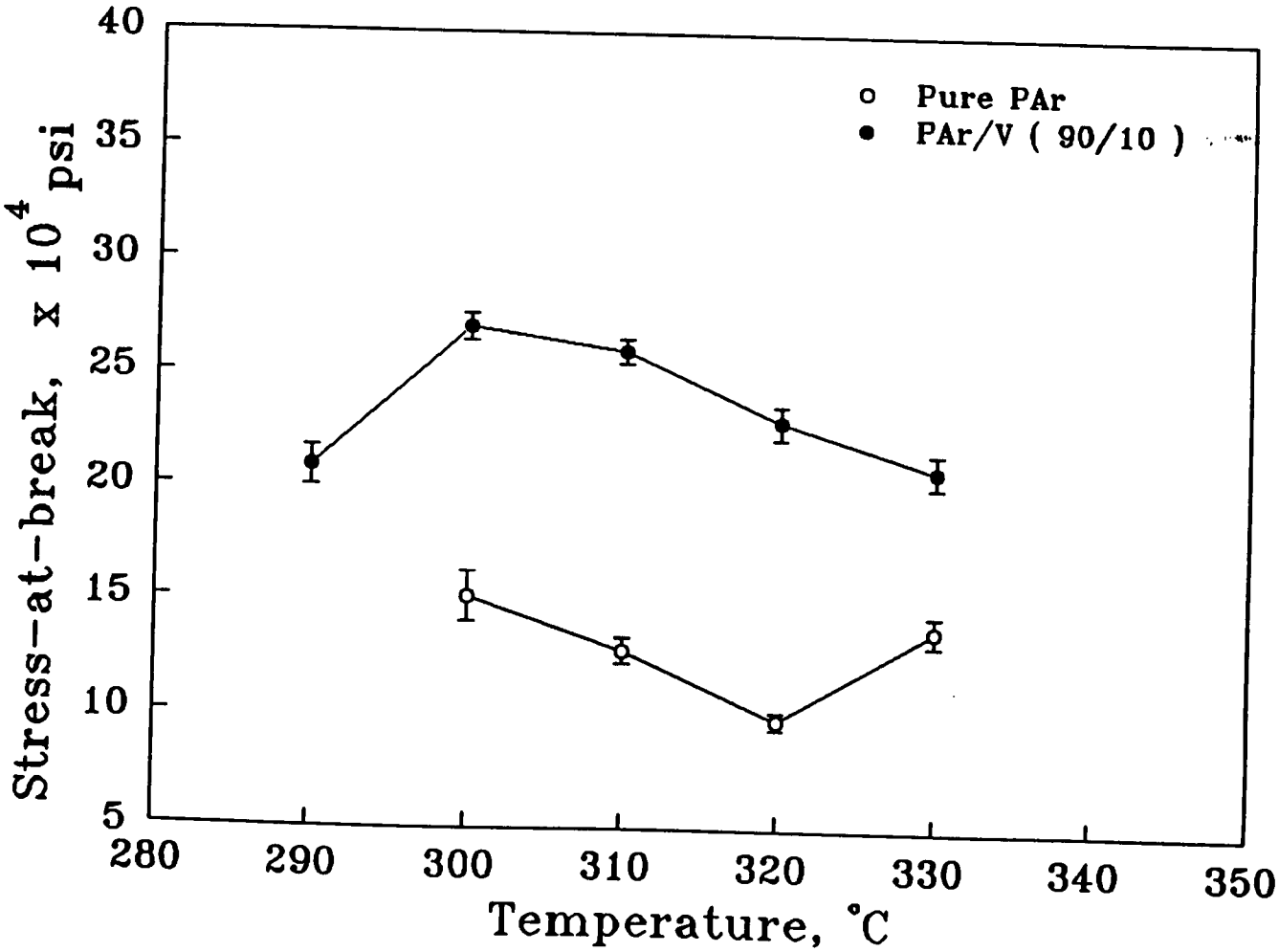

Fig. 3.27: Stress-at-break of fibers spun at different melt temperatures.

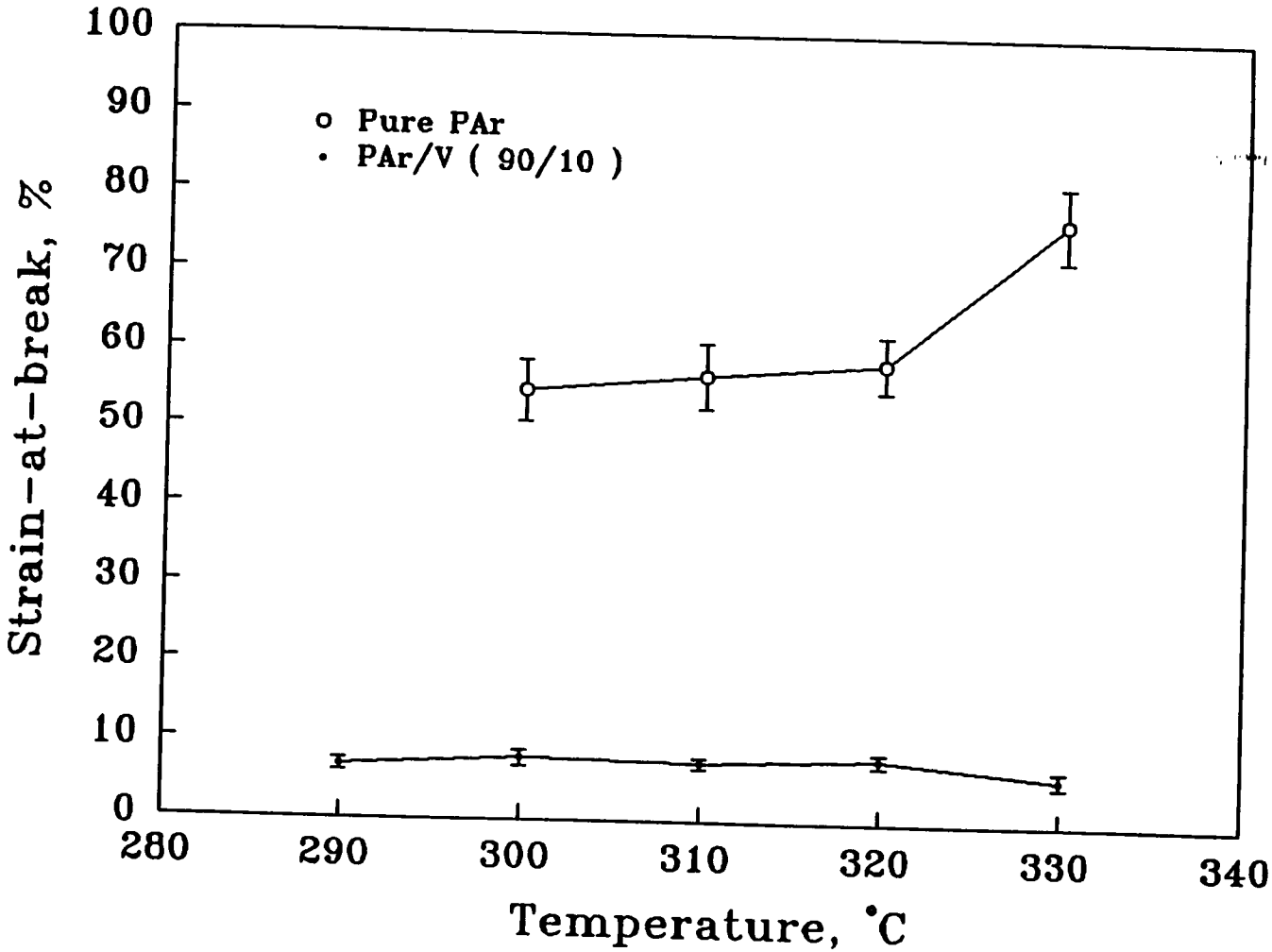

Fig. 3.28: Strain-at-break of fibers spun at different melt temperatures.

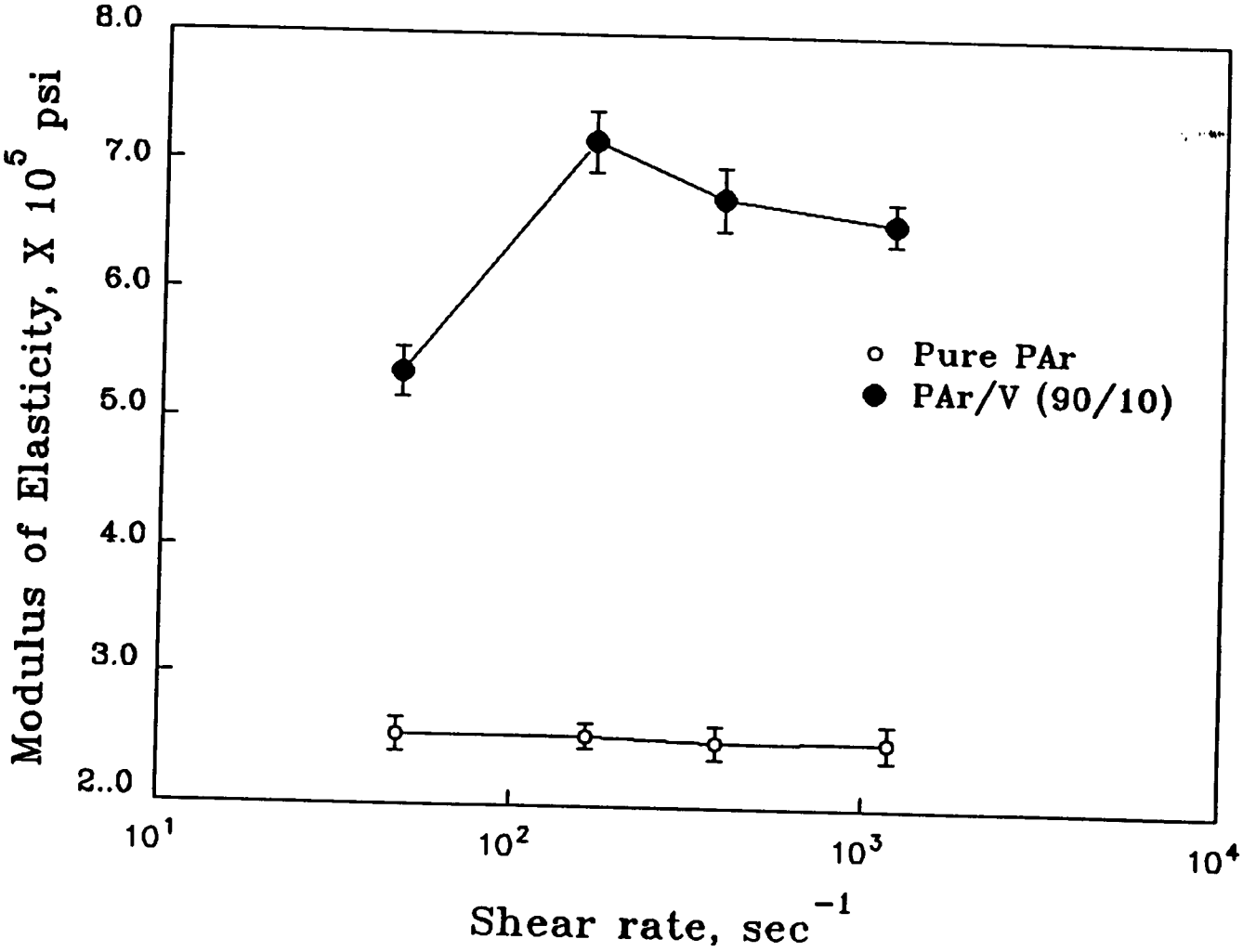

Fig. 3.29: Modulus of elasticity of fibers spun at different melt shear rates.

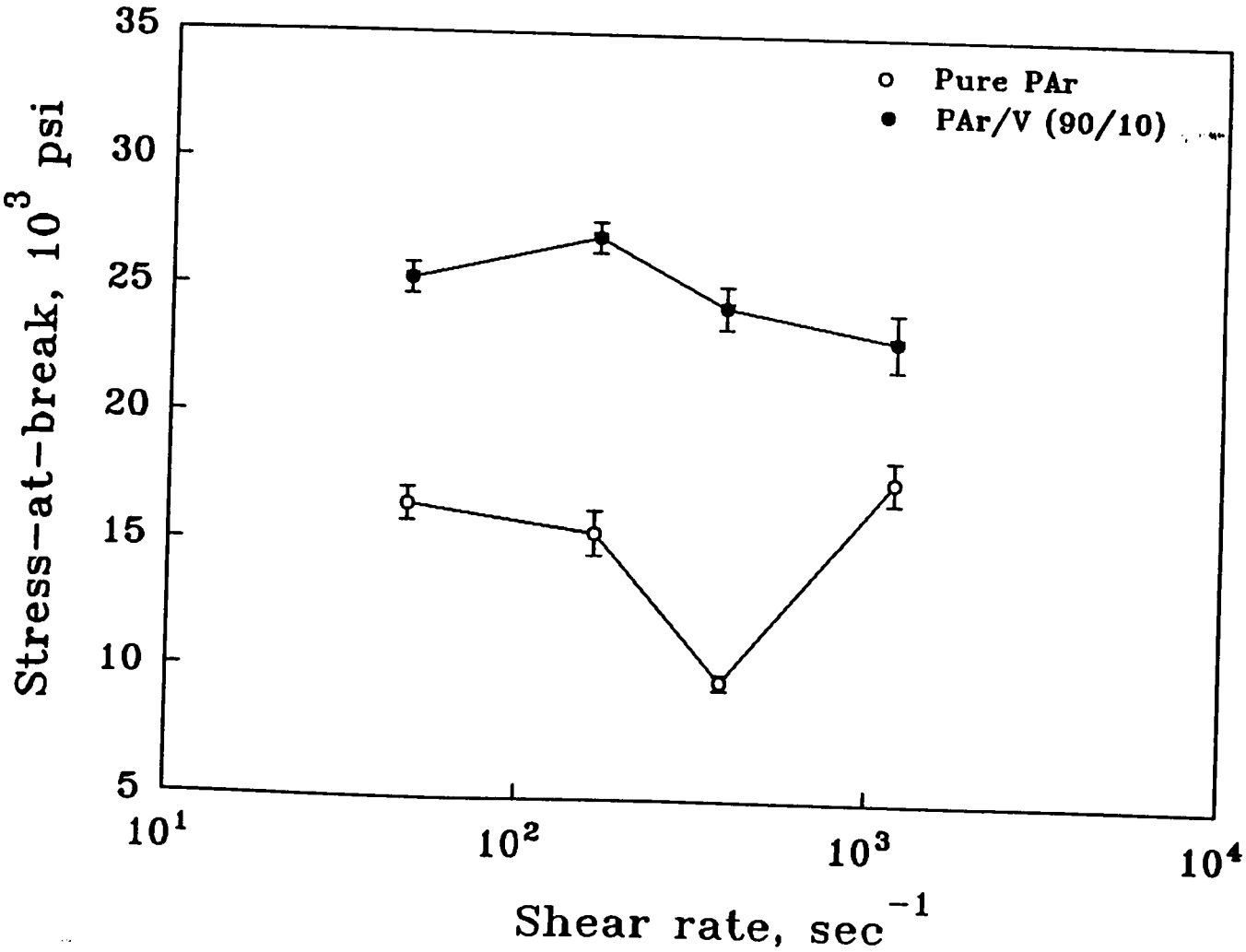

Fig. 3.30: Stress-at-break of fibers spun at different melt shear rates.

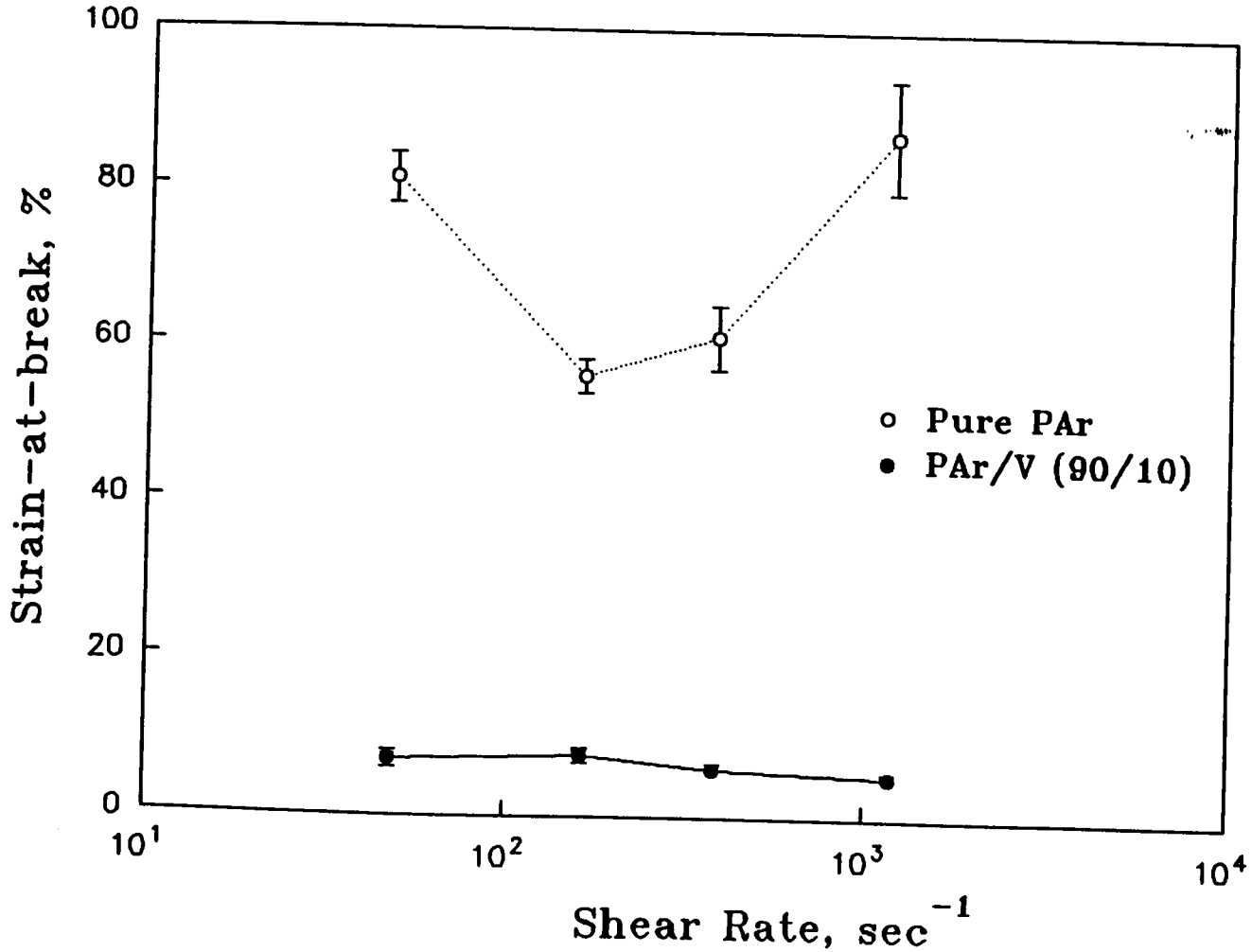

Fig. 3.31: Strain-at-break of fibers spun at different melt shear rates.

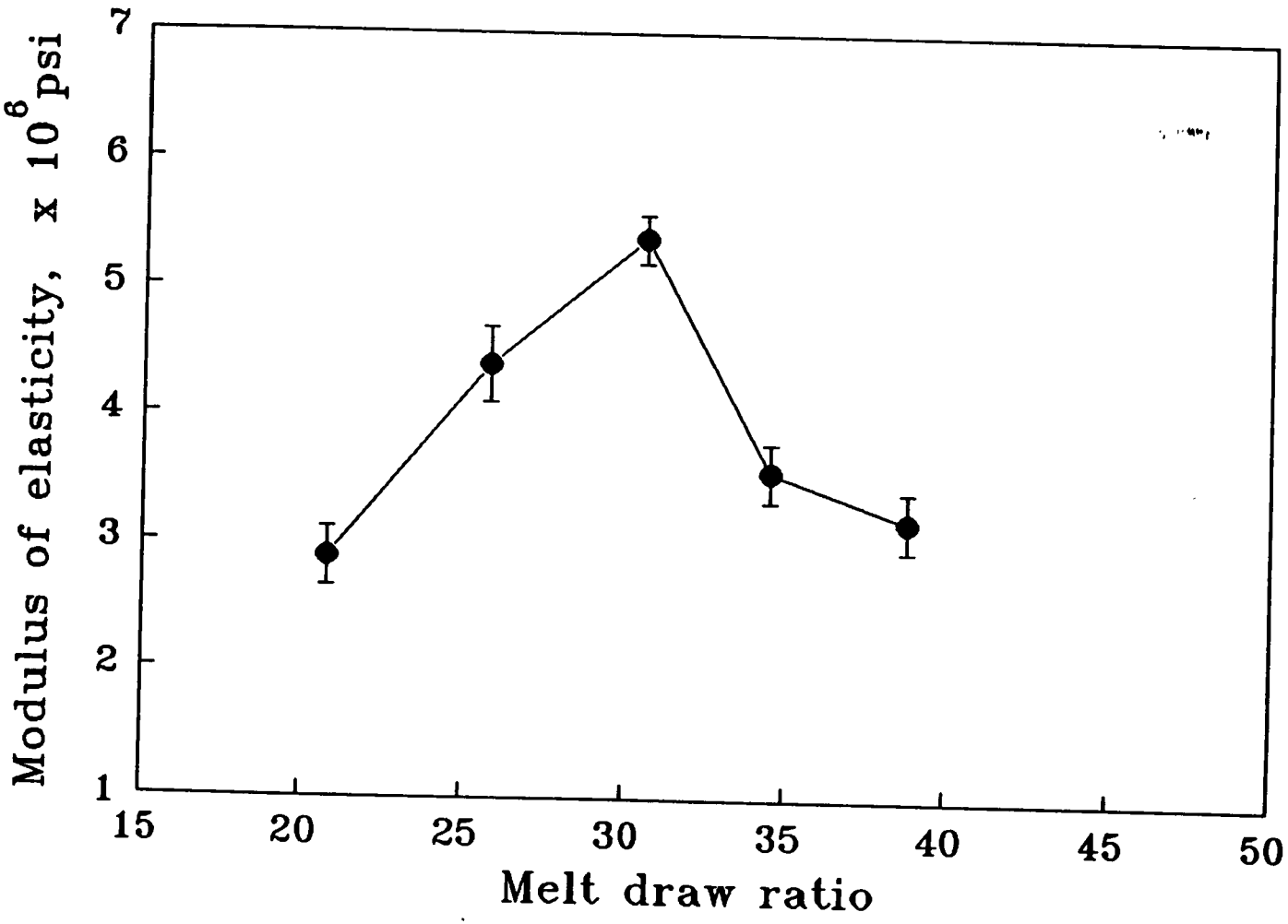

Fig. 3.32: Modulus of elasticity of fibers spun from pure LCP (Vectra) at different draw ratios.

CHAPTER 4

DISCUSSION

4.1 Thermal Analysis of Neat Polymers and Blends

Differential scanning calorimetry analysis of the as received samples of polyarylate showed an erratic glass transition in the range of 175 to 200°C. This can be explained in terms of a previous thermal and mechanical history imparted during the synthesis and extrusion of this material. Such frozen-in stresses due to fast cooling steps may cause enormous entropy relaxations during the glass transition processes while they are heated for the first time. Irreversible release of such stresses hinder the heat flow measurements, therefore an erratic glass transition behavior is obtained. Quenching of the melt from 250°C at a uniform cooling rate of 200°C/min apparently destroys the previously unknown thermal and mechanical history of the sample and allows a reproducible measurement of glass transition temperature. Therefore the second heating experiment in the DSC showed a typical glass transition for polyarylate at 183°C.

However the DSC traces of one of the several runs made in the as received condition showed a glass transition at 178°C followed by an exotherm probably due to the crystallization of occasional impurities induced by traces of residual solvent. This situation can be considered similar to that of polymers which crystallize due to incorporation of solvent, e.g. atactic polystyrene crystallizes due to carbon

disulfide[121]. Such traces of crystalline impurities show some evidence of melting during the second heating of the specimen quenched from the melt at 250°C. A T_g of 178°C obtained during the third subsequent heating run following the quenching of the melt from 375°C apparently reflect a state free from any residual solvent. A lower T_g of 178°C as compared to 183°C obtained previously for the samples quenched from a melt temperature of 250°C merely reflect an increased amount of free volume trapped upon quenching from a higher melt temperature. A decreased glass transition temperature of 178°C observed during the first heating run in DSC using as received polyarylate can be explained in terms of plasticization caused by the absorbed moisture.

Polyarylate has been found to be sensitive to the atmospheric moisture. Glass transition temperature of the polyarylate decreases fairly rapidly for the material exposed to humid air at room temperature (Fig. 3.3). This could be explained in terms of the plasticization induced by the absorbed moisture. The plasticization is reduced significantly for the samples kept under drierite inside a dessicator. The T_g of polyarylate decreased by about 4°C due to small amount of residual moisture with in the material due to limited drying efficiency of the drierite.

A glass transition temperature of 92°C observed for the thermotropic copolymer of HBA/HNA (75/25) reflect considerable reduction as compared with 161°C for the homopolymer of POB. This could be explained in terms of decrease in the symmetry of the chain disrupting the crystalline order of the POB homopolymer. The broad nature of this glass transition along with low heat capacity

jumps can be compared with the enormous transition breadth of some of the PON rich copolymers[122] (about 200°C). The endothermic transition centered at 279°C can be associated with a crystal-mesophase transition for this copolymer composition[123]. The first endothermic peak at about 240°C which turns significant only after annealing at 260°C, is reportedly associated with the transformation of an orthorhombic crystalline form into a pseudo-hexagonal phase[124]. According to this investigation, it was shown that the second endotherm for this copolymer is believed to arise due to the transition of initially generated hexagonal crystals into an anisotropic mesophase. Therefore, these authors suggested that the annealing of the as received Vectra is shown to produce a more stable orthorhombic form from the initially produced hexagonal phase. The mesophase associated with this copolymer system has recently been recognized as having conformationally disordered structure (condis phase) up to a very high temperature[125]. This bears support from the observation of low heats of transition associated with these endotherms. The condis phase as opposed to the liquid crystalline structure is believed to have enhanced conformational mobility with a high degree of axial and three dimensional order[126]. Sclerian textures associated the copolymer melt above the crystal-mesophase transition traditionally associated with the nematic structure of the LC phase[127] have now been shown to remain unchanged for this copolymer from room temperature up to the decomposition temperature[128]. Quenching of the melt from 375°C at a cooling rate of 40°C followed by a second heating of the copolymer apparently improves the overall crystallinity. This is supported by higher heats of

transition with accompanying narrow peak widths for the different endotherms shown in the DSC traces. Similarly, isothermal annealing done at 260°C tends to perfect the different crystalline modifications contributing to an increase in overall crystallinity. There is, however, no well defined peak shown reflecting a transformation of the mesophase melt into the isotropic state up to a temperature of 400°C.

A moderate decrease in the T_g of the immiscible polyarylate phase of the blends particularly for in the 3-4% LCP in the blend may be associated with the plasticization caused by a partially miscible low molecular weight end of the LCP material. However, a constant low T_g of the blends containing 3 and 4% by weight of LCP was found reproducible in the cyclic heating and cooling experiments done in the DSC. This evidence eliminates the possibility of plasticization of the polyarylate caused by any traces of moisture. Additional evidence supporting partial miscibility of component polymers have also been obtained through tan δ peak temperatures recorded for different composition up to 10% of LCP (Fig. 1, appendix B). T_g of the neat immiscible polyarylate is however evident in the blends with the LCP compositions of 10% and above. At a concentrations of 40% LCP in the blend , a slow decrease in T_g of the polyarylate phase accompanied by broadening of transition is probably indicative of a substantial interphase region.

4.2 Polarized Optical Microscopy of the Blends

The thermotropic copolymer from HBA/HNA (Vectra A) is shown to give an immiscible system with two phase morphology as shown by the optical microscopy of

its blends with polyarylate. A physically immiscible nature of the two components was also noted earlier in the DSC measurement on the blends. However, unlike as suggested from the DSC studies, blend containing 2% LCP by weight does not show any appreciable signs of miscibility.

Blends prepared by extrusion in the Brabender single screw extruder were shown to contain fairly uniform distribution of LCP particles having spherical diameter in the range of 0.5 to 2 microns. Such fine dispersion of the LCP particles could be generated due to strain deformation of the large LCP phases caused by small regions of vertical pins installed in the conventional parallel flow channel of the screw. The spherical shape of the dispersed LCP particles observed in the microtomed sections of the extruded strands can be expected due to the balancing of interfacial forces between the immiscible phases. Converging flow at the die entrance may generate high extensional forces to produce LCP particles that are deformed along the flow direction. Such deformations of dispersed LCP phases will have transient existence and would quickly relax back into spherical shapes as observed in the solidified extruded strands. It is however highly unlikely that such spherical shapes would have been formed due to breaking of the deformed LCP phases as has been suggested elsewhere for similar blends containing LCP[75]. No direct experimental evidence for the possible flow morphologies in such situations has ever been obtained.

4.3 Scanning Electron Microscopy of Fracture Surfaces

The dispersed LCP phase in the blends has been shown to be roughly spherical in shape in the extruded filaments that were not drawn during the cooling of the melt. This was supported by the observations in the optical microscopy of these extrudates. Spherical droplets of embeded LCP were also clearly evident in the SEM view of the fractured extrudate filaments. This is shown in Figure 3.8a for a blend composition containing 10% by weight of LCP. A similar morphology can also extrapolated to other compositions as well. The size of these particles was found to be in the range of 0.2 to 1.5 microns. This size distribution compares very well with the observation made earlier in the optical micrographs of the microtomed sections of the extrudates for the same composition of the blend. Breaking of this filaments formed by free extrusion apparently shows poor adhesion as revealed by the voids generated by the dewetting the spherical particles from the matrix during fracture.

The fibril shaped morphology for the dispersed LCP was shown to be present in the extruded fibers obtained by drawing of the cooling melt in the post die conditions. Apparently, the dispersed LCP fibrils observed in the fracture surface obtained from fibers were most probably formed during the melt drawing following the extrusion through the capillary die. The tapering ends of the protruding fibrils obtained on the fracture surface of these fibers could have arisen from the ductile failure of the preformed LCP fibrillar phases during the tensile stretching. This can be anticipated on the basis of high ductile properties of the microfiber structures

which apparently develop high degree of chain orientation.

The fibrils observed in the melt drawn fibers were shown to be highly oriented parallel to each other and to the overall fiber axis of the spun fibers. This is clearly shown by the bundle of stacked LCP fibers obtained after stripping of the matrix polyarylate by dissolving it selectively in chloroform. By looking at the fracture surface, a similar morphology can be anticipated in the case of fibers obtained from other compositions as well. The aspect ratio of the separated LCP fibrils of the fibers containing 10% LCP can be estimated to be in the range of 50 to 200 (Fig. 3.8b). An exact estimate of this range could not ascertained due to extensive interpenetration and poor resolution of fibrils. The diameter of these fibrils is found to be in the range of about 0.05 to 0.3 microns. The approximate volume of each of these fibrils may be estimated for an aspect ratio of 100 and a diameter of 0.2 microns. An average fibril volume of 0.628 $(micron)^2$ obtained in this way can be compared with the volume of spherical droplets that were seen in extruded filaments without any drawing on the melt for an identical composition. The later quantity is estimated to be about 0.268 $(micron)^2$ for average estimated diameter of 0.8 microns. Therefore it is evident that some of these particles do coalesce to generate larger particles during the converging flow at the die entrance at low extrusion rates used for fiber spinning. These large particles could then deform further due to the elongational forces from post die drawing of the melt.

The formation of such fibrillar phases of the dispersed LCP could be attributed to high melt viscosity of PAr as compared to a dispersed LCP phase. Such

flow morphology develop quickly in the case of two immiscible Newtonian fluid when their viscosity ratios substantially exceeds unity. Formation of such fibrillar phases and the variables affecting them have been analyzed in studies conducted on different systems[89,75]. Dispersed LCP was also shown to possess fibrillar morphology in the blends with PS and PS/PPE as the matrix[118]. Such elongated structure for the LCP was shown at compositions as low as 2% by weight of LCP with apparently low aspect ratios.

A geometric analysis assuming a random distribution of these highly oriented fibril like structure of dispersed LCP can be given to predict and correlate the mechanical properties of the fibers in terms of the aspect ratio of these reinforcing LCP phases. Tentative values of the aspect ratio can be ascertained first for the fiber made from the blend containing 10% by weight of LCP. Assuming an aspect ratio of 100, the average fibril volume was calculated above to be 0.628 $(microns)^2$. Now the number of pulled out fibrils observed in a tensile break would then be given for a typical scanning cross section of area of 96 $(micron)^2$ as,

$$v_t * A * L * 2 / V_1$$

where L is taken as 3 microns, equal to the maximu

m length of the pulled out fibril. v_t and V_1 are the total volume fraction and volume of a single fibril respectively. Area 'A' is taken as 96 $(microns)^2$ equal to photographed region. This gives an expected value of 46 for the fibers from the blends containing 10% by weight of LCP. The actual number of the pulled out fibrils on the fracture surface of the fiber is found to be about 62. An increased value of

number of pulled out ends is indicative of an lower aspect ratio than an assume value of 100 for the reinforcing fibrils. For the fibers from 15% blend, an identical calculations leads to an expected value of 70 pulled out ends against an actual number of 68. The aspect ratio of the dispersed fibrils in the case of 15% blend is evidently greater and is perhaps equal to the assumed value of 100. If part of the fibril ends seen in the fracture surface were formed by a ductile fracture, then it would reduce the actual number of pulled out fibrils to raise the estimated value of the aspect ratios in each case. The observations of fracture surface morphology based on the aspect ratios of the reinforcing fibrils is found to be in agreement with the mechanical properties of these fibers. A similar calculations have also been made for the low LCP composition blends resulting in low aspect ratio of the reinforcing particles.

An estimate of the actual fraction of the total volume of fibrils shown as pulled out ends on the fracture surface may also be obtained from the rule of mixtures. This has been plotted Figure 4.1. It may be seen from this plot that a large fraction of the total volume of LCP is associated with the fibril ends especially at low LCP contents. Alternatively, it may be explained in terms of a large deviation from the rule of mixtures in case of low LCP blend fibers due mainly to small aspect ratios of the reinforcing fibrils.

The adhesion between the fibrillar LCP particles and the matrix was seen to be poor primarily because of the low aspect ratio of the reinforcing fibrils. This is clearly shown through a number of holes visible on the fracture surface of the fibers

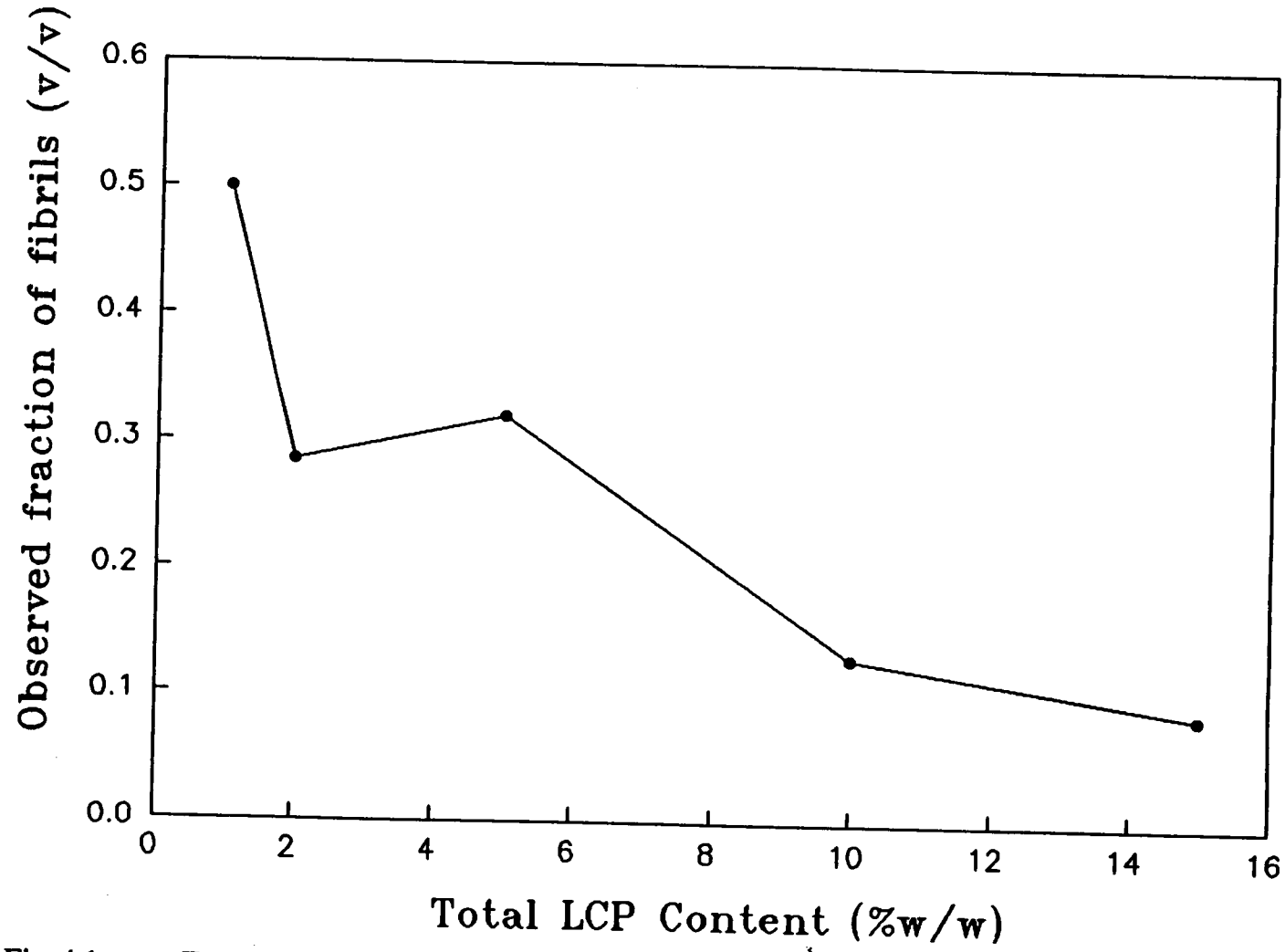

Fig. 4.1: Fraction of added LCP volume seen as pulled out fibrils on the fracture surface of the blend fibers.

prepared out of different compositions. Due to lower relaxation time of the deformed LCP phases they relax quickly in the post die conditions when the melt still hot. Therefore, undrawn extrudates contain LCP particles that are spherical in shape. High surface tension of the dispersed LCP melt can also induce a faster relaxation by overcoming the weak orienting influence of the shear field. In the presence of extensional forces due to pulling of the melt at the die exit these relaxation effects are more than offset. These extensional forces induce further deformation of the LCP phases improving their aspect ratios significantly before it is stopped by increasing viscosity of the cooling melt.

Fibers spun at low melt temperatures (290°C) apparently do not develop high aspect ratios from relatively smaller LCP droplets (Fig. 3.12a). This can be due to low diffusion of dispersed LCP phase through a high viscosity matrix. Elongation of the smaller droplets will only give rise to smaller fibril lengths. At a melt temperature of 300°C, however, medium viscosity is low enough to permit diffusion and agglomeration of the droplet more uniformly across the matrix. Larger LCP phases developed in this way are about the right size that can elongate into long, parallel fibrils having the necessary uniaxial orientation. In such cases the fibrils have better adhesion with the matrix which itself gets oriented due to elongational flow field. Fiber spun from high melt temperatures (330°C), however, represent an extreme case when the matrix viscosity is very low to allow rapid diffusion and agglomeration into large LCP phases that deform inadequately into tapering fibrils (Fig. 3.13c).

Fibers spun at low shear rate of 48 sec^{-1} give rise to poorly aligned matrix chains, therefore poor adhesion to well oriented LCP fibrils (Fig. 3.15). Any crack initiated at one of weak surface flaws can then propagate easily across the fiber dewetting a poor interface generated around these oriented LCP fibrils (Fig 3.14). Fibers spun at high shear rate (1134 sec^{-1}) probably developed low aspect ratio fibrils because of a rapid elongation of the smaller droplets which prevents their diffusion and growth into larger particles. Intermediate shear rates (e.g. 164 sec^{-1}) however provide the right balance between the between the particle growth and deformation into fibrils having close to uniaxial orientation. High draw ratios imposed on the melt during spinning, however, show evidence of plastic deformation of the matrix improving the orientation of the matrix chains (Fig. 3.13a). This will be reflected in further improvement in adhesion of the reinforcing fibrils to the matrix.

4.4 Melt Rheology of the Blends

Dynamic melt viscosities of the LCP blends have been shown to influence the morphology developed in the extruded fibers. Melt viscosity of all the blends of polyarylate and the HBA/HNA copolyester were found to be much reduced as compared to that of the neat polyarylate. Except for very low LCP content (1% w/w Vectra blend), a continuous decrease in the shear viscosity of the melt was obtained up to 5% LCP content (Fig. 3.16). The viscosity data has been collected from Figures 3.14 and 3.15 for a steady shear rate of 100 sec^{-1}. All the blends were shown to exhibit Newtonian behavior like the polyarylate with viscosities largely remaining

unchanged in the shear rate range of 10 to 200 sec^{-1}. Blend with 1% LCP however showed a non-Newtonian shear thinning behavior up to about 100 sec^{-1} with a small plateau region. Large decrease in the viscosity of the blends measured for the capillary flow may be attributed largely to the deformation of the dispersed LCP phases.

A number of factors such as the viscosity ratio, extensional flow in the converging region[75], elongational and shear forces and other processing variables[118,119] play important roles in describing the flow morphology. Deformation of LCP droplets dispersed in a amorphous matrix can be described in terms of an assumed Newtonian behavior[129]. A simple calculation using a melt temperature of 300°C for this blend system assuming a matrix viscosity of 10^4 Pa-s at a shear rate of 100 s^{-1} and a droplet diameter of one micron with an interfacial tension of 10^{-3} N/m, leads to a value of Weber number, We = ~500. A Weber number value substantial exceeding 1, therefore, typically meets the condition for melt processing which will deform the dispersed LCP particles. But in true viscoelastic systems like this, the behavior is much more complicated requiring precise identification of conditions. Since the polymer elasticity effects due to LCPs are poorly understood, only qualitative correlations have been made so far.

Newtonian behavior of the blends studied here can be explained in terms of a dominating influence of the immiscible polyarylate matrix. The flow of the immiscible polyarylate phase becomes increasingly facial in the presence of a deforming anisotropic LC phase. Pure LCP melts show high shear thinning behavior

under anisotropic stresses due to easy orientation of the rigid macromolecular chains present in the mesomorphic state. Low intermolecular interactions between the rigid chains result in the low yield stresses leading to plastic flow and the liquid like behavior[130,131]. Newtonian behavior of the similar blends have been reported for LCP contents up to about 50 to 70 % by weight of LCP[66]. Then, when the LC phase becomes the continuous phase, the blend tends to show the shear thinning behavior of the pure LCP. A continuous decrease in the viscosity with increasing content of LCP was, however, noted in general from other investigations of similar blends[65,52]. Blends of polyarylate/LCP, however, show a minimum in the viscosity at 5% LCP level. The reversal of viscosity trends with the LCP composition are apparently related to the nature of the continuous phase. No simple explanation of phase changes can however be given in this case at compositions as low as 5% by weight of LCP. Similar findings were reported for the blends of LCP with wholly aromatic polyamides[81].

Increased melt temperature is shown to decrease the melt viscosity of the PA/V blend in the range of 290 to 310°C. This is shown in Figure 3.18 for the blend containing 10% LCP. An estimate of the flow activation energies (ΔE_η) calculated for this composition showed improved values compared to average values reported in literature for the melt from wholly aromatic polyesters (54.4 to 83.7 KJ/mole). Higher flow activation energies for the blends suggests that the reduced viscosities of the melt is relatively unaffected by the temperature increase. It is also evident from the plot shown in Fig. 3.17 that the nature of flow changes from

Newtonian to non-Newtonian with shear thinning in the range of 0.1 to about 20 sec^{-1}. as the temperature of the melt is raised from 300 to 310°C.

4.5 Mechanical Properties of the Blends

Tensile mechanical properties of the fibers extruded from the blends are shown to be greatly improved over that measured for neat polyarylate fibers. Morpholgy of the LCP phase dispersed in these fibers was shown to be fibrillar with predominant orientation in the direction of fiber axis. Elastic modulus and tensile strength measured for these fibers can be used to predict the aspect ratio of these fibrillar LCP assuming a composite model. The relationship between the modulus and the volume fraction of the reinforcing species for such transversely isotropic composite materials (i.e. fibers of uniform aspect ratio embedded in a matrix, and all oriented in one direction) can be described by the Tsai-Helpin equation[130],

$$E_{11} = E_m (1+\zeta\eta V_f)/ (1-\eta V_f)$$

$$\eta = (E_f/ E_m -1)/ (E_f/ E_m -1), \quad \zeta = 2*(L/D)$$

For continuous fiber reinforcement (i.e. infinite L/D), this equation reduces to well known rule of mixtures to predict the modulus as a fuction of composition,

$$E_c = E_f v_f + E_m v_m$$

where the subscripts f and m refer to embedded LCP fiber and matrix polymer respectively, E is the measured elastic modulus of the pure polymers spun under high draw to achieve uniaxial conditions. Volume fraction 'v' for each of the polymers were calculated from the density obtained from the specifications supplied by the

manufacturer. Using these data, E_c was calculated for each different composition of blend and plotted as shown in Fig. 3.20. As may be apparent from this plot, the experimentally observed tensile modulus falls slightly short of the calculated values represented by the straight line. It would be worthwhile to note that the experimental data for the blend fibers relate to an extrusion temperature of 290°C, whereas the computed data was obtained from an experimental value for pure polymers spun at 300°C. By noting an increasing trend in modulus values of 10% blend LCP blend fibers upon raising the temperature to 300°C, one can extrapolate the same situation with other compositions as well. Therefore, the experimental data conform well with predictions of the composite theory under the base conditions studied here.

Apparently, there seem to be good adhesion between the LCP fibrils and the polyarylate matrix at low strains. This is clearly shown by a strict adherence to the rule of mixtures as shown by the modulus of the fibers extruded from 1-3% LCP blends (Fig. 3.19). Due to low intrinsic strain to break of the LCP (< 1.5%), it can not follow the plastic deformation of the matrix all the way to high strains. The adhesion between the matrix and the fibrils seem to collapse at high strains as is shown by a decrease in the breaking strength of the blends with low LCP contents (Figure 3.20). This results in large number of fibrils getting pulled out of the matrix as shown in the fracture surface micrographs obtained for the fibers containing up to 10% LCP. Tensile stress data has been modelled by assuming the volume occupied by the fibrils as mechanical voids for at the point of break[118]. This model

reportedly gives a good qualitative fit for the decrease in tensile strength data for low LCP blends. For high LCP composition blends both the elastic modulus and the breaking stress data tends to approach values predicted by the rule of mixtures as shown in the Figures 3.19 and 3.20. This could be explained in terms of a continuous reinforcement (high L/D) due to uniaxially oriented LCP fibrils providing good adhesion to the matrix. Such conditions are typically attained for the short fiber reinforced composites when the aspect ratio of the fibrils attains a value of 100. This has been supported by the calculation of aspect ratios done earlier for the fibers containing 10 and 15% by weight of LCP using the fracture surface micrographs. Long LCP fibrils observed in the blends with high LCP contents frequently develop good adhesion to the matrix. This is also seen in the fracture surface micrographs of blends having greater than 5% LCP by weight. Therefore, at high LCP contents, the LCP will dominate the mechanical behavior of the blends when the reinforcing fibrils are stressed up to the break resulting in catastrophic failure of the matrix at break point. At low LCP contents, on the contrary, the mechanical properties such as breaking strength and breaking elongation is determined by the matrix properties. This is clearly apparent from the corresponding plots shown in Figures 3.20 and 3.21. Slight increase in the strain-to-break observed for the low LCP content fibers is probably attributed to the poor adhesion of a rigid LCP phase to the polarylate matrix. At LCP contents higher than 3%, however, the fibrils can be easily imagined to constrain the plastic deformation of the matrix, restricting the elongation to break of the fibers (Fig. 3.21).

The decrease in the breaking strength of the low LCP content fibers can be explained in terms of failure of adhesion between the reinforced LCP and the matrix polymer reducing the effective load bearing area. This was supported by similar studies carried out on other LCP blends[118]. Good adhesion of PC with an LCP phase has been shown to give enhanced mechanical properties above those predicted by the rule of mixtures at LCP concentrations of less than 10% [65].

High melt temperatures were shown to improve the mechanical properties of the composite fibers obtained from the blends (Fig. 3.26 and 3.27). Increased melt temperatures apparently ensure increased deformation to produce long LCP fibrils. In the post die melt, the elongational forces continues to further deform the dispersed LCP before it solidifies[119]. At high temperatures beyond about 310 °C, the mechanical properties of the PA/V blends is shown to decrease. This could be attributed to a combination of reduced viscosity differences between the matrix and dispersed phase and an increased chances of coalescence of droplets through a reduced viscosity matrix at the die entrance. Eventually deformation of these large particles results in thicker fibrils with reduced aspect ratios and consequent low adhesion properties. This is clearly supported by the SEM micrographs of the fracture surface of these fibers (Fig. 3.12). Therefore at melt temperature of 300 °C, an optimum advantage in terms of a favorable morphology can be obtained.

Dispersed LCP particles seem to deform better in the capillary at an intermediate shear rate of 150-200 sec^{-1}. For 10% LCP blend, the elastic modulus and tensile strength were shown to go through a maximum in these shear rate range

(Figures 3.29 and 3.30). This could be due to an intrinsic behavior of pure Vectra, which reportedly shows maximum in tensile strength when processed at a shear rate of 150 sec^{-1}. According to some authors the deformation of the LCP phase occurring as a result of extensional forces at die entrance tend to relax in a weak and prolonged shear field[75]. Decrease in the mechanical properties at high shear field exceeding 200 sec^{-1} may be explained in terms of a competition between phase agglomeration to form larger droplets and a faster deformation of the smaller LCP droplets at the die entrance due to high extensional forces. This was supported by a large number of small aspect ratio LCP fibrils seen on the fracture surface from fibers extruded at 1134 sec^{-1} (Fig. 313b). According to some studies[66] it may have been caused by competing effects of viscous and interfacial tension causing either the relaxation or break up of the elongated fibrillar phases.

Increased melt draw ratio of the extruded fibers is shown to improve the elastic modulus and ultimate breaking strength as has been shown for the 10% LCP composition (Fig.3.23). This result shows that a significant part of the deformation of the dispersed LCP phases is occurring in the post die elongational flow of the melt. The linearly increasing values of the modulus and the breaking strength up to a maximum draw ratio of 114 indicates a morphology which is still far from uniaxial with respect to fibrillar LCP phases in the solidified fibers. Polyarylate matrix seem to exhibit plastic flow at a higher melt draw ratio of 114 as has been shown in the fracture surface of fibers containing 10% LCP (Fig. 3.11b). Improved orientation of the matrix due to plastic flow may also have contributed to increased mechanical properties.

CHAPTER 5

CONCLUSIONS AND FUTURE WORK

1. Dynamic shear viscosity of pure polyarylate melt is shown to decrease by over 12 fold by the addition of 5% by weight of LCP at a steady shear of 100 sec^{-1}. Substantial reduction in the melt viscosity can be achieved with 3% LCP and breaking elongation of the spun fibers were found improved to 62% compared to 50% for the neat polyarylate.
2. Fibers obtained by melt drawing of the extrudates gave high elastic modulus value with 300% improvement over those of neat polyarylate at 15% LCP loadings. About 100% improvement in breaking strength have been achieved for an identical composition. Breaking elongation values for the fibers, however was decreased significantly for the blend fibers.
3. Estimates of the aspect ratios of insitu produced LCP fibrils have been obtained using fibril end counts observed on the fracture surface. The values obtained for fibers containing 10 and 15% by weight of LCP agrees well with those suggested by the composite model calculations using rule of mixtures as applied to the mechanical properties.
4. High melt draw ratios during spinning has been shown to yield vastly improved elastic modulus and breaking strength of the resulting composite fibers. A melt shear rate of 150-200 sec^{-1} and temperature of 300°C are

shown to favor improved morphologies of the dispersed LCP with enhanced elastic modulus and breaking strength values. A tendency to fracture by shear was seen to occur along these highly oriented fibril-matrix structure for the fibers processed at low shear rates.

5. Adhesion of the embedded LCP fibrils with the matrix was seen to improve with the aspect ratios i.e. finer and longer fibrils apparently showing better adhesion to matrix.

Further studies on this type of system may stress the effects of the chemical and morphological structure of the filler LCP on the mechanical properties of the resulting fibers. Annealing of the fibers to improve the crystallinity of the LCP phase may be investigated for a possible influence on the uniaxial reinforcement effects. Blending with thermoplastic elastomers will be another area that can help improve the toughness of the material. There is need to understand the phase diagram of the these systems in order have better control over the structure development in the extruded fibers.

BIBLIOGRAPHY

1. A. Siegmann, M. Narkis, M. Puterman and A. T. DiBenedetto, *Polymer*, **20**, 89 (1979).

2. A. Siegmann, M. Narkis, M. Puterman and A. T. DeBenedetto, *J. Polym. Sci., Phys.*, **17**, 225 (1979).

3. G. Kiss, A. J. Kovacs and J. C. Whittmann, *J. Appl. Polym. Sci.*, **26**, 2665 (1981).

4. R. H. Baughman, and E. A. Turi, *J. Polym. Sci., Phys. Ed.*, **11**, 2453 (1973).

5. R. H. Boughman, H. Gleiter and N. Sendfield, *J. Polym. Sci., Phys. Ed.*, **13**, 187 (1975).

6. F. Reinitzer, *Monatash. Chem.*, **9**, 421 (1888).

7. M. G. Fridel, *Ann-Phys., Paris*, **18**, 273 (1922).

8. C. Robinson, *Trans. Faraday Soc.*, **52**, 571 (1956).

9. C. Robinson, J. C. Ward and R. B. Beavers, *Nature*, **180**, 1183 (1957).

10. W. J. Jackson and H. F. Kuhfuss, *J. Polym. Sci., Polym. Chem. Ed.*, **14**, 1043 (1976).

11. B. Wunderlich, "Thermal Analysis", *Ed. Academic Press Inc.* NY (1990).

12. T. Chung, *Polym. Eng. Sci.*, **26**, 13 (1986).

13. J. L. Fergason, *Scientific American*, **211**, 77 (1964).

14. D. B. DuPre, E. T. Samulski and A. V. Tobolsky, "The Mesomorphic State: Liquid and Plastic Crystals", p123 in "Polymer Science and Materials", A. V. Tobolsky and H. Mark, Eds., Wiley and Sons, Inc., NY (1974).

15. F. C. Frank, *Discuss. Faraday Soc.*, **25**, 19 (1958).

16. R. E. Jerman and D. G. Baird, *J. Rheol.*, **25** (2), 275 (1981).

17. E. Joseph, G. L. Wilkes and D. G. Baird, *Polymer*, **26**, 689 (1985).

18. F. E. McFarlane, V. A. Nicely and T. G. Davis, ' Contemporary Topics in Polymer Science', Vol 2, Ed., E. M. Pearce and J. R. Schaefgan, Plenum Publ., NY (1977).

19. J. Menczel and B. Wunderlich, *J. Polym. Sci., Polym. Phys. Ed.*, **18**, 1433 (1980).

20. A. E. Zachariades, J. Economy and J. A. Logan, *J. Appl. Polym. Sci.*, **27**, 2009 (1982).

21. K. F. Wissbrun, *Br. Polym. J.*, 163 (Dec. 1980).

22. D. G. Baird, *J. Appl. Polym. Sci.*, **2**, 2701 (1978).

23. G. Kiss and R. S. Porter, *Polym. Prepr. Am. Chem. Soc.Div. Polym, Chem.*, **20**, (1), 45 (1979).

24. Z. Z. Zhou, X. Wu and M. Wang, *Polym. Eng. Sci.*, **28**, (3), 136 (1988).

25. F. N. Cogswell, P. B. Griffin and J. B. Rose, U. S. Patent No. 4,386,174 (1983).

26. G. Gebhard, G. Rehage and J. Schwartz, *J. Non-Crystalline Solids*, **81**, 177 (1977).

27. W. Huh, R. A. Weiss and L. Nicholas, *Polym. Eng. Sci.*, **25**, 779 (1983).

28. A. Buckley, A. B. Conciatory and G. W. Colundann, U.S.Patent 4,434,262 (1984).

29. J. W. Doane, N. A. Vaz, B. G. Wu and S. Zumer, *Appl. Phys. Lett.*, **48**, 269 (1986).

30. G. P. Montgomery, N. A. Vaz, *Appl. Optics*, **26**, 738 (1987).

31. P. S. Drazaic, *J. Appl. Phys.*, **60**, 2142 (1986).

32. J. L. West, *Molec. Cryst. Liq. Cryst.*, **157**, 427 (1988).

33. T. Kajiyama, S. Washizu and M. Takayanagi, *J. Appl. Polym. Sci.*, **29**, 3955 (1984).

34. S. Washizu, I. Terada, T. Kajiayama and M. Takayanagi, *Polym. J.*, **16**, 307 (1984).

35. P. J. Flory, *Macromolecules*, **11**, 1119 (1977), ibid., **11**, 1112 (1977), **11**, 1126 (1977), **11**, 1134 (1977), **11**, 1138 (1977), **11**, 1141 (1977).

36. M. Ballauff, *Molec. Cryst. Liq. Cryst.*, **4**, 15 (1986).

37. B. Kronberg, I. Bassignana and D. Patterson, *J. Phys. Chem.*, **82**, (15), 1714 (1978).

38. A. Debault, C. Casagrande and M. Veyssie, *Molec. Cryst. Liq. Cryst.*, **72**, 189 (1982).

39. P. Martinoty, A. Dubault, C. Casagrande, and M. Veyssie, *J. Phys. Lett.*, **44**, 935 (1983).

40. F. Dowell, *Molec. Cryst. Liq. Cryst.*, **155**, 457 (1988).

41. E. G. Joseph, G. L. Wilkes, and D. G. Baird, *Polymer Liquid Crystals*, A. Blumstein, ed., Plenum Press, NY (1984).

42. E. G. Joseph, G. L. Wilkes, and D. G. Baird, *Am. Chem. Soc., Div. Polym. Chem., Polym. Prepr.*, **24**, 304 (1983).

43. S. K. Sharma, A. Tendolkar, and A. Misra, *Molec. Cryst. Liq. Cryst.*, **157**, 597 (1988).

44. S. K. Bhattacharya, A. Tendolkar, and A. Misra, *Molec. Cryst. Liq. Cryst.*, **153**, 501 (1987).

45. M. Takayanagi, T. Ogata, M. Morikawa, and T. Kai, *J. Macromol. Sci., Phys.*, **B17**, (4), 591 (1980).

46. M. Paci, C. Barone, and P. Luigi, *J. Polym. Sci., Polym. Phys.*, **25**, 1595 (1987).

47. J. Malthete, N. Isaert, and B. Soulestein, *Molec. Cryst. Liq. Cryst.*, **27**, 321 (1976).

48. M. Hess, K. Friedlich and R. Kosfield, *Int. Conf. Liq. Cryst. Polym.*, Bordeaux, France, Paper 7P8 (July 1987).

49. R. Kosfield, K. Friedlich, and M. Hess, *18th Euro-physics Conf. on Macromolec. Phys.*, **11c**, 81 (1987).

50. B. Bresci, M. Paci, D. Lupinacci and P. L. Magagnini, *Int. Conf. Liq. Cryst. Polym.*, Bordeaux, France, Paper 19P3 (July. 1987).

51. P. Zhuang, T. Kyu, and J. L. White, *SPE ANTEC Tech. Papers*, **34**, 1237 (1988).

52. M. R. Nobile, E. Amenadola, L. Nicholais, D. Acierno, and C. Carfagna, *Polym. Eng. Sci.*, **29**, 244 (1989).

53. S. Huang, A. C. Griffin and R. S. Porter, *Polym. Eng. Sci.*, **29**, 55 (1989).

54. M. Kimura and R. S. Porter, *J. Polym. Sci., Polym. Phys. Ed.*, **22**, 1697 (1984).

55. K. Friedlich, M. Hess, and R. Kosfield, *Macromol. Chem., Macromol. Symp.*, **16**, 251 (1988).

56. Z. Zhou, X. Wu, and M. Yu, *18th Europhysics Conference on Macromolecular Physics*, **11c**, 82 (1987).

57. R. R. Luise, *Polym. Liq. Cryst., Faraday Diss.*, **79**, 290 (1985).

58. M. Pracella, D. Dainelli, G. Gallie, and E. Chiellini, *Makromol. Chem.*, **187**, 2387 (1986).

59. M. Pracella, D. Dainelli, G. Galli, and D. Dainelli, *Molec. Cryst. Liq. Cryst.*, **153**, 525 (1987).

60. A. Nakai, T. Shiwaku, H. Hasegawa, and T. Hashemoto, *Macromolecules*, **19**, 3008 (1986).

61. T. Kyu, and P. Zhuang, *Polym. Commun.*, **29**, (4), 99 (1988).

62. H. H. Chuah, T. Kyu, and T. Halminiak, *Polymer*, **28**, 2130 (1987).

63. M. J. Seurin, J. M. Gill, A. T. Bosch, and P. Sixou, *Polymer*, **25**, 1073 (1984).

64. J. Billard, A. Blumstein, and S. Vilasagar, *Molec. Cryst. Liq. Cryst.*, **72**, 163 (1982).

65. T. M. Malik, P. J. Carreau, and N. Chapleau, *Polym. Eng. Sci.*, **29**, (9), 600 (1989).

66. A. Kohli, N. Chung, and R. A. Weiss, *Polym. Eng. Sci.*, **29**, (9), 573 (1989).

67. B. Y. Shin and I. J. Chung, *Polym. J.*, **21**, (11), 851 (1989).

68. T. Limtasiri and A. I. Isayev, *J. Appl. Polym. Sci.*, **42**, 2923 (1991).

69. A. Mehta, and A. I. Isayev, *ACS Polym. Prep.*, **30**, (2), 548 (1989).

70. R. A. Weiss, W. Huh and L. Nicolais, *Int. Conf. Liq. Cryst. Polym.*, Bodeaux, France, Paper 8P8 (1987).

71. R. A. Weiss, W. Huh, L. Nicolais, and A. Kohli, Conf. on Emerging Tech. Mater., AIChe, Paper CO1.50 (Aug. 1987).

72. R. A. Weiss, W. Huh, L. Nicolais and P. Yanisko, *SPE RETEC Tech. Papers*, 267 (1987).

73. F. N. Cogswell, B. P. Griffin, and J. B. Rose, U.S. Patent, 4,433,83 (1984).

74. F. N. Cogswell, B. P. Griffin, and J. B. Rose, U.S. Patent, 4,438,236 (1984).

75. K. G. Blizard and D. G. Baird, *Polym. Eng. Sci.*, **27**, 653 (1987).

76. D. Acierno, E. Amendola, C. Carfagna, L. Nicholais, and R. Nobile, *Molec. Cryst. Liq. Cryst.*, **153**, 533 (1987).

77. B. Lee, *SPE ANTEC Tech. Papers*, **34**, 1088 (1988).

78. L. Lorenzo, S. K. Ahuja, and H. Chang, *Am. Chem. Soc., Div. Polym. Chem., Polym. Prepr.*, **29**, 488 (1988).

79. M. T. DeMeuse and M. Jaffe, *Molec. Cryst. Liq. Cryst.*, **157**, 535 (1988).

80. C. U. Ko and G. L. Wilkes, *J. Polym. Sci.*, **37**, 3063 (1989).

81. A. Siegmann, A. Dagan, and S. Kenig, *Polymer*, **26**, 1325 (1985).

82. S. Swaminathan and A. I. Isayev, *Proc. ACS Div. of polym. Mater.*, **57**, 330 (1987).

83. S. G. James, A. M. Donald and W. A. Macdonald, *Molec. Cryst. Liq. Cryst.*, **153**, 491 (1987).

84. M. F. Froix, M. Park, and N. Trouw, *U.S. Patent* 4,460,736 (1984).

85. A. Zaldua, E. Munoz, J. J. Pena and A. Santamaria, *Polymer*, **32**, (4), 682 (1991).

86. T. Chung, *Plast. Eng.*, **43**, 39 (1987).

87. T. Chung, *SPE ANTEC Tech. Paper*, **33**, 1404 (1987).

88. A. I. Isayev and M. J. Modic, *Polym. Compos.*, **8**, 158 (1987).

89. R. A. Weiss, W. Huh, and L. Nicolais, *Polym. Eng. Sci.*, **27**, 684 (1987).

90. P. R. Subramanium, and A. I. Isayev, *Polymer*, **32**, (11), 1961 (1991).

91. P. R. Subramanium, and A. I. Isayev, *SPE ANTEC Papers*, **36**, 489 (1990).

92. A. Apicella, P. Iannelli, L. Nicodemo, L. Nicolais, A. Roviello, and A. Sirigu, *Polym. Eng. Sci.*, **26**, (9), 600 (1986).

93. A. Zaldua, E. Munoz, J. J. Pena, and A. Santamaria, *Polymer*, **32**, (4), 682 (1991).

94. T. Asada, H. Yanase and A. Onogi, "*Rheology*", G. Astarita, G. Marrucci and L. Nicolais, Eds., vol. 1, pg. 127, Plenum Press, NY (1980)

95. G. G. Viola and D. G. Baird, *J. Rheol.*, **30**, 601 (1986).

96. D. G. Baird, "*Polymer Liquid Crystals*", A. Blumstein, Ed., Plenum Press, NY (1985)

97. A. E. Zachariades and J. A. Logan, *Polym. Eng. Sci.*, **23**, 797 (1983).

98. G. W. Farrel and J. F. Fellers, *J. Polym. Eng.*, **6**, 264 (1986).

99. T. G. Ryan, *Molec. Cryst. Liq. Cryst.*, **157**, 577 (1988).

100. W. J. Jackson, Jr. and H. F. Kuhfuss, *J. Polym. Sci., Polym. Chem. Ed.*, **14**, 2043 (1976).

101. O. A. Nehme, C. A. Gabriel, R. J. Ferris, E. L. Thomas, and M. F. Malone, *J. Appl. Polym. Sci.*, **35**, 1955 (1988).

102. E. G. Joseph, G. L. Wilkes and D. G. Baird, *Am. Chem. Soc., Div. Polym. Chem., Polym. Prepr.*, **25**, 94 (1984).

103. G. Kiss, *Polym. Eng. Sci.*, **27**, 410 (1987).

104. M. Wellman, G. Hussman, A. K. Kulshreshtha, T. Helminiak, D. Wiff, C. Benner, and W.F. Hwang, *ACS Orgnic Coat. Plast. Chem.*, **43**, 783 (1980).

105. G. Husman, T. Helminiak, W. Adams, D. Wiff, and C. Benner, *ACS Symposium Ser., EMS*, **132**, 203 (1980).

106. G. Husman, T. Helminiak, M. Wellman, W. Adams, D. Wiff, and C. Benner, *Tech. Rep. AFWAL-TR-80-4034* (1980).

107. M. Takayanagi and G. Goto, *J. Appl. Polym. Sci.*, **29**, 2547 (1984).

108. T. Kajiama, S. Washizu, A. Kumano, I. Tereda, M. Takayanagi, and S. Shinkai, *J. Appl. Polym. Sci., Appl. Polym. Symp.*, **41**, 327 (1985).

109. M. Takayanagi, *Pure Appl. Chem.*, **55**, 819 (1983).

110. F. Schubert, K. Friedlich, M. Hess and R. Kosfield, *Molec. Cryst. Liq. Cryst.*, **155**, 477 (1988).

111. C. Carfagna, E. Amendola, L. Nicolais, D. Acierno, O. Francescangeli, B. Yang and F. Rustichelli, *J. Appl. Polym. Sci.*, **43**, 839 (1991).

112. R. A. Weiss, W. Huh and L. Nicolais, *High Modulus Polymers, A. E. Zachariades and R. S. Porter, ed.*, p 145, Mercel Deckker Inc., NY (1988).

113. T. Sun, D. S. Done and D. G. Baird, *Abstracts of Polymer Processing Society Summer Meeting*, Amherst, Mass., 9B (1989).

114. D. Dutta, H. fruitwala, A. Kohli, and R. A. Weiss, *Polym. Eng. Sci.*, **30**, 17, 1005 (1990).

115. M. Amano and K. Nakagawa, *Polymer*, **28**, 263 (1987).

116. R. Ramanathan, K. Blizard, and D. Baird, *SPE ANTEC Tech. Papers*, **34**, 1123 (1988).

117. R. Ramanathan, K. G. Blizard and D. G. Baird, *SPE ANTEC Tech., Papers*, **33**, 1399 (1987).

118. G. Crevecoeur and G. Groeninckx, *Polym. Eng. Sci.*, **30**, (9), 532 (1990).

119. K. G. Blizard, C. Federici, O. Federico, and L. L. Chapoy, *Polym. Eng. Sci.*, **30**, (22), 1442 (1990).

120. M. Kimura, R. S. Porter and G. Salee, *J. Polym. Sci., Phys. Ed.*, **21**, 367 (1983).

121. J. Francois, J. Y. S. and J. M. Guenet, *Macromolecules*, **19**, 2755 (1986).

122. R. A. Chivers, J. Blackwell and G. A. Gutierrez, *Polymer*, **25**, 435 (1984).

123. S. Z. D. Cheng, *Macromolecules*, **21**, 2475 (1988).

124. M. Y. Cao, B. Wunderlich, *J. Polym. Sci., Phys. Ed.*, **23**, 521 (1985).

125. H. Bechtold, J. H. Wendorff and H. J. Zimmerman, *Makromol. Chem.*, **188**, 651 (1987).

126. J. Blackwell, A. Biswas and R. C. Bonart, *Macromolecules*, **18**, 2126 (1985).

127. D. Demus and L. Richter, *Textures of Liquid Crystals*, Chemie, New York (1978).

128. M. Cao and B. Wunderlich, *J. Polym. Sci., Polym. Phys Ed.*, **23**, 521 (1985).

129. M. V. Tsebrenko, G. P. Danilova, and A. Y. A. Malkin, *J. Non-Newt. Fluid Mech.*, **31**, 1 (1989).

130. H. C. Tseng, D. L. Silver and B. A. Finlayson, *Phys. Fluids*, **15**, 1213 (1976).

131. S. Onogi, and T. Asuda, "Rheology, V.1", G. Astarita, G. Marucci, and L. Nicolais, ed., Plenum Press, N.Y. (1980).

APPENDIX

APPENDIX A

Table 1 : Mechanical properties of injection molded specimens of Isotropic polymer/ LCP blends (Ref. 103).

Material	Tensile Strength (MPa)	Elongation (%)	Tensile Modulus (GPa)	Flex Strength (MPa)	Flex Modulus (GPa)	Izod Impact (J/m)
Aclon	27.0	21.7	1.70	52.4	2.75	23.5
Aclon/LC polyester	70.3	2.5	5.24	83.4	3.83	14.5
Ardel	71.0	155	1.52	67.2	1.76	45.6
Ardel/LC polyester	102	5.3	4.27	100.6	3.32	18.6
Ardel/LCP esteramide	51.7	2.0	3.28	90.3	2.94	8.4
Celcon	56.5	58	2.37	81.3	2.36	41.5
Celcon/LC polyester	36.5	3.8	2.81	72.4	2.94	17.1
Celanex	51.7	5.8	2.58	89.6	2.66	-
Celanex/ LC polyester	37.9	1.2	3.54	52.4	2.75	-
Lexan	66.9	100	2.32	93.1	2.47	462
Lexan/LC polyester	121	3.49	5.72	132	4.54	14.8
Lexan/LCP esteramide	154	4.2	6.55	136	5.00	12.8
Nylon	73.1	436	2.06	76.5	2.01	31.9
Nylon/LC polyester	66.9	14.6	2.65	93.8	2.52	20.3
Nylon/LCP esteramide	60.7	2.5	3.16	86.2	3.38	11.6
PEEK	84.1	48	3.5	(extruded strand)		
PEEK/LC polyester	71.7	2.5	4.3	(extruded strand)		
Ultem	91.0	59	3.05	141	3.34	24.7
Ultem/LC polyester	129	4.3	5.15	156	4.78	19.1
Ultem/LCP	95.8	1.54	7.45	103	6.18	18.6

APPENDIX B

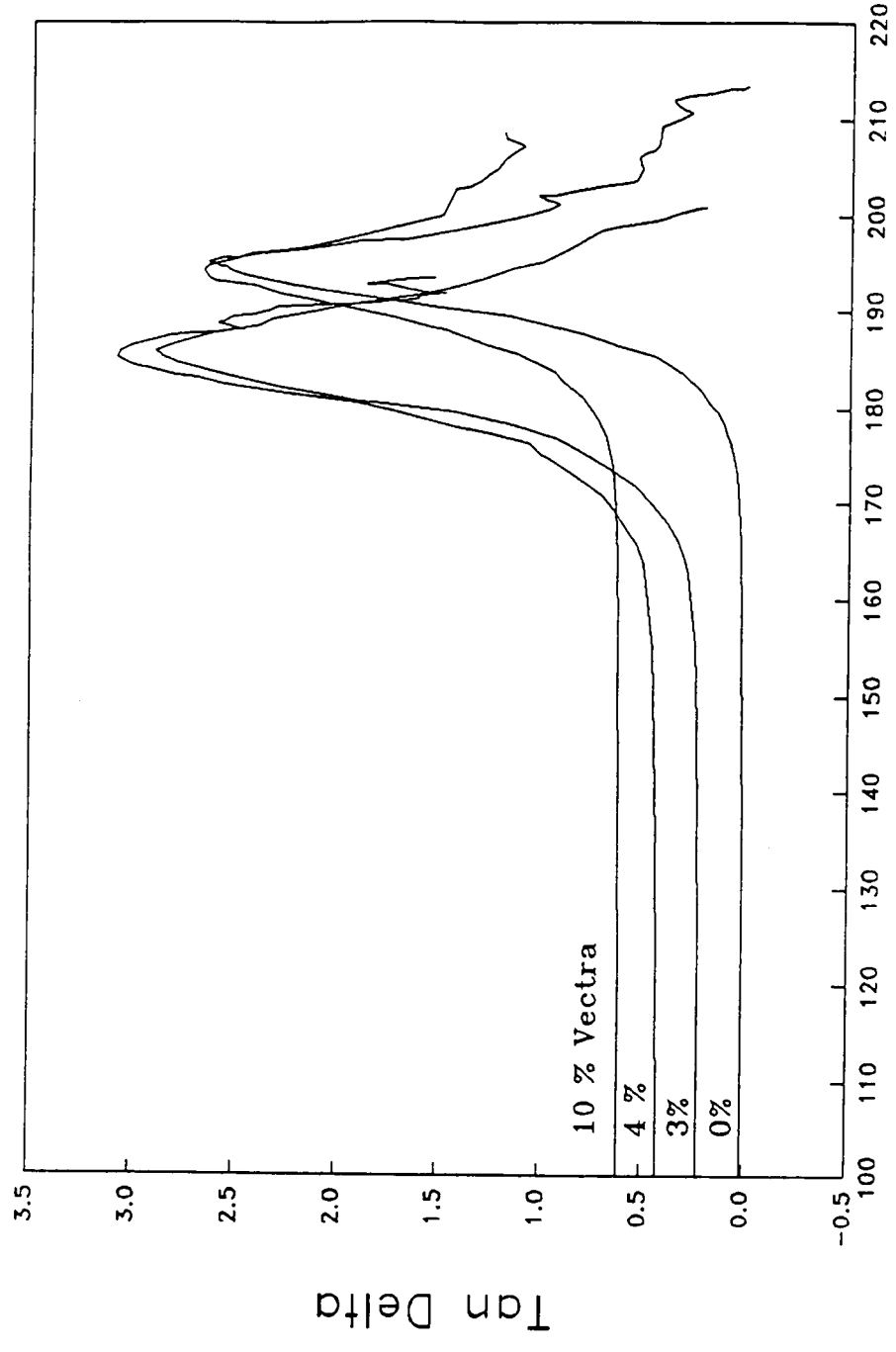

Fig. 1 : **Tan δ loss traces of PAr / Vectra (V) blends obtained through dynamic mechanical analysis (DMA) at a frequency of 1.1 Hz.**

VITA

Ravinder Nair was born in Kerala state, India on March 29, 1959. He studied at Delhi University, Delhi and received a Master degree in Chemistry in 1980. He then attended Indian Institute of Technology (IITD), Delhi for two years and received a M. Tech degree in Fiber Science and Technology.

After graduating from IITD, he joined Oil and Natural Gas Commission, Bombay in May, 1983. Having worked as a Production Chemist for about 5 years, he decided to continue his education in the area of polymers. With this aim, he joined the University of Tennessee at Knoxville in August, 1989 to study Polymer Engineering.

He is member of American Chemical Society and the Society of Plastic Engineers.